AALBORG UNIVERSITET

Institute of Energy Technology

M. Sc. in Power Electronics and Drives

Master Thesis

Fault Current Contribution from VSC-based Wind Turbines to the Grid

Massimo Valentini

Denmark, June 2008

AALBORG UNIVERSITET

Institute of Energy Technology
Pontoppidanstræde 101
DK-9220, Aalborg, Denmark
Tel. 96 35 92 40
Fax 98 15 14 11
www.iet.aau.dk

Title: Fault current contribution from VSC-based wind turbines to the grid

Project period:
4. February - 4. June 2008

Project group number:
PED10 - 1015C

Conducted by:
Massimo Valentini

Supervisor from Aalborg University:
Florin Iov, Associate Professor, PhD

Supervisors from Siemens Wind Power A/S:
Kenneth Pedersen, PhD
Vladislav Akhmatov, PhD
Kim Hoj Jensen, PhD

Number of copies: 5

Number of pages: 102

Finished: 4. June 2008

The cover picture represents the wind park Burbo (Great Britain). Courtesy of Siemens Wind Power.

Institute of Energy Technology,
Aalborg University
ISBN 978-87-89179-73-5

Synopsis:

When performing short-circuit investigations in power systems including wind power, valuable and accurate results can only be obtained by considering the real behaviour of wind turbines which is specified in national grid codes. This requires the consideration of the exact active and reactive current injections during the fault.
In this master thesis an equivalent VSC-based wind turbine model for short-ciruit calculations at steady-state conditions is developed; it is based on the Thevenin equivalent where paramenters are adjusted by a routine in order to force the model to behave as required by the German grid code, which is considered as reference regarding the grid voltage support. The routine, including the adjustable wind turbine model, is implemented in DigSILENT PowerFactory using the DPL-Programming Language.
The developed wind turbine model is validated by comparison with a valiadated dynamic model provided by Siemens Wind Power. The comparison in some significant cases proves that the routine accurately implements the injection of the desired active and reactive current components according to the German grid code.
The wind turbine model is finally rescaled to obtain an aggregate wind farm model and used to perform short-circuit calculations in a real power system including wind power. The Danish transmission system is considered and a large offshore wind farm with VSC-based wind turbines is included in the investigation. Test results in significant study cases prove that the current contribution from the wind farm has been successfully implemented in a general way and, thus, initial project goals have been completely achieved.

Preface

The present Master Thesis is entitled *Fault Current Contribution from VSC-based Wind Turbines to the Grid* and documented by group PED10-1015C in the 10^{th} semester at the Institute of Energy Technology, Aalborg University. The project period is from 4^{th} February to 4^{th} June 2008. The project is carried out in collaboration with Siemens Wind Power A/S that has provided supervision, finantial support and confidenial model results required for the validation of the developed wind turbine model for short-circuit studies.

Literature references are mentioned in square brackets by numbers. Detailed information about literature is presented in Bibliography. Appendices are assigned with letters and are arranged in alphabetical order. Equations are numbered in format *(X.Y)* and figures are numbered in format *Fig.X.Y*, where X is the chapter number and Y is the number of the item. The enclosed CD-ROM contains the material used throughout the project time; details regarding the CD-ROM content are provided in Appendix D.

The report is conducted by:

Massimo Valentini

Ringraziamenti

Questa tesi rappresenta per me e per tante altre persone a me legate un traguardo molto importante; rappresenta la fine del mio percorso accademico che ha dato tantissime soddisfazioni. Sebbene da parte mia devozione, impegno e volontá sia stati importanti per raggiungere questo traguardo, é stato altrettanto fondamentale il contributo di altre persone che vorrei qui ringraziare.

In primis, vorrei ringraziare i miei genitori per aver devotamente provveduto tutto il sostegno economico necessario per raggiugere questo ambito obiettivo. Senza il loro sostegno sarebbe stato molto piú difficile, se non addirittura impossibile, raggiungere gli stessi risultati. Spero di cuore di aver ricompensato i loro sacrifici con tante soddisfazioni.

Vorrei ringraziare di cuore Paola che ha dolcemente condiviso con me tutte le gioie e i sacrifici dal primo all'ultimo giorno di universitá. Sebbene durante gli ultimi due anni la lontananza ci abbia messo a dura prova, siamo riusciti insieme a superare anche questa sfida. Grazie per tutto il supporto morale, le emozioni, le attenzioni e le botte d'allegria.

Infine vorrei ringraziare tutte le persone, parenti ed amici, che hanno gioito per i risultati da me ottenuti e che sono state orgogliose di me.

Acknowledgements

This thesis represents the end of my accademic career as student; it is therefore worthy to thank not only people that have contributed to the project but also people that have been important for me throughout my accademic career.

First, I would like to acknowledge all important persons that have contributed to the project in this semester.

I would like to thank Prof. Florin Iov, my supervisor at Aalborg University, who has actively contributed to lead me to a higher level by providing me ideas and feedbacks. I really appreciated his critical supervision which has been crucial for me to achieve good results.

I am grateful to Dr. Vladislav Akhmatov, the supervisor from Siemens Wind Power A/S, for spending his time helping me to develop a good project, not only from the accademic point of view. I was very glad to work with a widely recognized expert like him on the wind power technology.

I also acknowledge Dr. Kenneth Pedersen and Dr. Kim Hoj Jensen, my supervisors from Siemens Wind Power A/S, who have succesfully provided me a very good environment to develop my final project.

I really enjoy the collaboration with Siemens Wind Power A/S; I worked in a professional environment and I was also financially supported. Thanks to the contribution from Siemens Wind Power A/S, the project is focused on a challenging engineering topic and has been developed using a professional approach where my own contribution is validated by comparisons with confidential models and data kindly provided by the company.

Here, I would like to acknowledge all fundamental contributions throughout my accademic career, starting from the Bachelor.

First, I am grateful to my parents for having supported my study and provided everything I needed; I fortunatelly did not miss fundamental things and, thus, I could completely focus and devote myself to my studies.

I would like to acknowledge Prof. Silvano Vergura; he was the first helping me to start the wonderful adventure in Denmark. I am also grateful for the interesting conversations that helped me very much when I was confused about my professional future.

I am very grateful to Prof. Remus Teodorescu because he really made my dream of studying abroad possible. I have been working with him throughout the entire master, gaining practical experience in Power Electronics for renewable energy systems. With this student job I could improve my skills and, even more important, I earned some money that made my stay in Denmark possible. I really appreciated him for everything he has done trying to make me a good engineer. I have also appreciated very much his personality: a friend, a wise professor and a very distinguished person.

I would like to thank the entire Institute of Energy Technology where I spent two unforgettable years; I will definitely miss the kindness in which I lived and studied throughout the master.

I would like to thank all together Prof. Remus Teodorescu, Prof. Florin Iov, Prof. Stig Munk-Nielsen, Prof. Marta Molinas, Prof. Pedro Rodriguez, Prof. Marco Liserre and Dr. Vladislav Akhmatov for considering me a possible future PhD student with great potential; I know that they would have been pleased to have me in their own research groups and I would have been the same.

I would like to thank my flatmates Alin, Andreea, Antonio, Emanuele and Karolina for the nice atmosphere in which we lived together; without them, my stay in Aalborg would not have been the same.

Throughout my accademic career, the only person with whom I shared all satisfactions and problems is my wonderful girlfriend Paola; she has been very patient with me by letting me devote most of the time and energy to my studies. I really appreciated what she has done for me and, thereby, I would like to kindly acknowledge her.

Contents

Chapter 1

Project definition

Contents

1.1 Introduction

In the recent years an increasing attention has been paid to alternative methods of electricity generation as a consequence of increasing environmental concern and growing global energy demand. The very low environmental impact of the renewable energies make them a very attractive solution. The progress of wind technology experienced in the last years has exceeded all expectations, leading to cost reduction to levels comparable, in many cases, with conventional methods of electricity generation [1]. As a result wind turbines participate actively in the power production of several countries around the world. This development raises a number of challenges regarding grid stability, power quality and behaviour during fault situations. The growing importance of wind power, which can be observed in many European countries, the USA, Canada and also Australia [1], requires detailed analysis of the impact of wind power on electric power systems. Therefore, a number of studies are currently carried out for identifying required network reinforcement, reserve requirements and the impact of wind power on the power system stability [2][3][4][5].

This chapter is an introduction to the project. Section 1.2 provides a general backgroud on the wind energy technology and describes wind turbine (WT) concepts; section 1.3 defines the problem of the short-circuit current contribution from WTs to the grid; in section 1.4 project limitations are specified. In section 1.5 the power system simulation tool used in the project for short-circuit studies is briefly introduced; it will be deeply described in section 3.6. In section 1.7 the outline of this project is provided.

1.2 Background to Wind Energy Technology

Wind turbines interact with the wind, capturing part of its kinetic energy and converting it into usable energy. Depending on the position of the rotor axis, wind turibines are classified into vertical-axis and horizontal-axis ones. Nowadays, almost all commercial wind turbines connected to the grid have horizontal-axis three blades rotors [6]. The rotor is located on the top of the tower, in a nacelle, where wind has more energy and is less turbulent. The tower holds up a nacelle where gearbox and generator are assembled. There is also a yaw mechanism that turns the rotor and nacelle to face the wind in order to capture as much energy as possible when the wind turbine is working in normal operation. The WT rotor speed is usually low; for multi-MW wind turbines the nominal rotational speed is around $10 - 15rpm$. In order to efficiently convert the mechanical energy captured from the wind into electrical energy by means of an electrical generator, it is convenient to speed up the rotational speed of the WT rotor using a gearbox. In case of multi-pole generators, the gearbox can be avoided or reduced as the generator rotational speed, which corresponds to a high energy convertion, is lower.

Power electronics is nowadays used to efficiently interface renewable energy systems to the grid [7][8]. It plays a very important role in modern wind energy conversion systems (WECSs) especially for multi-MW wind turbines in large wind farms. The control of WECSs, performed by means of power electronics, contributes to the fulfilment of grid requirements, a better use of the turbine capacity by means of variable-speed operation and the allevation of aerodynamic and mechanical loads improving the lifetime of the installation [6]. The active control of the wind energy leads to higher performance that is essential to enhance the competitiveness of the wind technology.

1.2.1 Wind turbine concepts

Wind turbines can be distinguished on the basis of the speed control capability and power control capability [2][8].

Regarding the speed control capability, they are distinguished in *fixed-speed WTs*, operating in a narrow range of rotor speed slightly above the synchrounous speed, and *variable-speed WTs*, operating in a wide range of rotor speed both above and below the synchrounous speed, allowing the maximization of the captured power depending on the incoming wind.

Regarding the power control capability, they are distinguished in *fixed-pitch WTs*, with fixed blades, and *variable-pitch WTs* with pitch angle control to increase the output power depending on the incoming wind in normal operation or to limit the captured power in case of wind speed above the rated value (i.e. power limitation mode [8]).

The most commonly used WT designs can be categorized into four categories [6][7][8][9]:

- fixed speed WTs (FSWTs);
- partial variable speed WTs with variable rotor resistance (PVSWTs);
- variable speed WTs with partial-rating frequency converter, known as doubly-fed induction generator-based concept (DFIGWTs);
- variable speed WTs with full-rating power converter, also known as Voltage Source Converter (VSC)-based WTs (VSCWTs).

Fig.1.1 shows the structure of the above concepts which are described in the following [8].

Fixed speed WTs are characterized by a squirrel cage induction generator (SCIG) directly connected to the grid by means of a transformer [7]. The rotor speed can be considered locked

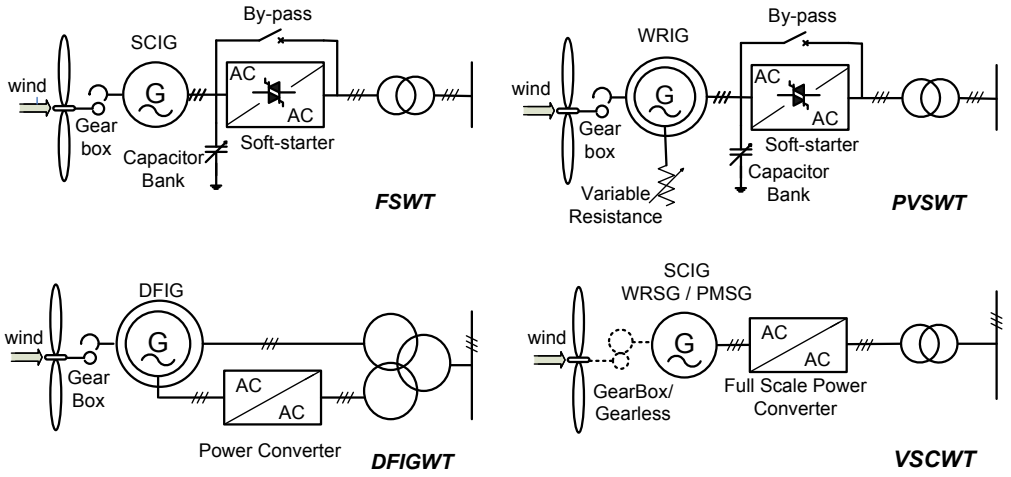

Figure 1.1: *Common wind turbine concepts [7][8].*

to the grid frequency as very low slip is encountered in normal operation (typically below 2%). The reactive power absorbed by the generator is locally compensated by means of a capacitor bank following the production variation (5-25 steps) [7]. A soft-starter can be used to perform a smooth grid connection. This configuration is very reliable because of the robust construction of the standard SCIG and the simplicity of the applied power electronics [6].

Partial variable speed WTs with variable rotor resistance use a wound rotor induction generator (WRIG) connected to the grid by means of a transformer [6][10]. The generator rotor windings are connected in series with a converter operated as an external resistance used to change the torque characteristic and the operating speed in a narrow range (typically $0-10\%$ above the synchrounous speed) [7]. A capacitor bank performs the reactive power compenastion and smooth grid connection occurs by means of a soft-starter.

In DFIGWTs, the stator is directly coupled to the grid while a partial-rating power converter controls the rotor frequency and, thus, the rotor speed [6][7]. The partial-rating power converter is rated at $20\% - 30\%$ of the WRIG rating so that the speed can be varied within $\pm$ 30% or more of the synchronous speed. However, slip rings reduce the reliability and increase the maintenance.

Variable speed VSCWTs are characterized by the generator connected to the grid by means of the full-rating frequency converter [6][7]; the converter performs the reactive power compensation and a smooth grid connection [11].

1.3 Problem definition

Short-circuit studies form an important part of power system analysis. The problem consists of determining bus voltages and line currents during various types of faults. When a power system is subject to a fault, all currents change as the impedances seen from generation units have changed. Currents flowing into the system in case of a fault are called *fault currents* or *short-circuit (SC) currents* and, depending on the type and location of the fault and the fault impedance, can be several times higher than the pre-fault currents.

Faults in power systems are divided into *three-phase balanced faults* and *unbalanced faults* [12]. Different types of unbalanced faults are *single line-to-ground*, *line-to-line* and *double line-to-ground faults*.

Short-circuit studies are frequently requested and performed by power system companies as they provide the maximum fault current used for the design of electrical components (i.e. cables, transformers, circuit breakers) and the minimum fault current for proper relays' setting and coordination. They are normally perfomed using commercially available power system simulation tools.

For network planning purposes, short-circuit studies only consider steady-state SC currents; the attention is paid to the expected maximum currents for the rating of the components and the minimum currents to make sure the protection systems will properly work. Short-circuit calculations at planning stage will mostly use calculation methods that require less detailed network modelling (e.g. load information are not considered) and might apply worst-case estimations. These calculation methods apply the IEC/VDE and the ANSI standardized methods [13][14]. Power system simulation tools normaly provide SC calculation modules based on the above standardized methods. They take into account the SC current contribution of conventional grid components such as synchrounous generators used in power plants and induction motors connected up to the subtrasmission levels (66kV-110kV); in fact since they have been used for many years, their behaviour during a fault condition is well known [12][15]. However they do not consider the SC current contribution of VSC-based components (i.e. [16]).

In the last thirty years power electronics has rapidly changed and, as a consequence, the number of grid-connected applications has increased, mainly due to the development of semiconductor devices and microprocessor technology [7]. Although the level of penetration of VSC-based grid-connected components is increasing thank to the control capability provided by power electronics, the steady-state short-circuit current contribution of these components is not treated yet in present IEC, VDE and ANSI standards. As a consequence, their SC contribution is still not implemeted in power system symulation tools.

Wind turbines with full-rating power converters are VSC-based grid-connected components. Accordingly, their short-circuit current contribution can not be taken into consideration when performing SC studies with commercially available power system simulation tools. On the contrary, for fixed speed WTs (FSWT), partial variable speed WTs with variable rotor resistance (PVSWT) and doubly-fed induction generator-based WT (DFIGWT), the short-circuit current contribution can be evaluated only considering the generator without power electronics as explained in international standards and in the literature (i.e. [14][17]).

In the past, wind turbines were allowed to disconnect from the power system during a grid fault, meaning that they had no contribution to the fault. As wind turbines begin to displace conventional power plants, an increasing support of the grid during faults is required; for this reason, in specific conditions, they are expected to remain connected to the power system during faults. Recently, system operators in many countries have established grid connection requirements, known as grid codes (GCs), that specify the range of voltage conditions for which wind turbines must remain connected to the power system [18][19][20][21]. They specify requirements for the fault ride-through (FRT) capability of WTs. Many investigations have been performed within the area of fault ride-through operation of wind turbines (i.e [21][22][23]) but only limited attention has been paid on the investigation of the SC current contribution from VSC-based wind turbines.

Some national grid codes (i.e. in German and Spanish), require WTs not only to remain connected when subject to a specified voltage dip profile but also to support the grid during faults. The grid voltage support, known as voltage control, is performed by injecting reactive current up to 100% of the rated value. This affects the voltage level at the WT terminals and in the nearby power system of the WT connection point. When considering the SC current contribution from such full-rating converters based WTs, it is necessary to evaluate the exact reactive current injection; this is

fundamental to obtain valuable results from fault studies in case of high wind power penetration. However, at the beginning of this project, there is no standardized method to perform short-circuit studies at steady-state conditions that include the fault current contribution from VSC-based wind turbines. The reason of this lack is that there is not enough experience; however the interest in this topic will increase as the wind power penetration grows. Nowadays, the SC contribution from VSC-based grid-connected components can only be evaluated by performing full dynamic simulations based on a dynamic network model for electromagnetical and electromechanical transients (i.e. [16]). This is a time consuming analysis and therefore it is not preferred to the SC calculation at steady-state conditions according to international standards.

As the level of penetration of the wind energy increases, detailed analysis about the impact of the wind power on the power system operation have to be performed [3]. Therefore increased demand for experience, knowledge and simulation models for the SC current contribution from VSC-based WTs to the grid is already required.

1.4 Project limitations

In this work the investigation on the short-circuit current contribution from wind turbines to the grid is limited to *VSC-based wind turbines* (see section 1.2.1). In fact, for other wind turbine concepts, stator windings of the generator are directly connected to the grid by means of transformers and power electronics is not always involved in the grid connection in normal operation (i.e. for FSWT and PVSWT power electronics is involved only at the startup when a soft-starter is used to smooth the grid connection). As a consequence, in case of a grid fault, those types of wind turbine basically behave as the electric generator involved, whose behaviour is well known for of induction and synchrounous generators [17].

The investigation is carried out with balanced three-phase short-circuit faults. Some statistics prove that the three-phase short-circuit is not the most frequent grid faults. Some data regarding the faults in the transmission system of the Nordic countries are presented by Nordel[1] in [24]; according to [24], more than 50% of the total number of faults per year in the period 2000-2005 in Denmark, Finland and Sweden were located on overhead lines as shown in Fig.1.2; Norway is an exception as faults located in substations were predominant compared with faults on overhead lines. Moreover the single-phase fault on overhead lines has the highest probability to occur compared with other types of faults [20]. Although the three-phase short-circuit is not the most frequent grid fault, it is the only one considered in this work because *(i)* it is often the most severe fault condition and *(ii)* is often assumed that not cleared faults may develop into a three-phase short-circuit [25].

The evaluation of the short-circuit current contribution to the grid from VSC-based grid-connected components is of common interest. This means that it is not only referring to VSC-based wind turbines but also to other distributed generation (DG) units. However this work is only focused on WECSs.

The investigation is carried out with the support of a power system simulation tool. Among several possible tools, the simulation tool DIgSILENT PowerFactory is chosen for this work as it is among the tools used by Siemens Wind Power which has collaborated on the present project work.

[1]Nordel is the collaboration organization of the Transmission System Operators of Denmark, Finland, Iceland, Norway and Sweden.

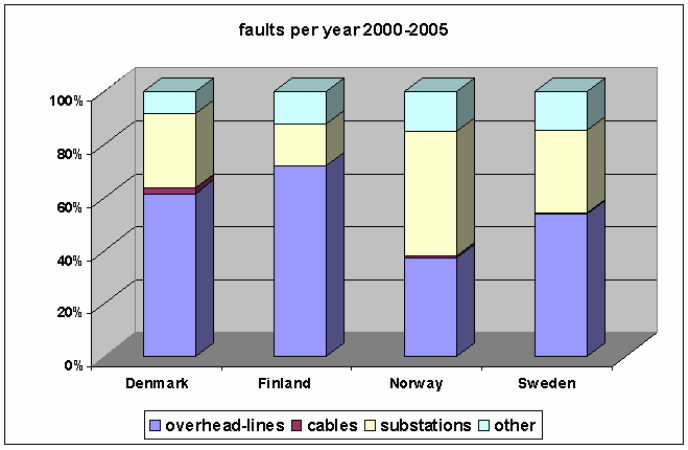

Figure 1.2: *Sharing of faults in the transmission systems of Nordic countries [20].*

1.5 Power system simulation tool

The routine to perform short-circuit calculations with current contribution from wind turbines to the grid is implemented in the commercially available power system simulation tool DIgSILENT PowerFactory.

DIgSILENT (DIgital SImuLator for Electrical NeTwork) features several simulation functionalities; the one of interest in the this work is the short-circuit calculation functionality which is based on international standards as well as the most accurate DIgSILENT General Fault Analysis (GFA) method, identified as the *complete method*. The following features are supported for all the implemented SC analysis methods:

- calculation of all three symmetrical components as well as phase quantities;
- user definable fault impedance Z_f;
- calculation of short-circuit quantities at a specific, selected busbar or along a defined section of a line/cable;
- calculation of Thevenin impedances as seen from the faulty node.

It provides a complete implementation of the IEC 60909/VDE 0102 and IEEE 141/ANSI C37 SC calculation methods according to the latest published versions.

Given the structure of the WT model during grid faults, a routine (i.e iterative process) will lead to the selection of proper parameters so that the WT behaves as expected at steady-state conditions. At each iteration, one or more SC calculations will be performed as further explained in section 4.3. The routine is implemented in DigSILENT PowerFactory using the DIgSILENT Programming Language (DPL). Features of the DPL-Programming Language are briefly presented in the following [26][27]:

- it offers a flexible interface for automating tasks:
- it can access all objects in the network models;
- it can be used to create new standardized DPL commands that can be used over and over again (i.e. the SC calculation including the current contribution from VSC-based WTs);

- it can configure and execute all PowerFactory commands (e.g. load flow and short-circuits calculation commands);
- it may contain other DPL commands which will then act as subroutines and be tested independently from each other.

1.6 Project goals

In this section, the project goals are summarized:

- overview on the wind energy technology;
- analysis of requirements for fault ride-through capability of wind turbines in some significant national grid codes;
- deep analysis of fault ride-through capability and grid voltage support according to the German grid code which is the one that provides the most described specifications;
- short-circuit calculations: analysis of calculation methods and standards;
- deep analysis of the implementation in DIgSILENT PowerFactory of calculation methods for SC studies;
- development of an equivalent model of VSC-based wind turbines for short-circuit calculations at steady-state conditions;
- development of a DPL-based routine for SC calculations including the fault current contribution from VSC-based WTs to the grid;
- comparison of the developed wind turbine model for SC calculation to the validated WT dynamic model provided by Siemens Wind Power;
- rescaling of the developed wind turbine model to represent a large scale wind farm;
- application of the developed wind farm model for short-circuit investigations in the Danish power system.

1.7 Project outline

The project is organized as a single-task work which is the development of a DPL-based routine for short-circuit calculations including the fault current contribution from VSC-based wind turbines to the grid. In this introductory chapter, the problem has been defined and project limitations are given regarding the considered WT concept, considered grid fault and the chosen power system simulation tool.

In **chaper 2**, requirements for fault-ride-through capability for wind turbines are presented according to some elected national grid codes. First it is explained how fault-ride-through requirements enhance the grid voltage support from WTs in case of grid fault by means of reactive current injection. Then the attention is paid on the relevand grid codes; the Danish, German and Spanish grid codes are analysed concerning the fault ride-through and grid voltage support specifications.

In **chapter 3** the short-circuit calculation is introduced. After describing reasons for short-circuit studies and the time behaviour of SC currents, grid faults are classified. Then, four methods

for SC calcuations are presented. International standards regarding SC calculations at steady-state conditions are analysed and finally the model implementation in the simulation tool DIgSILENT PowerFactory is deeply described.

In **chapter 4** an equivalent WT model for short-circuit calculation at steady-state conditions is described. It is based on a general approach using a Thevenin equivalent whose parameters are adjusted by the DPL routine to match the steady-state operation required by the German grid code regarding the reactive current injection into the grid during a voltage dip. The developed SC calculation routine is presented and the implementation using the DIgSILENT Programming Language is explained.

In **chapter 5** focuses on the validation of the developed DPL-based WT model for SC calculation. This is based on the comparison with results obtained with the validated SWP 3.6MW WT dynamic model provided by Siemens Wind Power. The comparison is based on some study cases agreed with Siemens Wind Power.

In **chapter 6** the developed DPL-based WT model is rescaled to represent a large wind farm used for SC investigations in the Danish power system model as application example. It shows that the short-circuit current contribution to the grid from wind farms complying with fault-ride-through and grid voltage support specifications can be taken into consideration when performing calculation at steady-state conditions.

At the end some general conclusions are given. Moreover suggestions about future work and future improvements are given.

Chapter 2

Requirements for fault ride-through capability for wind turbines

Contents

2.1 Introduction

In order to ensure the electrical system stability with significant wind power penetration, trasmission system operators in many countries are setting grid connection requirements for wind generators also known as *grid codes*. They provide several technical requirements; this chapter only focuses on requirements for fault ride-through capability of wind turbines. FRT is the ability of WTs to remain connected to the grid during a voltage dip. In most national grid codes, this capability is specified by a voltage profile that wind turbines shall withstand remaining connected to the grid. Only in few GCs (i.e. Germany and Spain), WTs are not only supposed to remain connected during a grid fault but also to support the grid voltage due to well-formulated requirements.

In section 2.2 general technical requirements for wind turbines included in national grid codes are briefly described. In section 2.3 the relationship between requirements for fault ride-through capability and short-circuit current contribution for wind turbines is presented. It yields that requirements for FRT play an important role in this work as the study of the short-circuit current contribution from WTs to the grid makes only sense if they are required to remain grid-connected and support the grid voltage in case of grid faults. Section 2.4 focuses on requirements for fault ride-through capability included in the Danish, German and Spanish grid codes. The Danish grid code is important because it provides a detailed description of the simulation model, including the type of the power grid model, to verify basic stability properties of WTs. The German and Spanish grid codes are important because they are the only ones well-describing the grid voltage support requirements during a grid fault by means of reactive current injection. In section 2.5 a

brief comparison between several requirements for FRT are graphically compared. The comparison is based on the specified voltage profiles that wind turbines shall withstand without disconnecting from the grid.

2.2 Grid connection requirements

Significant incorporation of wind power into a power system might affect the system operation especially in case of weak grids. In the past, requirements for wind turbines were primarily focused on their protection in case of grid faults (e.g. rules for disconnection); they did not consider the impact that WTs might have on the power system if the WTs stayed grid-connected [28]. However, with the increasing wind power penetration level, the loss of a considerable part of the wind generators in case of grid fault has become unacceptable as the stability of the power system can be negatively affected.

To ensure the electrical system stability, trasmission system operators in many countries are setting grid connection requirements for wind generators also known as *grid codes*. For MW-size WECSs and depending on the country, the grid connection rules are formulated; the most common requirements of concern are [7][11][29][30]:

- *active power control*: several GCs require the active control of the wind farm output power in order to participate to the energy dispach as conventional power plants and to prevent overloading of lines.

- *frequency control*: some GCs require wind farms to participate to the frequency control as conventional power plants; the frequency is kept within the required limits to ensure the security of supply, prevent the overloading of electric equipment and fulfil the power quality standards.

- *frequency and voltage ranges*: ranges of voltage amplitue and frequency are provided for continued operation in case of voltage and frequency stability problems.

- *voltage control*: some GCs require wind farms to perform the voltage control as conventional power plants; this is performed by controlling the reactive power.

- *voltage quality*: a whole set of different requirements is included in national GCs with respect to rapid changes, flickers and harmonics.

- *tap-changing transformers*: some grid codes (i.e. E.On Netz, ESBNG) require that wind farms are equipped with tap-changing grid transformer in order to be able to vary the voltage ratio between the wind farm and the grid when needed.

- *fault ride-through capability*: some GCs require wind turbines to remain connected in case of grid fault and, in some cases, to support the power system by injecting specified reactive power in order to ensure the system stability.

- *wind farm modelling and verification*: some GCs require wind farm owners to provide models and system data, to enable the Transmission System Operator (TSO) to investigate by simulations the interaction between the wind farm and the power system; they also require the installation of monitoring equipments to verify the actual behaviour of the farm during faults and to check the delivered model.

- *communications and external control*: most GCs require that the wind farm operator provides on-line measurement of some important variables for the system operator to enable proper operation of the power system (i.e. voltage, active and reactive power, operating status and wind speed). Only in few cases (i.e. Denmark and E.On), it is required the possibility to connect and disconnect the wind turbines externally.

WECSs must provide the power quality required to ensure the stability and reliability of the power system they are connected to and to satisfy the customers connected at the same grid. Voltage and frequency at the point of common coupling (PCC) must be kept as stable as possible. In general, frequency is a quite stable variable, frequency variations are always due to power unbalance between generation and consumption (i.e. generators accelerate when the supplied power exceeds the consumption, hence increasing the frequency; on the contrary they slow down when they can not cover the power demands, thereby frequecy decreases) [8]. Voltage variations take place as a consequence of variation of the mean wind speed; the amplitude of these variations depends on the impedance of the grid connected at the PCC, on active and reactive power flows. A way of attenuating voltage variations, without affecting the power extraction, is to control the reactive power flow. In the past, when fixed speed wind turbines were the State-of-the-Art, the reactive power compensation was performed by means of capacitor bank following the production variation (5-25 steps); nowadays the most effective way to perform the reactive power control is based on power electronics [8].

In the next years, the major research challenge is directed towards the grid integration of large wind farms in the electrical power system. It implies that the survival of some WT concepts is strongly connected to their ability to support the grid, to handle faults in the grid and to comply with grid requirements of the utility companies [7].

2.3 Fault Ride-Through capability and short-circuit current contribution from WTs to the grid

The fault ride-through capability of generators, also known as low-voltage-ride-through capability, is the ability of generators to remain stable and connected to the network when faults occur on the transmission network [20][29][31]. Faults in the transmission systems can cause a large transient voltage depression across the power system. Conventional large synchronous generators are normally expected to trip only if a permanent fault occurs on the circuit to which they are directly connected. Every power system is designed and operated to withstand a maximum sudden loss of a defined amount of generation capacity. If generation connected to healthy circuits does not remain connected and stable during and after the grid fault, this generation will be lost in addition to that disconnected by the original fault. Clearly, when a big loss of generation occurs, the system frequency drops rapidly and load shedding become necessary to ensure the stability [32].

Requirements for fault ride-through capability for wind turbines play an important role in this work as the study of the short-circuit current contributions from wind turbines to the grid makes sense only if WTs are required to remain connected in case of grid fault. In the past, wind turbines were subject to very simple requirements concerning their expected behaviour in case of grid fault; they where expected to disconnect in a time dependent on the voltage amplitude and frequency variations. Nowadays, requirements for FRT require WTs to remain connected and, in some countries, to support the grid to ensure the stability of the power system.

In order to highlight the importance of fault ride-through capability when interested on the short-circuit current contribution from wind turbines to the grid, a SC calculation performed in

the network owned by the German transmission system operator Vattenfall Europe Transmission (VE-T) is presented in [28] and reshown in Fig.2.1; it considers a balanced three-phase SC in the north-east part of Germany, where there is a high wind power penetration. Fig.2.1 reveals that a

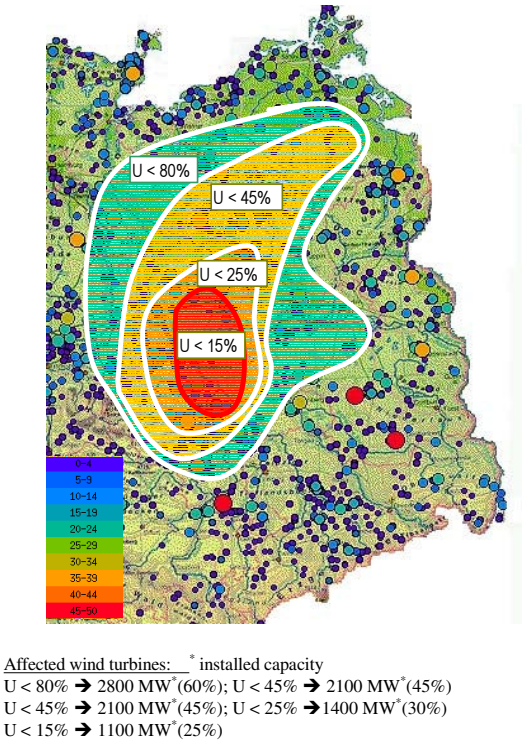

Figure 2.1: *Voltage collapse during a three-phase short circuit in the north-east part of Germany [28].*

large amount of the wind power (60% of the installed capacity in the considered area) is subjected to a voltage drop below 80%. According to the old rules for WTs in that area, they must disconnect when the voltage is below 80% [28]. This means that most of the wind power would be lost when previous rules are applied; such a big loss of generation (i.e. $2800MW$) would definitely affect the stability of the power system. The important consideration that follows is that, when old rules are applied, most wind turbines are disconnected in case of grid fault due to undervoltage protection settings; this means that their short-circuit current contribution is not relevant as only few WTs would remain connected. On the contrary, when present FRT requirements are fulfilled, almost all wind turbines are expected to remain connected and support the grid in case of fault, leading to a strong short-circuit current contribution which should be taken into consideration.

2.4 Requirements for FRT Capability in national grid codes

As it has been explained in the previous section, requirements for fault ride-through for wind turbines are important when considering their short-circuit current contribution to the grid. Therefore, among typical subjects of grid codes (see section 2.2), only the FRT requirements are considered in this work.

This section is intended to provide a background on the fault ride-through requirements of three relevant grid codes: the Danish, German and Spanish ones. They are the only grid codes actively involved in this project work. The description of FRT requirements from some other national grid

codes is beyond the purpose of this work; deep analysis and comparison is extensively presented in the literature [20][30][31][33][57].

Fault ride-through requirements are advanced grid-connection requirements technically justified only in countries with high wind power penetration; in fact, when the wind power integration is low, there is no need to require wind turbines to remain connected and support the grid during the fault. The assessment of the need for such requirements should be made by government bodies or TSOs that are fully separated from any generation activities, to avoid biased decisions [29].

Some national grid codes (e.g. Denmark and Ireland) have different fault ride-through requirements for distribution and transmission networks, whereas other national GCs have focus only on the transmission level (e.g. Germany and Spain). Some details about the existing grid codes for connection of wind power to transmission and distribution networks are given in Tables 2.2[1] and 2.3. However only some GCs specify requirements for FRT.

In the following, fault ride-through requirements for wind farms installed in Denmark, Germany and Spain are presented.

2.4.1 Denmark

Different requirements for wind farms connected to the distribution level ($< 100kV$) and the transmission level ($\geq 100kV$) are specified.

Distribution level

According to specification of Energinet.dk, wind turbines connected to grids with voltages below $100kV$ shall disconnect or remain connected to the grid in case of grid fault as shown in Fig.2.4.

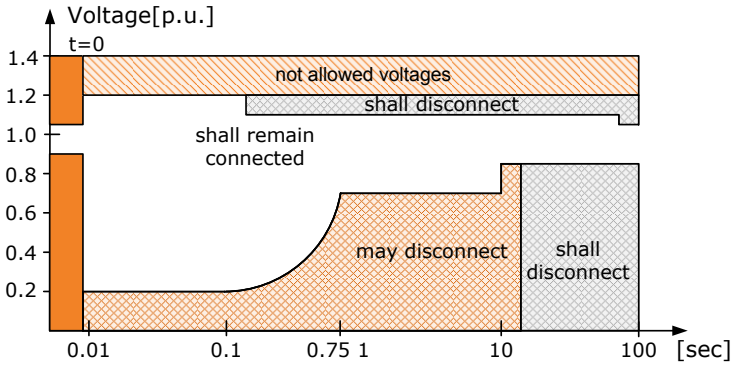

Figure 2.4: *Requirements for disconnection of wind turbines in the event of voltage dip. At time $t = 0$ an operating disturbance occurs [34].*

Protection devices against internal defect in the WT must have higher priority with respect to requirements graphically shown in Fig.2.4. As special requirement, a WT and the compensation equipment must not be disconnected from the electrical network in the following conditions [34]:

- three-phase short-circuit for $100ms$;
- two-phase short-circuit with or without ground for $100ms$ followed after $300 - 500ms$ by a new short-circuit of $100ms$ duration.

[1] In Table 2.2 the new Spanish grid code for connection to the transmission level is missing; it the called *PO.12.3-Requisitos de respuesta frente a huecos de tension de las instalaciones de produccion de regimen especial*, released in November 2005 [37].

Country	Document ref.	Title	Reference, year	Scope
Austria	TOR	Technische und organisatorische Regeln für Betreiber und Benutzer von Netzen	E-Control 2004	Grid code for transmission & distribution
Belgium	Royal Decree 19/12/2002	Koninklijk besluit houdende een technisch reglement voor het beheer van het transmissienet van elektriciteit en de toegang ertoe	Staatsblad, 2002	Transmission Code
	ELIA internal doc.	Voorschriften en uit te wisselen informatie voor de aansluiting van productie-eenheden (Draft)	ELIA, 2004	Wind connected to transmission level
Denmark	TF 3.2.5	Wind turbines connected to grids with voltages above 100 kV	Energinet, 2005 (Eltra & Elkraft)	Wind connected to transmission level
Finland	-	No specific grid code available	-	-
France		Référentiel technique de RTE	RTE 2005	Transmission Code
Germany	Transmission Code 2003	Netz- und Systemregeln der deutschen Übertragungsnetzbetreiber	VDN, 2003	Transmission Code
	VDN Richtlinie	EEG Erzeugungsanlagen am Hoch- und Höchstspannungsnetz	VDN, 2004	Connection of renewable energy auto-production to the high-voltage level
Greece	Transmission Code, 30/5/2001	Transmission System Operation Code	HTSO	Transmission Code
Ireland	Grid Code	Grid Code, Version 1.1	ESB National Grid, 2002	Transmission Code
	WFPS1	Wind farm power station grid code provisions	ESB National Grid, 2004	Wind connected to transmission level
Italy	CEI 11-32	Impianti di produzione di energia elettrica connessi a sistemi di III categoria	Comitato Elettrotecnico Italiano	Connection of generators to HV (transmission level)
Netherlands	Grid Code	Netcode	DTE 2005	Grid code for transmission & distribution
Norway	guideline for wind farms >10MW (in preparation assisted by SINTEF)	guideline for wind farms >10MW (available on www. statnett.no from fall 2005	Stattnet	Connection of wind turbines
Poland		Instruction of Transmission System Operation and Maintenance		
Portugal		Regulamento do Acesso às Redes e às Interligações.	Entidade Reguladora do Sector Eléctrico (ERSE), 2001	Grid code for access to transmission & distribution
Spain	P.O. 12.1 P.O. 12.2	P.O. 12.1 Solicitudes de acceso para la conexión de nuevas instalaciones a la red de transporte P.O. 12.2 Instalaciones conectadas a la red de transporte: requisitos mínimos de diseño, equipamiento, funcionamiento y seguridad y puesta en servicio	MITYC	Grid code for transmission
Sweden	SvK	Affärsverket Svenska Kraftnäts föreskrifter om driftsäkkerhetsteknisk utformning av produktionsanläggningar	Svenska Kraftnät 2002	Decentralized generation connected to transmission level
UK	Engineering Recommendation G75/1	Recommendations for the connection of embedded generating plant to Public distribution systems above 20kV or with outputs over 5MW	Electricity Networks Association 2002	Embedded generation (large systems)

Figure 2.2: *National grid codes for connection to the trasmission level [29].*

Country	Document	Title	Organisation	Scope
Austria	TOR	Technische und organisatorische Regeln für Betreiber und Benutzer von Netzen	E-Control 2004	Grid code for transmission & distribution
Belgium	Lastenboek C10/11	Technische aansluitingsvoorschriften voor gedecentraliseerde productie-installaties die in parallel werken met het distributienet	BFE 2004	Decentralized Generation connected to distribution level
Denmark	TF 3.2.6	Wind turbines connected to grids with voltages below 100 kV	Energined 2004 (Eltra & Elkraft)	Wind connected to distribution level
Finland	-	No specific grid code available	-	-
France		Le référentiel technique	EDF Reseau Distribution	Distribution Code
	Arrêté du 17 mars 2003	Arrêté du 17 mars 2003 relatif aux prescriptions techniques de conception et de fonctionnement pour le raccordement à un réseau public de distribution d'une installation de production d'énergie électrique	Journal officiel de la République Française	Grid connection of production units to distribution level
Germany	Distribution Code 2003	Regeln für den Zugang zu Verteilungsnetzen	VDN 2003	Code for connection to distribution level
	Technische Richtlinie	Parallelbetrieb von Eigenerzeugungsanlagen mit dem Mittelspannungsnetz des EVU	VDEW 1999	Connection of distributed generation to the medium voltage level
Greece	Distribution Directive 129	Interconnection of power stations to the distribution grid	PPC	Connection of distributed generation to the low and medium voltage level
Italy	CEI 11-20	Impianti di produzione di energia elettrica e gruppi di continuità collegati a reti di I e II categoria	Comitato Elettrotecnico Italiano	Connection of generators to LV and MV (distribution level)
Netherlands	Grid Code	Netcode	DTE 2005	Grid code for transmission & distribution
Norway	TR A5329 / EBL-K 17-2001	Retningslinjer for nettilkobling av vindkraftverk	J.O. Tande, Sintef 2001	Connection of wind turbines
Poland		Instruction of Transmission System Operation and Maintenance		
Portugal		Regulamento do Acesso às Redes e às Interligações	Entidade Reguladora do Sector Eléctrico (ERSE), 2001	Grid code for access to transmission & distribution
Spain	RD 436/2004 OM 5/9/1985	Real Decreto 436/2004, de 12 de marzo, por el que se establece la metodología para la actualización y sistematización del régimen jurídico y económico de la actividad de producción de energía eléctrica en régimen especial	MITYC	Grid code for distribution
Sweden	AMP	Anslutning av mindre produktionsanläggningar till elnätet	Svensk Energi 2001	Code for connection to distribution level
UK	Engineering Recommendation G59/1	Recommendations for the connection of embedded generating plant to the Public Electricity Suppliers distribution systems	Electricity Networks Association 1991	Embedded (distributed) generation, small systems
	Engineering Recommendation G75/1	Recommendations for t he connection of embedded generating plant to Public distribution systems above 20kV or with outputs over 5MW	Electricity Networks Association 2002	Embedded generation (large systems)

Figure 2.3: *National grid codes for connection to the distribution level [29].*

The required fault ride-through capability is represented by the voltage profiles in Fig.2.5; in those cases, WTs are supposted to remain connected. The high voltage limit HVL and the low

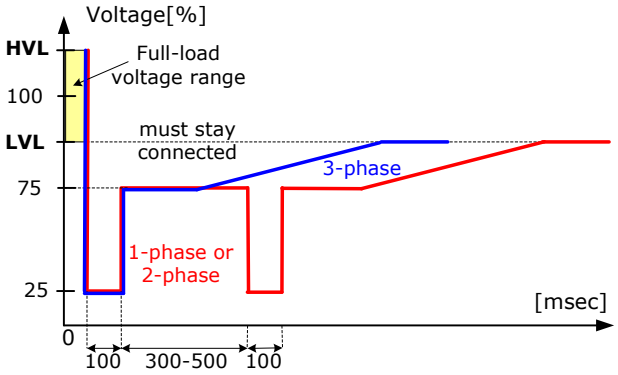

Figure 2.5: *Fault ride-through capability of wind turbines connected to the Danish distribution system [20][34].*

voltage limit LVL in the Danish distribution networks are defined in Tab. 2.1.

Nominal voltage [kV]	Low voltage limit LVL [kV]	High voltage limit HVL [kV]
0.4	0.380	0.440
10	10	11
15	14.5	16.5
20	20	22
30	28.5	33
50	47.5	55
60	57	66

Table 2.1: *Voltage levels in the Danish distribution networks [20].*

A wind turbine shall have sufficient capacity to fulfil the above mentioned requirements when two faults (two-phase or three-phase SCs) occur in two minutes interval [34]. There shall also be sufficient energy reserve (emergency, hydraulic and pneumatic) to cope with at least six faults (two-phase or three-phase SCs) with five minutes interval [34].

Transmission level

The fault ride-through requirements for wind farms connected to grids with voltages above 100 kV are specified in [35]. According to [35], WTs shall remain connected to the grid in the following situations:

- three-phase short-circuit up to $100ms$;
- two-phase short-circuit with/without ground for up to $100ms$ followed after $300-500ms$ by a new SC of maximum $100ms$ duration;
- single-phase short-circuit for up to $100ms$ followed after $300-500ms$ by a new SC of maximum $100ms$ duration.

A wind turbine shall have sufficient capacity to fulfil the above mentioned requirements when two faults occur in two minutes interval [35]. There shall also be sufficient energy reserve (emergency, hydraulic and pneumatic) to cope with at least six faults with five minutes interval [35].

In order to verify basic stability properties of all WT types included in the wind farm, it is required that the design of a wind turbine shall be verified by means of a turbine test carried out by simulation of the wind farm stability by applying a symmetric three-phase short circuit fault to the power grid [35]. Additionally, the impact on the wind farm of asymmetrical faults, with unsuccessful automatic reclosure, must be documented. In this case the wind turbine shall not be disconnected from the grid.

The wind farm owner must provide to the TSO a report detailing the simulation model and results of the test which is done with the voltage profile with a slowly recovering time shown in Fig.2.6.

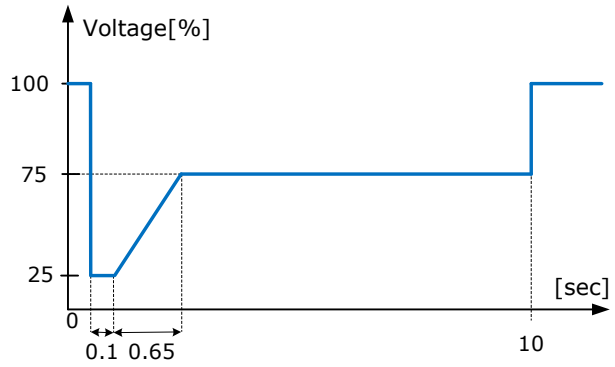

Figure 2.6: *Voltage profile for simulation of symmetric three-phase faults [35].*

The power system shall be modelled by the Thevenin equivalent as shown in Fig.2.7.

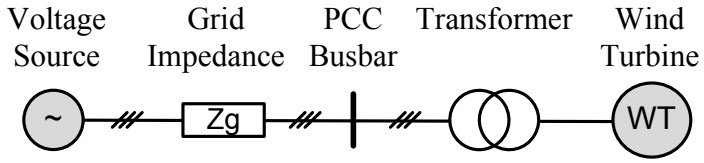

Figure 2.7: *Thevenin equivalent model of the power system for symmetrical fault analysis [20][35].*

The voltage source shall simulate the voltage profile given in Fig.2.6 with a correction factor such that the pre-fault PCC voltage is $1pu$. The power grid shall have a short-circuit power S_k at the PCC ten times the wind farm rated power, $S_k = 10S_{WF,n}$, and the ratio $R_g/X_g = 0.1$, corresponding to a phase angle of 84.3°. Initial conditions for simulaions are rated wind speed, rated rotor speed and zero reactive power at the PCC. In the report the simulation tool used for the stability analysis shall be specified; the simulation model shall be described to a level of detail that makes possible to repeat the calculation in the analysis tool.

The wind farm meets the interconnection requirements when [35]:

- the output power reaches the rated value no later than $10s$ after the PCC voltage is above $0.9pu$.

- the active power at the PCC during the voltage dip meets the following condition:

$$P_{actual} \geq k_p P_{t=0} (\frac{V_{actual}}{V_{t=0}})^2 \tag{2.1}$$

where P_{actual} and V_{actual} are active power and PCC voltage during the simulated fault, $P_{t=0}$ and $V_{t=0}$ are pre-fault power and voltage, $k_p = 0.4$ is a reduction factor considering any voltage dips at the generator terminals.

- the reactive power exchange at the PCC shall be in the normal limits (see Fig.2.8) no later than $10s$ after the voltage is above $0.9pu$; during the voltage dip the reactive current shall not exceed the rated value.

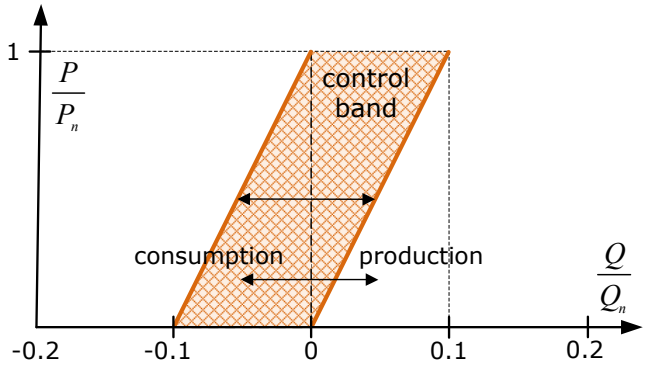

Figure 2.8: *Reactive power control range for normal operation of a wind turbine [35].*

- during the voltage dip the reactive power control must change from normal operation to maximum voltage support such that the normal pre-fault grid voltage is re-established as soon as possible; this control must also be able to avoid overshoots.

Beside the symmetrical short-circuit analysis, the results of asymmetrical faults with unsuccessful reclosure is requied [35]. The wind farm must withstand the impacts from the asymmetric faults in the grid without requiring the disconnection of any wind turbine of the wind farm. The following two asymmetrical faults are considered:

- two-phase SC with unsuccessful reclosure (see Fig.2.9a);
- single-phase SC with unsuccessful reclosure (see Fig.2.9b).

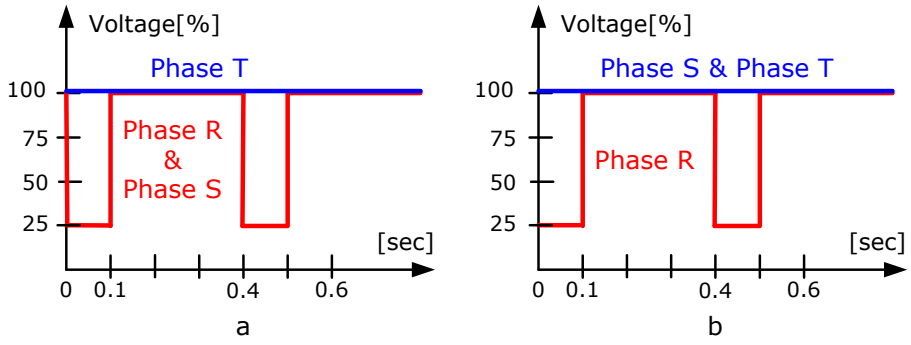

Figure 2.9: *Voltage profiles for asymmetrical faults. a) two-phase SC with unsuccessful reclosure; b) single-phase SC with unsuccessful reclosure. Based on [35].*

When the PCC is on the secondary side of the transformer, its vector group and phase shift must be considered in the fault analysis. Unless otherwise agreed, it shall be assumed that the transformer is YNd11-connected.

Besides, the owner of the wind farm connected to the transmission level shall guarantee that [35]:

- the WT can withstand the thermal impact in case of repetiton of the above symmetrical fault after two minutes;
- the WT can withstand the thermal impact in case of repetiton of the above asymmetrical faults after two minutes;
- the WT has sufficient energy reserve (emergency, hydraulic and pneumatic) to withstand the thermal impact of the symmetrical fault for at least six symmetrical faults with five minutes interval;

2.4.2 Germany

Different requirements for WTs connected to the distribution level ($< 60kV$) and the transmission level ($\geq 66kV$) are specified [18][36]. However, requirements for fault ride-through are only specified at the transmission level; therefore German GCs for the distribution level are not treated here.

Transmission level

The general grid connection requirements in Germany for distributed generation connected at the trasmission level are given by E.On in [18]; they apply to wind farms connected to high voltage (i.e. $60kV$ and $100k$V) and extra-high voltage (i.e. $220kV$ and $380k$V). It is required that, in the event of grid fault outside the protection range of the generating plant (i.e. over/under frequency and over/under voltage protections), there must be no disconnection from the grid [18][30]. Moreover, the generating unit shall inject short-circuit current into the grid during the fault period in a way agreed with the TSO. It is recommended to use the over/under frequency and the over/under voltage protections at the PCC for each generating unit; this is normally referred as automatic system. After the disconnection due to the automatic system, the grid synchronization must be performed as soon as the PCC voltage is above $105kV$ in $110kV$ grid, $210kV$ in $220kV$ grid and $370kV$ in $380kV$ grid. After reconnection, the active power shall increase with a maximum rate of 10% of the rated power per minute.

The limit voltage profiles for grid-connected generating plants in case of three-phase fault or faut-related voltage dips are shown in Fig.2.10.

As shown in Fig.2.10, if the PCC voltage is above the limit line 1 (i.e. the red line), wind turbines within the wind farm must remain connected. Below the limit line 2 (i.e. the blue line), wind turbines may disconnect; however, if the voltage is below low voltage limit LVL, equal to 95% of the rated voltage longer that $1.5s$, the WT must be disconnect by the automatic system. Within the limit lines 1 and 2, the following applies [18][20]:

- all generating plants shall remain connected to the grid during the fault; if, due to constraints of the plant concept, a generating plant cannot fulfil this requirement, it is permitted with agreement with E.On to shift the limit line while, at the same time, reducing the resynchronisation time and ensuring a minimum reactive power injection during the fault;

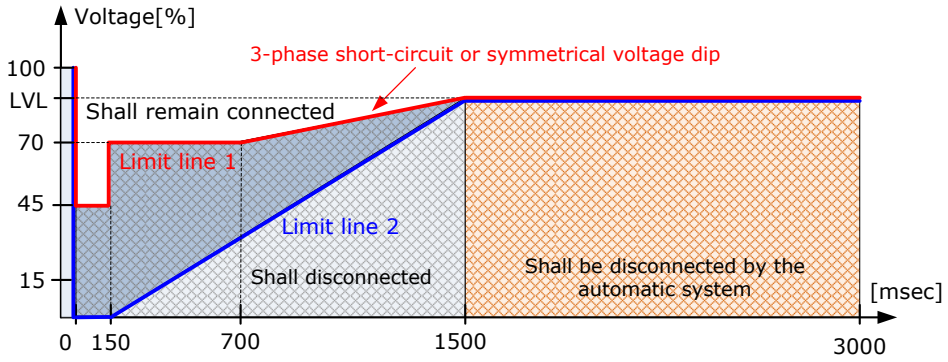

Figure 2.10: *Voltage limits for disconnection of generating units in the case of grid faults [18].*

- if, when experiencing the fault, the individual generators becomes unstable or the generator protection responds, a brief disconnection of the generating plant from the grid is allowed by agreement with E.On; after the disconnection, the grid synchronisation shall take place within $2s$. The active power infeed must be increased to the original value with a gradient of at least 10% of the rated generator power per second.

In the following cases, the generating plant shall disconnect in case of grid fault [18][20]:

- if the PCC voltage goes and stay below 85% of the rated voltage and with a leading operation, the generating unit shall disconnect after $0.5s$.;
- if the voltage on the low voltage side of each individual generator transformer goes below 80% of the lower value of the voltage band (i.e. 95%), generators shall disconnected in the following way: one quarter of the generators after $1.5s$, after $1.8s$, after $2.1s$ and after $2.4s$ respectively;
- if the voltage on the low voltage side of each individual generator transformer goes and stay above 120% of the upper value of the voltage band (i.e. 105%), the affected generator shall disconnect with a time delay of 100 msec.

During a voltage dip, all generating plants shall support the grid voltage with additional reactive current. The reactive current injection shall be performed within $20ms$ after a voltage dip on the WT voltage (i.e. LV-side of the WT transformer) above 10% has occured; it shall act as shown in Fig.2.11. The generator unit shall provide a reactive current on the low voltage side of the transformer equal to at least 2% of the rated current per each percent of the voltage dip. If necessary, the generating unit shall be able to provide full rated reactive current. Within the dead-band, there are no specifications for the injected reactive current; this means that the manufacturer can inject some reactive power depending on the control strategy. However, according to [18], in normal operation all generating plants shall work with power factor within 0.95 (inductive) to 1, unless differently agreed with E.On. The blue line in Fig.2.11 represents a minimum requirement for the reactive current injection; in fact a higher reactive current can be injected, being on the safe side. After the voltage returns within the dead-band, the voltage support shall be maintained for further $500ms$. For extra-high voltage grids, the above voltage control may be required in normal operation as continuous control.

Throughout this work, the German grid code is considered as reference; therefore when evaluating the current contribution from wind turbines to the grid, it is assumed that WTs comply with

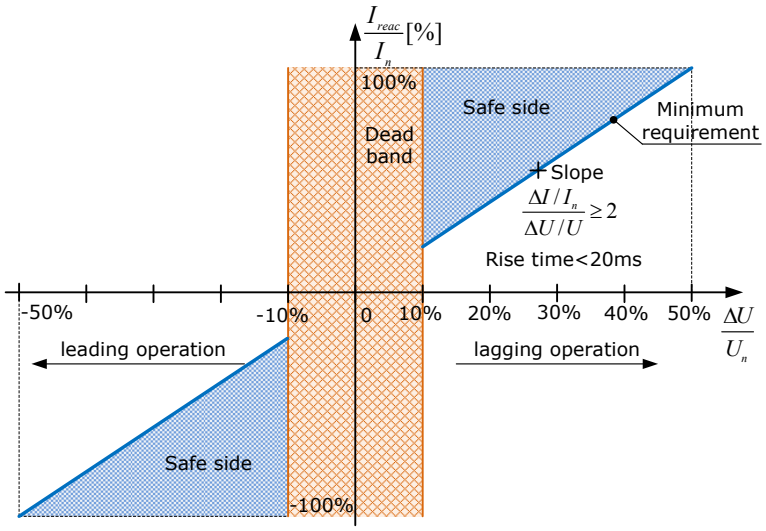

Figure 2.11: *Voltage support requirement from E.On Netz during voltage dips [18].*

it and, thus, perform the grid voltage support as specified in Fig.2.11. It is worthy to note that WTs are considered at least complying to the minimum requirement specified in Fig.2.11.

2.4.3 Spain

Minimal interconnection requirements for wind turbines connected to the Spanish transmission system have been issued by REE Spain [37] and it was published officially in October 2006. This document is only addressed to fault ride-through capabilities and grid voltage support (i.e. reactive power/voltage control) during faults; it applies to all operators connected to the main transmission grid. According to [38], requirements presented by REE are also valid for wind farms connected at the distribution level.

As minimum requirement, WTs shall remain connected during faults with the WT voltage profile shown in Fig.2.12.

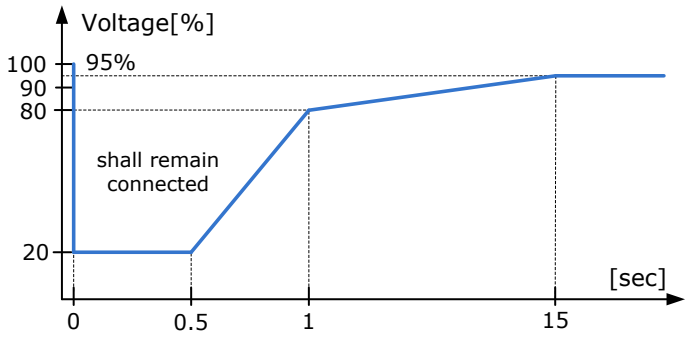

Figure 2.12: *Fault ride-through requirement for wind turbines in the Spanish transmission grid [37][20].*

After a voltage dip, wind power systems are required to stop drawing the reactive power within $100ms$ and to inject reactive power within $150ms$ according to Fig.2.13.

In Fig.2.13 it can be seen that the grid voltage support by means of reactive current injection is required for a WT voltage below 85% (i.e. voltage dip above 15%); below 50% of the rated WT

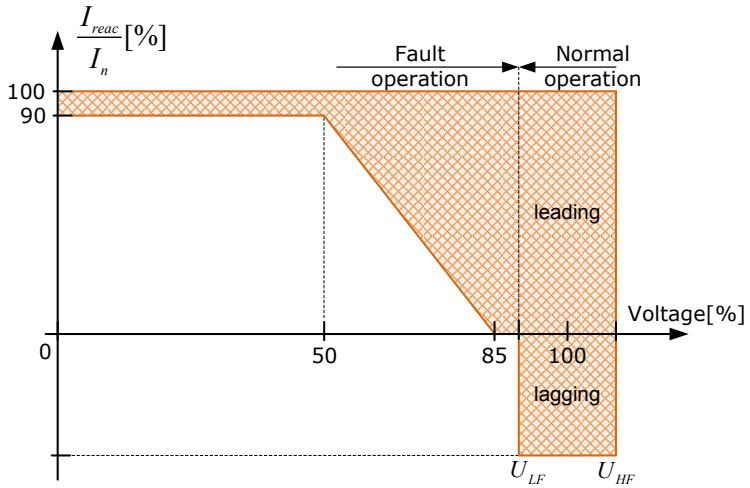

Figure 2.13: *Grid voltage support/reactive current injection requirement during voltage dips according to Spanish grid codes [37][20].*

voltage, a reactive current injection within $90\% - 100\%$ of the rated current is required.

2.5 Brief comparison of FRT requirements in national grid codes

This section is intended to provide a short comparison between fault ride-through requirements from several national grid codes. A deep comparison is presented in [20] and [31]. As a summary, requirements for FRT capability are compared based on the PCC voltage profile that wind turbines shall withstand without disconnecting from the grid in case of fault; considered countries are Denmark, Ireland, Germany, Great Britain, Spain, Italy, USA and Canada. The voltage profiles for fault ride-through capability are summarized in Fig.2.14. In some country different profiles are

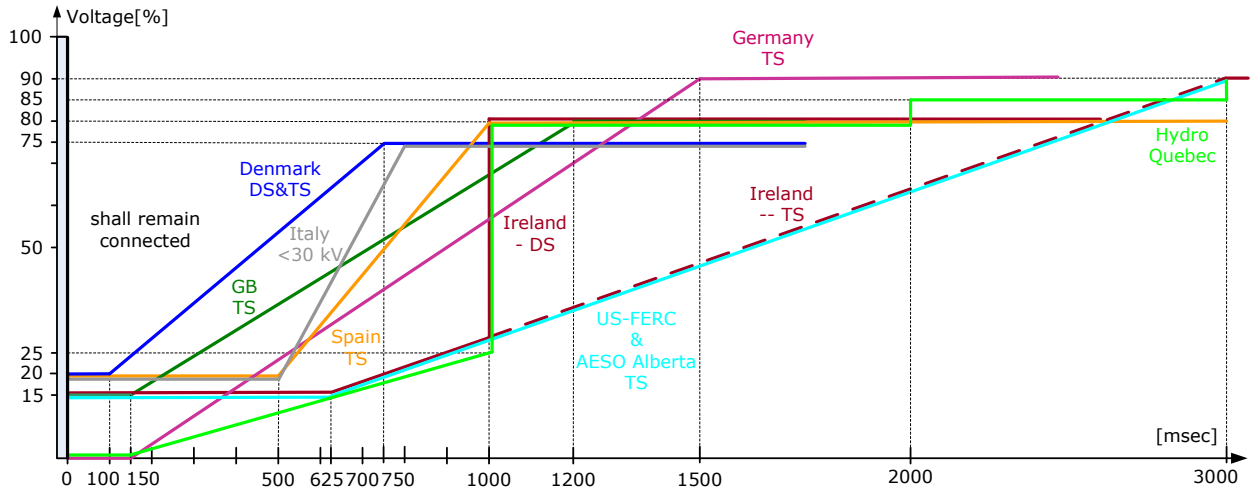

Figure 2.14: *Summary regarding fault ride-through requirements in national grid codes [20][31].*

specified for WTs connected to the transmission system (TS) and others connected to the distri-

bution system (DS). It can be seen that Denmark has the lowest short-circuit time duration with only $100ms$; however it requires that the wind turbines shall remain connected to the grid during excessive faults. From the poin of view of the fault duration, Ireland has the most demanding grid code as it requires wind turbines to withstand PCC voltage below $0.9pu$ for $3s$. The German grid code requires WTs to remain connected during voltage dips down to $0pu$ for a duration of $150ms$.

Among all considered national grid codes in Fig.2.14, only the German and Spanish GCs require the grid support during a grid fault by means of well-specified reactive current injection [18][37]. Their requirements are different as the required reactive current injection depending on the WT generator voltage are not the same; in both cases up to 100% reactive current injection is required in case of voltage dip at the WT generator voltage below $0.5pu$. Furthermore, both grid codes specify a minimum requirement for the grid voltage support; however WT manufacturers are free to inject more reactive current than required during a grid fault, leading to the operation on the safe side.

2.6 Summary

In this chapter the relationship between requirements for fault ride-through capability and short-circuit current contribution for wind turbines is presented. It can be concluded that requirements for FRT play an important role in this project work as the study of the short-circuit current contributions from WTs to the grid makes sense only if wind turbines are required to remain connected and support the grid voltage in case of grid fault.

Requirements for fault ride-through capability included in some national grid codes have been presented. The Danish grid code is important because it provides a detailed description of the simulation model, including the power grid model, to verify basic stability properties of wind farms. The German and Spanish grid codes are important as they are the only one requiring the grid voltage support by means of reactive current injection during a grid fault. Moreover they specify minimum requirements for the grid voltage support; however WT manufacturers are free to support the grid more than required, being on the safe side.

The German grid code is chosen as the reference of the grid voltage support requirement for this project work because of well-specified requirements to the reactive current demand.

Chapter 3

Short-circuit calculation

Contents

3.1 Introduction

A short-circuit is an undesired operation of a electricity network. It is caused by an abnormal connection by means of a fault impedance between two or more points at different voltage potentials in normal operaton. It causes unacceptable overloading of equipment (transformers, transmission lines, cables, generators, etc) that can even lead to damage of some components.

Planning, design and operation of electrical power systems require several studies to evaluate and assess performances, reliability and safety of the system; examples of these studies are: load flow, short-circuit, motor starting, stability, protective device coordination, reliability analysis [15][39]. Short-circuit studies are frequently performed by power system companies as those studies provide the maximum SC current used for the design of electrical components (i.e. cable, transformer, circuit breakers) and the minimum SC current for proper relays setting and coordination. In this way power systems can be correctly dimensioned and protected, allowing safe and economic operation. Some unpleasant consequences of wrong power system dimensioning and protection are [40]:

- impairment of safety and reliability of the power supply;
- interruption of the power supply;
- damage of electrical equipment;
- mechanical and thermal stresses of equipment;
- overvoltages.

An essential issue concerning short-circuit studies is the required calculation accuracy. The level of detail is chosen depending on the purpose that can either be (*i*) network planning and (*ii*) fault operation analysis [39][41]. At the stage of network planning, the interest is focused on the expected maximum currents, for the rating of the components, and the minimum currents, for relay setting and coordination. In this case SC calculations are performed by using methods that require less detailed network modelling and apply extreme-case estimations. Examples for these methods are the IEC/VDE and IEEE/ANSI calculation methods [13][14][42]. A different application of the SC calculation is the precise evaluation of the fault current in a specific situation (i.e. fault operation analysis).

Typical applications in system planning are [41]:

- ensuring that the defined short-circuit capacity of equipment is not exceeded with system expansion and system strengthening;
- co-ordination of protective equipment (fuses, over-current and distance relays);
- dimensioning of earth grounding systems;
- verification of sufficient fault level capacities at load points;
- verification of admissible thermal limits of cables and transmission lines.

Typical applications in system operations are [41]:

- ensuring that short-circuit limits are not exceeded when changing the system configuration;
- determining protective relay settings;
- analysis of system faults (e.g. mal-operation of protection equipment);
- analysis of possible mutual interference of parallel lines during system faults.

For system planning studies the system operating conditions are not known, and therefore estimates are necessary. For this purpose the method of the equivalent voltage source at the fault location has generally become accepted in Western Europe according to IEC 909 (VDE 0102). A revised version of this was published as IEC 60909 in July 2001. This method does not required the load-flow of the system. It is based on the nominal and/or calculated operating conditions and uses correction factors for voltages and impedances, to push the results towards the safe side.

For short-circuit calculations at a specific operating condition, the exact network information is well known. If the accuracy of the calculation according to IEC 60909 is not sufficient, or to verify the results of this method, the superposition method can be used. It calculates the expected short-circuit currents in the network on the basis of the existing network operating condition. If the system models are correct, it is more accurate than the method presented in IEC 60909. However the most unfavourable conditions with respect to the sizing of plant have to be chosen which may required extensive studies.

Nowadays short-circuit studies are also performed for enabling the connection of large amount of distributed generation to the distribution network (e.g. wind farms) [17]. Distributed generation resources are typically connected to distribution networks, at the low or medium voltage level, and contribute to the total fault level of the network. In case of SC in the distribution network, the fault current is determined by the combined contributions of the upstream grid and the various DG sources. Hence, a basic requirement for allowing the grid-connection of DGs is to ensure that

the resulting fault level remains below the network design value, under the most unfavourable conditions.

In this chapter the time behavior of the SC current is analysed to identify characteristic values. Then, types of short-circuit faults that can occur in a power system are classified. Common methods for SC current calculation are presented; standards concerning SC studies are analysed to identify similarities and differences in the methodology and approximations. Finally, the short-circuit calculation implemented in the chosen power system simulation tool is deeply described. This chapter ends with the selection of the mehod that will be used to perform SC current calculations to evaluate the current contribution from VSC-based wid turbines to the grid.

3.2 Time behavior of the short circuit current

The time behavior of the short-circuit current depends on the fault location and therefore faults are distinguished in far-from-generator and near-to-generator [14][40]. The time behavior of the SC current in both cases is shown in Fig.s 3.1 and 3.2.

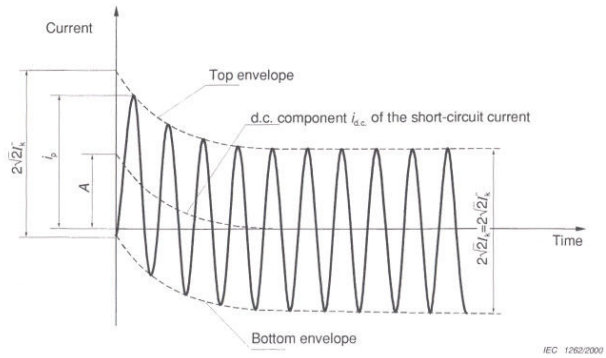

Figure 3.1: *Time behavior of the short-circuit current far-from-generator [14][40].*

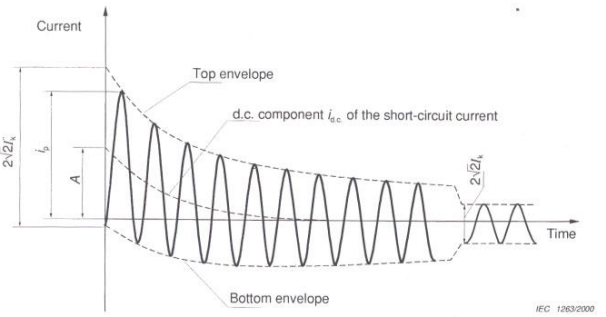

Figure 3.2: *Time behavior of the short-circuit current near-to-generator [14][40].*

where I_k'' is the initial symmetrical SC current, i_p is the peak SC current, i_{dc} is the decaying d.c. aperiodic component and A is the initial value of the d.c. aperiodic component. Fig.3.1a refers to a short-circuit far-from generating units and is characterized by a constant value of the symmetric a.c. periodic component. Fig.3.2b refers to a SC near a generating unit and is characterized by a variable value of the symmetric a.c. periodic component. Fig.s 3.1 and 3.2 refer to the short-circuit current at the fault location; it is distinguished from the *transferred SC currents* in the network branches [14].

3.3 Classification of grid faults

A short-circuit represents a structural network change equivalent with that caused by the addtion of an impedance at the fault location. If the fault impedance Z_f is zero, the fault is called *bolded* or *solid fault.*

The most important types of short-circuit fault in a three-phase network are schematically represented in Fig.3.3 [12][14][25][40][43]; their deep description is beyond the purpose of this project.

Fault	Circuit diagram of the fault point	Boundary conditions	Description
Three-phase SC	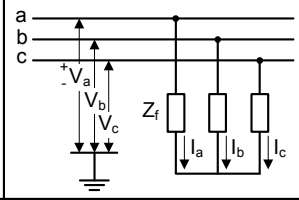	$I_a+I_b+I_c=0$ $V_a=Z_f\ I_a$ $V_b=Z_f\ I_b$ $V_c=Z_f\ I_c$	• Connection of all conductors with or without simultaneous contact to ground • Symmetrical loading of the three external conductors • Calculation on a single-phase basis
Line-to-line SC	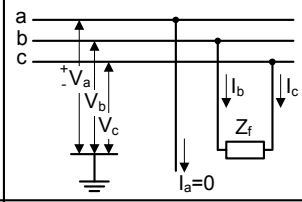	$I_a=0$ $I_b=-I_c$ $V_b-V_c=Z_f\ I_b$	• Unsymmetrical loading • All voltage non-zero • SC current high than in a three-phase SC near-to-to generator
Double line-to-ground SC	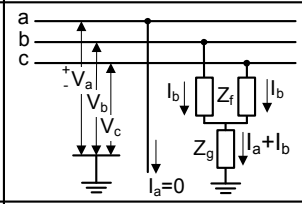	$I_a=0$ $V_b=(Z_f+Z_g)I_b+Z_g\ I_c$ $V_c=(Z_f+Z_g)I_c+Z_gI_b$	• The leakage current flowing to ground is a capacitive ground fault current
Single line-to-ground SC	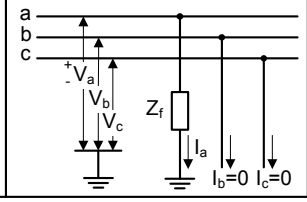	$I_b=I_c=0$ $V_a=Z_f\ I_a$	• Very frequent occurrence in low voltage networks

Figure 3.3: *Short-circuits in a three-phase network.*

The three-phase fault is defined as the simultaneous short-circuit across all three phases; since conductors are loaded symmetrically, it is a balanced fault and can be solved on a per phase basis; the other two phases carry the same current except for the phase shift. The line-to-ground SC, the line-to-line SC and the double line-to-ground SC are unsymmetrical faults as phases are loaded in different ways due to the fault.

3.4 Short-circuit analysis methods

Short-circuit studies in three-phase systems can be performed by using four calculation procedures:

- nodal method, based on the bus impedance matrix [12];
- symmetrical component method [12][14][43];
- superposition method for a defined load flow [40][41];
- dynamic time-based simulations.

The method selected for the SC study depends on the application and on the required accuracy. Table 3.1 shows the classification of SC calculation methods depending on the application.

Planning conditions	Operating conditions - on-line SC calculation
Approximative methods based on simplified network model (IEC, ANSI)	Detailed method based on a detailed network model
1) Nodel method 2) Symmetrical component method	1) Superposition method 2) Dynamic time-based simulations

Table 3.1: *Methods for short-circuit studies depending on the application*

Several methods for the short-circuit analysis are presented in the literature depending on the type of fault and the required accuracy. They are brifely introduced in this section; however the details about the application of the presented methods is beyond the purpose of this project work.

3.4.1 Short circuit calculation based on the nodal method

The anaysis in case of balanced three-phase short-circuit fault can be conveniently solved on a per-phase basis by assuming symmetrical network structure (i.e. transposed overhead lines); the Thevenin's method can be used [12]. When this procedure, based on the network reduction, is not efficient or applicable for large network, the method based on the bus impedance matrix can be used. It is a more general fault circuit analysis based on the nodal method where, by definig elements of the bus impedance matrix, fault currents and bus voltages can be easly calculated [12][32].

3.4.2 Symmetrical component method

Various methods for the solution of unbalanced faults are presented in the literature. However the *method of symmetrical components* is the most used as it simplifies the solution of unbalanced circuits by transforming them into a number of balanced circuits. Therefore it leads to the treatment of the problem to a per-phase basis. This method assumes a symmetrical network structure (i.e. transposed overhead lines); however it provides acceptable accuracy in case of untransposed overhead lines.

Using the symmetrical component method introduced by Dr. C. L. Fortescue in 1918, the currents in each line conductor are found by superposing the currents of three symmetrical components systems [12][14][40]:

- positive-sequence current I_1;
- negative-sequence current I_2;
- zero-sequence current I_0.

Taking a line conductor as reference, phase currents can be calculated from their symmetrical components as follows:

$$\begin{bmatrix} I_a \\ I_b \\ I_c \end{bmatrix} = \begin{bmatrix} 1 & 1 & 1 \\ 1 & \underline{a}^2 & \underline{a} \\ 1 & \underline{a} & \underline{a}^2 \end{bmatrix} \begin{bmatrix} I_0 \\ I_1 \\ I_2 \end{bmatrix} \tag{3.1}$$

where $\underline{a} = -\frac{1}{2} + j\frac{\sqrt{3}}{2}$ and $\underline{a}^2 = -\frac{1}{2} - j\frac{\sqrt{3}}{2}$. Eq.3.1 can be rewritten using the matrix notation as follows:

$$\mathbf{I}_{abc} = \mathbf{A}\mathbf{I}_{012} \tag{3.2}$$

where **A** is the symmetrical component tranformation matrix (SCTM) which transforms the phasor current $\mathbf{I}_{abc}$ into component currents $\mathbf{I}_{012}$ and is:

$$A = \begin{bmatrix} 1 & 1 & 1 \\ 1 & \underline{\alpha}^2 & \underline{\alpha} \\ 1 & \underline{\alpha} & \underline{\alpha}^2 \end{bmatrix} \tag{3.3}$$

Solving Eq.3.1 for symmetrical component currents, it yields:

$$\mathbf{I}_{012} = \mathbf{A}^{-1}\mathbf{I}_{abc} \tag{3.4}$$

The inverse of **A** is given by:

$$\mathbf{A}^{-1} = \frac{1}{3}\begin{bmatrix} 1 & 1 & 1 \\ 1 & \underline{a} & \underline{a}^2 \\ 1 & \underline{a}^2 & \underline{a} \end{bmatrix} \tag{3.5}$$

Substituting Eq.3.5 into Eq.3.4:

$$\begin{bmatrix} I_0 \\ I_1 \\ I_2 \end{bmatrix} = \begin{bmatrix} 1 & 1 & 1 \\ 1 & \underline{a} & \underline{a}^2 \\ 1 & \underline{a}^2 & \underline{a} \end{bmatrix} \begin{bmatrix} I_a \\ I_b \\ I_c \end{bmatrix} \tag{3.6}$$

For the calculation of the initial symmetrical short-circuit current I_k'' and the symmetrical short-circuit current I_k at the fault location, the positive, negative and zero-sequence equivalent circuits may be converted by network reduction into an equivalent SC impedances $\underline{Z}_{k0}$, $\underline{Z}_{k1}$ and $\underline{Z}_{k2}$ at the short-circuit location. In the sequence equivalent circuits each component of the network is represented by its model at the specific sequence as widely explained in references [12][14][25][43].

Once the positive, negative and zero-sequence equivalent circuits are reduced to equivalent SC impedances at the short-circuit location, symmetrical current component I_0, I_1 and I_2 can be calculated by considering constrains imposed by the faults (i.e. interconnection between positive, negative and zero sequence equivalent circuits which are independent in normal condition with the assumption of balanced network structure).

The symmetrical component method provides the equations for the steady-state symmetrical short-circuit current for different faults; these equations can be easily compared to assess upon which fault conditions the maximum and minimum SC currents are obtained. When using the symmetrical component method, the pre-fault currents are neglected.

3.4.3 Superposition method

The superposition method, also known as complete method, is an exact method for the calculation of the steady-state short circuit currents. It consists of the superposition of two steady-state operating conditions; it requires the following three steps [40][41].

In the first step pre-fault currents and voltages are calculated. The calculation consists of the load flow solution for the specified network configuration and operating conditions (e.g. excitation conditions of the generators, tap positions of regulated transformers and breaker/switching status reflecting the operational scheme).

In the second step the pre-fault voltage at the fault location with negative sign is applied to the passive network (i.e. this is the only voltage source while internal voltage source of generators are short-circuited). In this condition steady-state currents and voltages are calculated using the load flow calculation.

In the third step both conditions are superposed (complex adding) leading to a zero voltage at the fault location. As the complete method is a superposition of two special load flow solutions, the data necessary for the model network elements are exactly the same as for the load flow calculation. This method is accurate as long as pre-fault conditions are correct. Moreover, operating conditions (i.e. active and reactive power, bus voltages and tap settings for transformers) are often difficult to determine. Fig.3.4 illustrates the procedure of the superposition method.

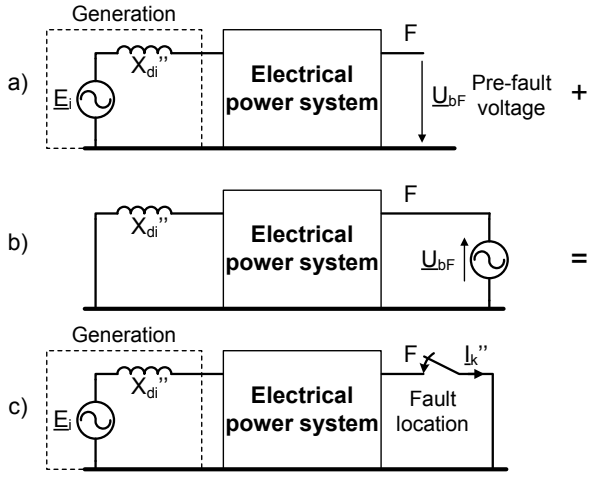

Figure 3.4: *Principle of the superposition method. a) Pre-fault operating condition; b) Operation with applied negative pre-fault voltage at the SC location; c) SC condition obtained by superposing a and b*

3.4.4 Dynamic time-based simulations

Short-circuit studies can be performed using time-step based simulation tools that include a detailed model of the entire network representing the dynamic behaviour of system components [44][45]. The model comprises a system of differential equations which are solved using iterative methods. The significant data manipulation requirement inherent with such method can make it slow and inefficient for large transmission systems [45]. The adoption of dynamic simulation is relatively recent and is related to the availability of powerful computers capable of handling large amount of data [39]. Due to the high level of detail of the network model, dynamic simulations are not the best solution for short-circuit calculation at the planning stage. However this is the only available method to evaluate the dynamic behaviour of the power system during a fault condition (i.e. none of the above mentioned methods provides information about the dynamic behaviour).

3.5 Standards for short-circuit calculations and standard methods

The development of computer hardware and software could have forced power system engineers to adopt dynamic simulation for short-circuit studies and overcome simplified procedures offered by standards. However, there is still a great interest in short-circuit current calculation according to international standards as much simpler models for network components are required. Moreover the computational demand of dynamic simulations is still too big for commercial computers, meaning that they still require an unacceptable computational time. The interest in short-circuit calculations at steady-state conditions is confirmed by the presence of many commercial power system simulation tools equipped with specific modules for SC calculation according to international standards.

The aim of the section is to introduce procedures for short-circuit studies based on standards, to highlight the specific fields of application and the limits. For SC calculation at steady-state conditions, the five important standards are:

- *IEC 60909-2001* - Short-circuit currents in three-phase a.c. systems. Part 0: Calculation of currents;
- *VDE 0102:2002-07* - Short-circuit currents in three-phase a.c. systems - Part 0: Calculation of currents (IEC 60909-0:2001); German version EN 60909-0:2001 [13];
- *IEEE 141-1993* - IEEE recommended practice for electric power distribution for industrial plants [42];
- *ANSI C37.010.1999* - IEEE application guide for a.c. high-voltage circuit breakers rated on a symmetrical current basis [46];
- *ANSI C37.5* Methods for determining the rms value of a sinusoidal current wave and normal-frequency recovery voltage, and for simplified calculation of fault currents [47];

The IEC 60909 is a revised version of the IEC 909; it has been published in July 2001. The first edition of the IEC 909 (1988) is a derivative work taken from the German Verband Deutscher Electrotechniker (VDE) VDE 0102 [48]. The IEC 60909 provides a standard procedure for the SC current calculation in low and high voltage networks up to 380kV at 50Hz or 60Hz which is intended to lead with sufficient accuracy to results on the safe side. In Augurst 2001 it has also been recognized as European standard DS/EN 60909 [14].

The ANSI standards, that apply to equipment rating values, include C37.010 for systems with l000V and above and C37.13 for systems below l000V [49][46]. The The IEEE 141-1993 (the IEEE Red Book) provides supplementary guidelines and interpretation of these ANSI standards. The ANSI C37.010-1999 is a revised version of the American ANSI C37.010-1979; it is focused on the sizing of a.c. high-voltage circuit breaker. The design procedure is based on the symmetrical short-circuit current. The ANSI C37.5 is an American standard which provides a simlified short-circuit procedure based on the total rated current. Regarding the SC current calculation, the ANSI C37.010-1999 and the ANSI C37.5 are quite similar as they provide the same calculation procedure; however slightly different curves for the a.c. and d.c. decaying are provided.

Some of the above standards are identical regarding requirements, approximations and methodologies for short-circuit current calculations. Therefore the the following two methods are normally considered:

- the IEC 60909/VDE 0102 method, identified as the *IEC method*;
- the IEEE 141/ANSI C37 method, identified as the *ANSI method*;

The outlines of the above mentioned methods are presented in the following by pointing out the most significant differences in methodologies and assumptions.

3.5.1 The IEC 60909/VDE 0102 (IEC) method

The IEC method is based on the method of the equivalent voltage source at the fault location which is generally accepted in Western Europe. It derives from the superposition method presented is section 3.4.3; it is based on an equivalent voltage source at the faulted bus with the goal of accomplishing a close-to-reality short-circuit calculation without the need of the preceding load-flow calculation and the associated definition of actual operating conditions. With respect to the

superposition method, the IEC method does not required the pre-fault load flow solution and, thus, pre-fault operating conditions. The main simplifications compared with the superposition method are the following [41]:

- nominal conditions are assumed for the whole network, i.e. $U_i = U_{n,i}$;
- load currents are neglected, i.e. $I_{op} = 0$.
- a simplified simulation network is used, i.e. loads are not considered in the positive and negative sequence network.

With the above simplifications, Fig.3.4c can be approximated as Fig.3.4b due to the low impact produced by the pre-fault operating conditions. At steady-state, this is acceptable for the following two reasons [50]:

- currents in normal operation (pre-fault condition) are, in magnitude, much smaller than the corrresponding SC currents;
- power systems are basically inductive especially at high voltage; in normal operation currents lag bus voltages with inductive power factor around 0.9, whereas SC currents lag bus voltages with a much lower power factor (i.e. phase shift close to 90^o).

With the above assumptions, the operating current and the SC current in steady-state condition can be represented by their correspondent phasors as shown is Fig.3.5.

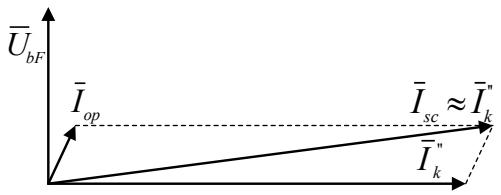

Figure 3.5: *Steady-state operating current and short-circuit current. U_{bF} pre-fault bus voltage, I_{op} pre-fault operating current, I_k'' steady state SC current, I_{sc} total short-circuit current obtained by superposition.*

As it can be seen, the higher is the ratio I_k''/I_{op} the better is the approximation $I_{sc} \approx I_k''$, meaning that operating currents can be neglected. Moreover, the pre-fault operation of the power system is assumed to be the rated one, meaning that the pre-fault bus voltage of the faulty busbar is assumed equal to the rated value U_n. To ensure that the results are estimated on the safe side, a correction factor c is applied to the voltage at the faulted busbar $U_{bF} = cU_n$. If there are no national standards, the correction factor c can be chosen according to table 3.2, considering that the highest voltage does not differ from the rated value by more than +5% in low-voltage systems and +10% in high-voltage systems [40][14]. This factor differs for the calculation of the maximum and the minimum short-circuit current of a network (e.g. c_{max} and c_{min} have to be respectively used) and depends on the voltage tolerance.

In the IEC, there are distinguishes between near-to-generator and far-from-generator (and motor) short-circuits. Near-to-generator, the prospective short-circuit current[1] presents a symmetrical component decaying with time, while far-from generator the symmetrical component is constant.

[1]The prospective short-circuit current is the current that would flow if the SC was replaced by an identical connection of negligible impedance without any change of the supply [14].

Nominal voltage U_n	**Voltage factor c for maximum SC current** c_{max}[1]	**Voltage factor c for minimum SC current** c_{min}
Low voltage $100V$ to $1000V$ IEC 60038, table I	 1.05[3] 1.10[4]	 0.95
Medium voltage $> 1kV$ to $35kV$ and IEC 60038, table III	 1.10	 1.00
High voltage[2] $> 35kV$ (IEC 60038, table IV)	 1.10	 1.00

1) $c_{max}U_n$ should not exceed the highest voltage U_m for equipment of power systems
2) If no nominal voltage is defined $c_{max}U_n = U_m$ or $c_{max}U_{min} = 0.9U_m$ should be applied
3) For low-voltage systems with tolerance of +6%, for example systems renamed from 380V to 400V
4) For low-voltage systems with tolerance of +10%

Table 3.2: *Voltage factor c [14]*

Different approaches are used according to the network configuration (i.e. radial or meshed) and fault location. Appropiate formulas are provided for modelling external network, two or three winding transformers, overhead lines and cables.

The following values of short-circuit current are considered [14][40]:

- initial symmetrical short-circuit current $I_k^{''}$;
- symmetrical short-circuit current I_k;
- peak short-circuit current i_p;
- d.c. component of the short-circuit current $i_{d.c.}$;
- symmetrical short-circuit breaking current I_b;
- thermal equivalent short-circuit current I_{th}.

Above mentioned values are briefly described in the following.

Initial symmetrical short-circuit current $I_k^{''}$

The initial symmetrical short-circuit current $I_k^{''}$ is the r.m.s. of the a.c. symmetrical component of the prospective SC current at the instant of short-circuit. The calculation method determines the SC currents at location F using the equivalent voltage source, $cU_n/\sqrt{3}$, defined as the voltage of an ideal source applied at the short-circuit location in the positive sequence system, whereas all other sources in the system are ignored (i.e. voltage sources are considered as short-circuits whereas current sources are considered as open-circuits). All network feeders, synchronous and asynchronous machines are replaced by their internal impedances[2]. All line capacitances, shunt admittances and non-rotating loads, except those of the zero-sequence system, are neglected. The equivalent voltage source method is illustrated in Fig.3.6.

[2]The contribution of asynchronous motors in low-voltage power system to the SC current $I_k^{''}$ may be neglected if their contribution is not higher than 5% of the initial short-circuit current $I_{kM}^{''}$ calculated without motors [14].

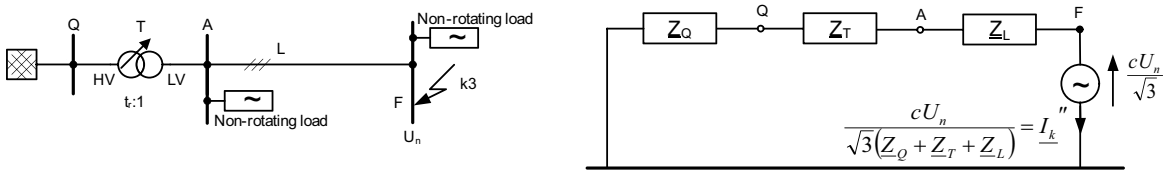

Figure 3.6: *Illustration of the equivalent voltage source method [14].*

In the case of balanced short-circuits, the initial symmetrical SC current is calculated as follows:

$$I_k'' = \frac{cU_n}{\sqrt{3}Z_k} \tag{3.7}$$

where Z_k is the magnitude of an equivalent short-circuit impedance of the upstream grid (essentially its Thevenin impedance) at the short-circuit location F (see Fig.3.6). According to the equivalent voltage source method, it is possible to calculate the short-circuit current at location F only using the nominal voltage and the rated characteristics of the equipment. The results are made sufficiently accurate by using some corrective factors, such as [51]:

- voltage factor according to table 3.2;
- correction factor K_G for the correct calculation of the generator impedance;
- correction factor for power station units.

In networks with different voltage levels, voltages, currents and impedances are converted to the voltage level of the short-circuit location using the rated transformation ratio of the transformers involved.

In distribution networks, with or without DG, the maximum fault level typically occurs at the busbars of the infeeding substation, due to the large contribution of the upstream grid, which is rapidly diminishing downstream the network.

In medium voltage networks,with or without DG, the maximum fault level typically occurs at the busbars of the infeeding substation, due to the large contribution of the upstream grid. In the presence of distributed generation, the resulting total fault level is the vectorial sum of the fault currents due to [17]:

- the upstream grid;
- the various generators (and possibly large motors) connected to the distribution network.

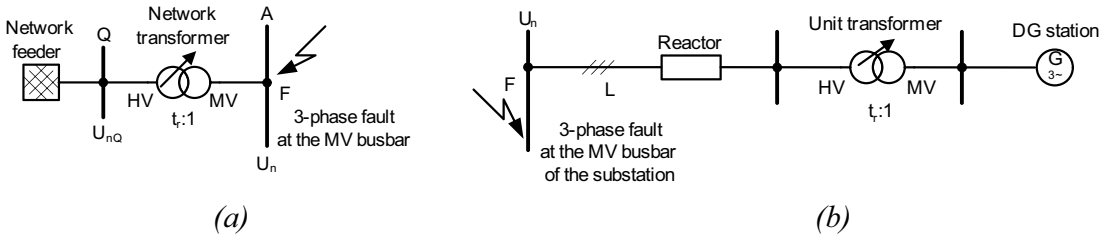

Figure 3.7: *Short-circuit current contributions in MV distribution networks (a) of the upstream grid and (b) of a DG*

The contribution of the upstream grid is depicted in Fig.3.7a and is calculated by:

$$\overline{I}_k^{''} = \frac{cU_n}{\sqrt{3}(\overline{Z}_Q + \overline{Z}_T)} \tag{3.8}$$

where Z_Q is the impedance of the network feeder (upstream grid) at the connection point Q and Z_T is the impedance of the transformer, both referred to the low-voltage side of the transformer.

The IEC 60909 has been developed without considering DGs and therefore their contribution is not taken into account [40]. The fault contribution of DGs depends on the generator type and technology (i.e. synchronous or induction, directly connected or interfaced to the grid via power electronics converters). For conventional generators, it is given by (see Fig.3.7):

$$\overline{I}_k^{''} = \frac{cU_n}{\sqrt{3}(\overline{Z}_G + \overline{Z}_T + \overline{Z}_L + \overline{Z}_L)} \tag{3.9}$$

where the impedances of the generator (G), the transformer (T) (if any), the interconnection line (L) to the substation and the series reactor (R) (if any) are included, all referred to the voltage at the short-circuit location.

For generators connected to the grid via power electronics converters, in case of SC at the connection point, the initial symmetrical SC current can be calculated as follows [17]:

$$I_k^{''} = kI_{rG}, 0 \leq t \leq \Delta t \tag{3.10}$$

According to Eq.3.10, the generator acts as a current source $I_k^{''}$, equal to k times the rated current of the generator I_{rG}, where Δt is the maximum duration of the contribution, before the DG is disconnected by its own protection. If the DG includes a transformer, the current is converted to the voltage level of the fault location F. A typical value for the fault current may be k=1.5, representing the short-time over-current capability of the grid-side converter, whereas Δt depends on the protection and fault ride-through capability of the DG unit [17]. This approximative fault current contribution from VSC-based DGs leads to inaccurate results as it does not consider the real behavior of the converter during the fault, such as the active and reactive current injection; it only predicts the magnitude of the fault current but not the phase shift with respect to the bus voltage.

Doubly-fed induction generators (DFIG), widely used in variable speed WTs, are a special case. Despite the presence of the converter in their rotor circuit, their fault current contribution is similar to that of the directly connected induction generators [17]. Hence, they are represented by the positive-sequience impedance Z_M calculated using Eq.3.11:

$$Z_M = \frac{1}{I_{LR}/I_{rG}} \cdot \frac{U_{rG}}{\sqrt{3}I_{rG}} = \frac{1}{I_{LR}/I_{rG}} \cdot \frac{U_{rG}^2}{S_{rG}} \tag{3.11}$$

where U_{rG}, I_{rG} and S_{rG} are respectively rated voltage, current and apparent power of the generator, I_{LR}/I_{rG} is the ratio of the locked-rotor current to the rated current and is assumed to be $I_{LR}/I_{rG} = 8$. $R_G = 0.1X_G$ is assumed for the calculation of resistance and reactance of the generator. The duration Δt of their contribution, however, should be limited to 3-5 cycles.

Those ways of taking into account the fault contribution of grid-connected DGs with power converters does not take into consideration the control of the converter which can make it injecting current with different power factors.

Symmetrical short-circuit current I_k

The symmetrical short-circuit current I_k is the r.m.s. of the a.c. symmetrical component of the prospective SC current (i.e. the aperiodic component, if any, is neglected). For the calculation, two different procedures are used for faults far-from or near-to generators. Far-from generators, I_k is assumed to be equal to the initial value $I_k^{''}$, whereas near-to generators, the calculation of I_k takes into account many effects, such as magnetic circuits saturation, excitation type, automatic voltage regulator, type of machine (turbogenerator or salient pole generator); details can be found in [14].

Peak short-circuit current i_p

The peak short-circuit current i_p is the maximum possible value of the prospective SC current; it occurs in the period immediately following the SC occurrence. The calculation depends on wheather the network is radial or meshed. In case of radial network, i_p is the sum of contributions i_{pi} from the $i-th$ path converging to the faulty bus:

$$i_p = \sum i_{pi} \tag{3.12}$$

Each contribution i_{pi} is computed as a function of $I_{ki}^{''}$, as $i_{pi} = k_i\sqrt{2}I_{ki}^{''}$, where each coefficient k_i depends on the $R_(ei/X_(ei$ ratio of the corresponding path (e.g. the dependence is represented by a graph in the IEC 606909). In case of meshed network, as the behaviour of the short-circuit current in each path depends on all network branch parameters, i_p can be calculated as $i_p = k\sqrt{2}I_k^{''}$, where k is the equivalent coefficient. The IEC 60909 suggests three different approximated methods, called A, B and C, to compute an equivalent coefficient k:

- procedure A: k is determined from the smallest R_{ei}/X_{ei} ratio of all branches in the network, thus obtaining the highest k on the graph; for low-voltage network, $k \leq 1.8$;
- procedure B: k is determined from the R_e/X_e ratio of the positive-sequence SC impedance at the fault location and multiplied by a safety factor of 1.5 in order to account different R_{ei}/X_{ei} ratios in parallel branches;
- procedure C: k is determined with an equivalent frequency as below:
  - calculation of positive-sequence reactances for all network branches i at the equivalent frequency f_c:
    $$X_{ci} = \frac{f_c}{f}X_i \tag{3.13}$$
    where f is the nominal frequency $(50-60Hz)$ and f_c is the equivalent frequency $(20-24Hz)$.
  - calculation of the equivalent impedance at the SC position using the resistances R_i and reactances X_i of the network branches in the positive-sequence system:
    $$\underline{Z}_c = R_c + jX_c \tag{3.14}$$
  - determination of the factor k from the graph in the IEC 60909 using the ratio:
    $$\frac{R_e}{X_e} = \frac{f_c}{f}\frac{R_c}{X_c} \tag{3.15}$$

A ratio $f_c/f = 0.4$ is assumed. Method C is recommended in meshed networks [14].

Direct current component of the short-circuit current $i_{d.c.}$

The d.c. component of the SC current can be calculated as [51]:

$$i_{d.c.} = \sqrt{2} I_k^{''} e^{-2\pi f t R_e/X_e} \tag{3.16}$$

where f is the nominal frequency, t is the time and R_e/X_e is the exact ratio for a radial network or an equivalent ratio for a meshed network. For meshed networks, the ratio R_e/X_e can be determined using one of the following procedures:

- procedure B: equivalent to procedure B for the peak SC current i_p calculation;
- procedure C: equivalent to procedure C for the peak SC current i_p calculation;
- procedure C': as in C, R_e/X_e is calculated using the equivalent frequency f_c; however, instead of using $f_c/f = 0.4$, f_c is calculated from the ratio f_c/f depending on $f \cdot t$ as follows:

$f \cdot t$	< 1	< 2.5	< 5	< 12.5
f_c/f	0.27	0.15	0.092	0.05

Table 3.3: *f_c/f ratio at different $f \cdot t$ [14].*

Symmetrical short-circuit breaking current I_b

The symmetrical short-circuit breaking current I_b is the r.m.s. of the a.c. symmetrical component of the prospective SC current at the istant t_m of contact separation of the first pole of the switching device. In the case of short-circuit far-from generators, as the amplitude of I_k is basically constant, the symmetrical breaking current is assumed to be $I_b = I_k = I_k^{''}$ independently on the network configuration. In the case of near-to-generator short-circuit, it is necessary to distinguish between radial and meshed networks. For a radial network, I_b can be expressed as the sum of different I_{bi} contributions from the $i-th$ path converging to the faulty bus:

$$I_b = \sum I_{bi} = \sum \varphi_i q_i I_{ki}^{''} \tag{3.17}$$

The factor φ_i can be determined by a formula or a graph as a function of the minimum contact parting time t_m[3] and of the ratio $I_{ki}^{''}/I_{ri}$, where I_{ri} is the rated current of the machine in the $i-th$ branch. The factor q_i can be determined by a formula or a graph as a function of the minimum contact parting time t_m and of the ratio P_{rG}/p, where P_{rG} is the rated active power in MW and p is the number of pole pairs of the machine. For meshed networks, it can be assumed $I_b = I_k^{''}$, according to a conservative approximation of a more complicated formula [17].

Thermal equivalent short-circuit current I_{th}

The thermal equivalent short-circuit current I_{th} is the r.m.s. value of a current having the same thermal effect and the same duration as the actual SC current. It is calculated by using the Joule integral $\int i^2(\tau) d\tau$, which is a measure of the energy dissipated in the resistive element of the system by the SC current. According to the IEC method, the Joule integral is calculated using a factor m

[3] Considered values are 0.02, 0.05, 0.1 and $\geq 0.25s$

for the time-dependent heat effect of the d.c. component of the SC current and a factor n for the time-dependent heat effect of the a.c. component of the SC current. It yields [14]:

$$\int_0^{T_k} i^2(\tau)d\tau = I''^2_k(m+n)T_k = I^2_{th}T_k \tag{3.18}$$

The thermal equivalent SC current is:

$$I_{th} = I''_k\sqrt{m+n} \tag{3.19}$$

where equations for m and n are provided in the IEC 60909 [14].

3.5.2 The IEEE 141/ANSI C37 (ANSI) method

The ANSI C37.010-1999 standard is addressed to a good sizing of medium and high-voltage circuit breakers (rated on symmetrical current basis) installed at 1000V and above.

One of the most important requirements of circuit breaker application is the determination of the maximum short-circuit duty imposed on the breaker; they are evaluated in the ANSI C37.010-1999 using two methods with different accuracy, the E/X_e *simplified method* and the E/X_e *method with adjustment for a.c. and d.c. decrements.*

Although the main goal is not the calculation of short-circuit currents, it provides a SC current calculation procedure based on the reduction of the electric system to an equivalent network comprising an ideal voltage source E and an equivalent reactance X_e, both expressed in *p.u.* [39]. The voltage magnitude E is the highest operating voltage at the faulty bus and represents the pre-fault voltage; when the operating voltage is not known, the nominal voltage can be used. The standard considers both the d.c. and the a.c. components of the short-circuit current by means of appropriate corrective factors. The aperiodic d.c. component is determined by the R_e/X_e ratio of the equivalent impedance seen from the faulty point. The a.c. decay takes into account the behaviour of rotating machines, which can either be near to or remote from the fault location. The effect of the remote contribution on the a.c. component is evaluated by means of the $NACD$ factor, which is the ratio of the remote current contribution and the total fault current:

$$NACD = I_{remote}/I_{sc} \tag{3.20}$$

The remote current contribution I_{remote} is the sum of all remote generator contributions, such as induction generators, synchronous machines, external grids. The $NACD$ factor takes values within $[0; 1]$; $NACD = 1$ means that there is no local generation (i.e. equivalent to far-from-generator in the IEC 60909/VDE 0102), whereas $NACD = 0$ means that there is no remote generation (i.e. equivalent to near-to-generator in the IEC 60909/VDE 0102). The calculation of the NACD factor may be very time consuming, as the contribution of each generator is calculated one by one. Therefore different approximative methods can be used.

The considered faults are both symmetrical and non-symmetrical; however particular attention is paid to three-phase and line-to-ground faults. Three types of duties are considered [39]:

- first-cycle duty;
- contact-parting duty;
- short-circuit current for time-delayed relaying devices.

Each duty is calculated using a different network. Above mentioned duties are briefly described in the following.

First-cycle duty

The first-cycle duty is the half-cycle r.m.s. short-circuit current and allows the evaluation of stresses during the first cycle after the fault. To evaluate it, a first-cycle network must be built; it requires to ignore static loads and to correct the subtransient impedances of rotating machines with multiplicative factors which take into account their typical a.c. decay. Reactances can be used instead of impedances. The multiplicative factors for subtransient reactances are collected in a table shown in [47]. The calculation of the first-cycle duty does not require any consideration about local or remote fault. Once the equivalent reactance of the first-cycle network X_{fc} is obtained, the first-cycle duty can be evaluated as:

$$I_{fc} = E/X_{fc} \tag{3.21}$$

This symmetrical duty must be lower than the breaker closing current and latching capability [39]. If the equivalent impedance Z_{fc} is used instead of X_{fc}, the standard recommends to use two different networks to evaluate X_{fc} and R_{fc}, one with only reactances and the other with only resistances; this procedure is more conservative than the one consisting of the calculation of the complex impedance. By using the first-cycle duty, the asymmetrical duty I_{Ad} and the peak value of the first-cycle SC current I_{Pd} can be calculated as follows:

$$I_{Ad} = 1.6 \cdot I_{fc} \tag{3.22}$$

$$I_{Pd} = 2.7 \cdot I_{fc} \tag{3.23}$$

The factors 1.6 and 2.7 are not empirically determined but they are derived in reference [52].

Contact-parting duty

The contact-parting duty is the r.m.s. current at the parting of the breaker poles. In the standard, only breakers with minimum contact-parting time in the interval 1.5-4 cycles are considered. An interrupting network has to be built, composed by the pre-fault voltage source and by an equivalent impedance. This equivalent impedance of the interrupting network Z_{int} (or reactance X_{int}, as permitted by the standard) is calculated by network reduction; corrective factors for subtransient reactances are different because the a.c. decay at minimum contact-parting time is larger than during the first cycle. The contact-parting duty is, then, calculated as E/X_{int}. This value is used to select the proper breaker; to do this two procedures, beyond the scope of this work, are provided [52].

Short-circuit currents for time-delayed relaying devices

The short-circuit current in case of time-delayed relaying device is calculated as E/X_{del}, where X_{del} corresponds to a network comprising only generators and passive elements (i.e. lines and transformers) and omitting motor contributions. Generators are represented by the transient reactance or by a larger reactance that takes into account the a.c. decay; moreover, the d.c. component is supposed to be zero.

3.5.3 Comparison between IEC and ANSI methods

This section is focused on the comparison between the two standard methods for the short-circuit studies at steady-state conditions. Calculation procedures have been presented in sections 3.5.1 and 3.5.2. Here they are analyzed to define common quantities, similarities and differences.

Common quantities

A first comparison considers the initial symmetrical SC current; $I_k^{''}$ considered in the IEC method can be related to the term E/X_{fc} of the ANSI method, where $E = cU_n$ in *p.u.* and X_{fc} is the reactance of the first-cycle network.

The peak short-circuit current i_p, considered in the IEC method, can be related to the peak value of the first-cycle SC current $I_{Pd} = 2.7 \cdot I_{fc}$ of the ANSI method.

The symmetrical short-circuit breaking current I_b of the IEC method can be related to the term E/X_{int} of the ANSI method, where the equivalent reactance X_{int} of the interrupting network is considered.

IEC 60909 near/far versus ANSI local/remote

In the IEC 60909/VDE 0102, motors and generators are subject to the near-to/far-from consideration. The SC contribution of each generator is taken into account in two different ways depending on if the short-circuit is considered far-from or near-to the generator. The IEC method calculates the initial symmetrical SC current for each electrical machine. For calculating breaking currents, motors are considered near if the sum of all $I_{kMi}^{''}$ exceeds 5% of the $I_{kM}^{''}$ without motors, otherwise all motors are considered far. Induction motors whose terminals are short-circuited are treated as a special case. Synchronous machines are considered near if their $I_{kG}^{''}$ is bigger than twice their rated current (i.e. if $I_{kG}^{''} > 2I_{rG}$).

The ANSI method does not take into accout the remoteness of induction and synchronous motors during the calculation of interrupting currents; they are always represented by fixed impedances. Generators are considered remote if the fault location is more than two transformers away or if the transfer reactance between the generator and short-circuit location is greater than 1.5 times the subtransient reactance of the generator. Otherwise, generators are considered to be local.

Radial and meshed networks

In the IEC 60909/VDE 0102, radial and meshed networks are well distinguished; different rules are applied for the calculation of all considered values of the SC current (see section 3.5.1).

The ANSI method does not distinguish radial and meshed networks, meaning that a bigger approximation is applied.

Accuracy

Some comparison studies between the IEC and the ANSI methods are presented in the literature (i.e. [39] and [48]). Reference [39] shows that, for the considered study case, the IEC 60909 produces a more conservative approximation of the short-circuit current than the ANSI C37.010 with respect to the exact value obtained by means of full dynamic simulations.

Although the ANSI method is designed for a good sizing of high-voltage circuit breakers, it produces a good approximation of the SC current. The IEC 60909/VDE 0102 presents a method that inherently more accurately models SC currents; however it requires significantly more complex modelling of the power system fault contributions than ANSI.

3.6 Short-circuit calculation in DIgSILENT PowerFactory

The power system simulation tool DIgSILENT PowerFactory allows short-circuit studies at steady-state condition; several methods are provided in the SC module of DIgSILENT. The selection of

the calculation method depends on the purpose of the study [41]. Short-circuit calculations at planning stage mostly use calculation methods that require less detailed network modelling (e.g. do not require pre-fault operating conditions) and apply extreme-case estimations. Examples of these methods are IEC 60909/VDE 0102 and IEEE 141/ANSI C37 methods (see sections 3.5.1 and 3.5.2). If the interest is focused on the fault current in a specific situation, the SC calculation method normally uses the superposition method, which is based on a specific load-flow situation (see section 3.4.3).

The goal of this section is to describe the implementation in PowerFactory of SC calculation methods at steady-state condition. The handling of PowerFactory, the different methods and the available options are presented in the following.

PowerFactory is able to perform single faults and multiple faults in power systems of nearly unlimited complexity. SC can be performed on busbars, terminals and lines; in case of SC on a line, the fault location can be specified in % of the line length or in absolute distance with respect to the selected reference end [41].

Short-circuit calculation options

PowerFactory provides the following calculation methods for short-circuit calculation:

- method of the equivalent voltage source at the fault location according to the International IEC 60909 standard;
- method of the equivalent voltage source at the fault location according to the German VDE 0102 standard (VDE 0102 is identical with IEC 60909);
- method of the equivalent voltage source according to the American IEEE 141/ANSI C37 standard;
- the complete method (i.e. superposition method) which considers the pre-fault load-flow solution.

Although two different options are available for calculation accordings to IEC 60909 and VDE 0102, as those standards are identical, the same results are obtained.

The following fault types can be analyzed:

- 3-phase SC;
- 2-phase SC;
- single-phase to ground SC;
- 2-phase to ground SC;
- 1-phase to neutral SC;
- 1-phase neutral to ground SC;
- 2-phase to neutral SC;
- 2-phase neutral to ground SC;
- 3-phase to neutral SC;
- 3-phase neutral to ground SC;

The fault types involving the neutral conductor only make sense when the lines include neutral conductors.

The IEC 60909/VDE 0102 method

The short-circuit calculation according to the IEC 60909/VDE 0102 provides some basic and advanced options. The window with basic options is shown in Fig.3.8.

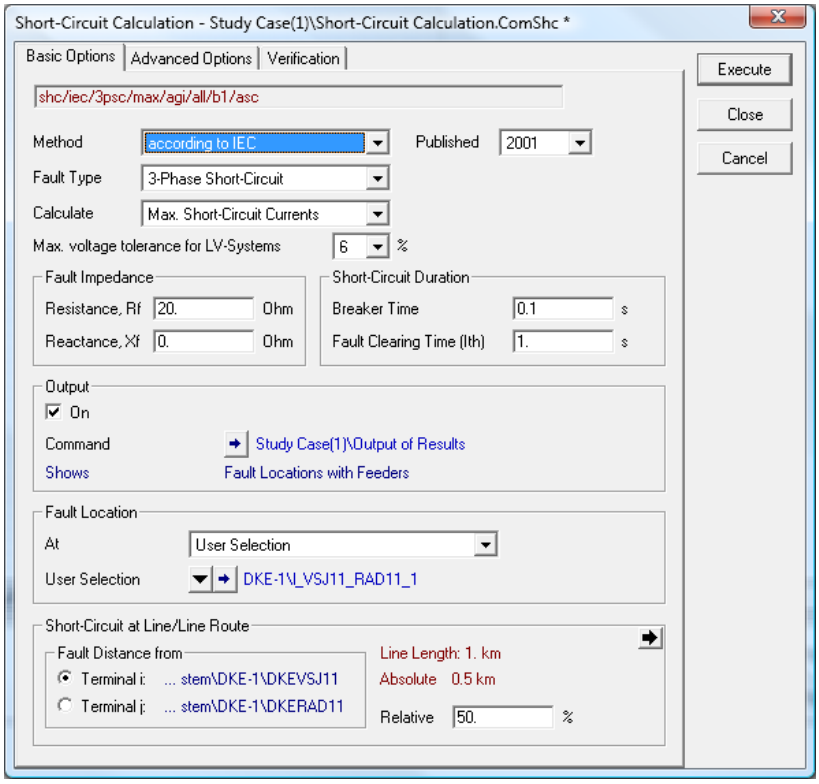

Figure 3.8: *Short-circuit calculation according to IEC 60909/VDE 60909. Basic options.*

The following basic options are available [41]:

- *Published*: it offers a sub-selection for the method, where the version of the used standard can be selected. Available versions of the IEC standard were issues in 2001 and 1990 (i.e. the 1990 is still available for the verification of documented results).
- *Fault Type*: the type of short-circuit can be selected.
- *Calculate*: the minimal or maximal short-circuit current can be selected as result.
- *Max. Voltage tolerance for LV systems*: the voltage tolerance is used to define the voltage correction factor c (see table 3.2). The voltage tolerance is not used when a user-defined correction factor is defined in the advanced options window.
- *Fault Impedance*: resistance and reactance of the SC path can be specified.
- *Short-Circuit Duration*: the *breaker time*[4] is used to calculate the symmetrical SC breaking current I_b of a circuit breaker, whereas the *fault clearing time*[5] is used for the thermal equivalent SC current I_{th}.

[4]Time between the SC occurence and the instant of contact separation of the first pole of the switching device
[5]Time between the SC occurence and the end of the SC current (i.e. duration of the actual SC current)

- *Output*: if enabled, a report is produced at the end of the SC calculation.
- *Fault location*: the SC can be produced on a used-defined element, at all busbars/junction and internal nodes or at all busbars. If a user-defined element is selected (i.e. busbar, terminal, lines), then the SC current at the faulty elements and the prospective SC currents at all other points are shown as result. Otherwise only SC currents at faulty elements are shown.
- *Short-Circuit at Line/Line Route*: if a line is selected as faulty element, the fault location can be specified in % of the line length or in absolute distance with respect to the selected reference end.

The window with advanced options is shown in Fig.3.9.

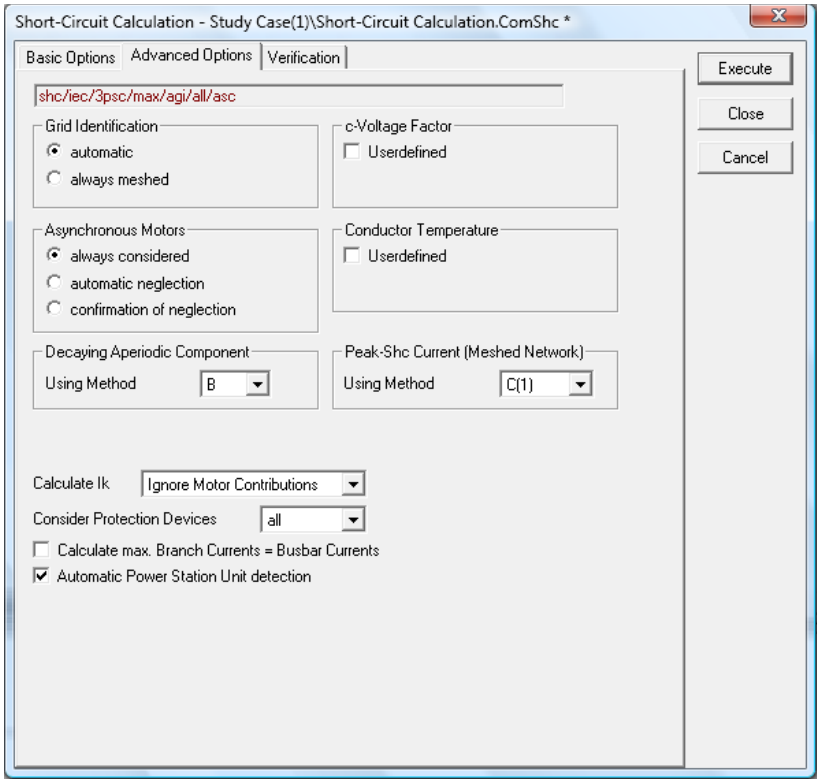

Figure 3.9: *Short-circuit calculation according to IEC 60909/VDE 60909. Advanced options.*

The advanced short-circuit options are used to tune the short-circuit calculations. The following advanced options are available [41]:

- *Grid Identification*: it can be specified if the grid feeding of the short-circuit is meshed or radial. Normally PowerFactory can automatically find the appropriate setting. The option always forces a meshed grid approach which affect the calculation of the peak SC current i_p.
- *c-Voltage Factor*: the *c*-factor can be specified by the user only if this option is enabled.
- *Asynchronous Motors*: the short-circuit currents contribution from asynchronous motors may be always considered, automatically neglected when possible or neglected with user confirmation[6].

[6]The contribution of asynchronous motors in low-voltage power system to the SC current $I_k^{''}$ may be neglected if their contribution is not higher than 5% of the initial short-circuit current $I_{kM}^{''}$ calculated without motors [14].

- *Conductor Temperature*: when activating this option, the pre-fault conductors temperature can be set manually. This will influence the calculated maximum temperature of the conductors caused by the short-circuit currents. If it is not specified by the user, the default value 0^oC is used.

- *Decaying Aperiodic Component*: the d.c. component of the SC current at the breaking time T_b is calculated using the R_e/X_e ratio which can be evaluated as follows:

  - method B, corresponding to the method B in IEC 60909/VDC 0102;
  - method C, corresponding to the method C' in IEC 60909/VDC 0102;
  - method C', corresponding to the method C in IEC 60909/VDC 0102.

  Some discrepancy in the notation has been identified between the IEC 60909/VDC 0102 and DIgSILENT PowerFactory (i.e. C and C').

- *Peak-Shc Current (Meshed network)*: i_p in meshed grid can be calculated using one of the following methods as general selection for all network branches:

  - method B, corresponding to the method B in IEC 60909/VDC 0102;
  - method C(1), corresponding to the method C in IEC 60909/VDC 0102;
  - method C(012), which is similar to C(1) but it uses the correct short-circuit impedance based on positive, negative and zero-sequence systems.

- *Calculate I_k*: the symmetrical short-circuit current can be calculated with different ways of considering asynchronous machines; the following options are available:

  - *Without Motors*, which disconnects all asynchronous motors before calculating I_k;
  - *DIgSILENT Method*, which considers all asynchronous motors by their breaker current; the breaker opens after their own tripping times;
  - *Ignore Motor Contributions*, which considers asynchronous motor impedances during the calculation but it does not consider motor contributions as results.

- *Consider Protection Devices*: it calculates measured currents for all protection devices and evaluates tripping times; if protection devices do not need to be analyses, this option can be disabled to increase the calculation speed.

- *Calculate max. Branch Currents = Busbar Currents*: this option is used to check the rating of the circuit breakers against the system breaker currents. Breaker currents are normally calculated as $max[I_{bus} - I_{branch}, I_{branch}]$. If this option is activated, the busbar short-circuit current I_{bus} is used as the breaker current, which is an over-estimation of the SC currents.

- *Automatic Power Station detection*: according to the IEC 60909/VDE 0102, different impedance correction factor are appied for separate generators and transformers and for a unit/block (power station) consisting of a generator including its step-up transformer. When selected, PowerFactory tries to detect power stations; when disabled, then the transformers have to be marked by setting the *unit Transformer* option in the transformer dialogue box.

The *Verification* option in the third page of IEC settings will, when enabled, write a loading report to the output window which shows the various maximum and calculated currents for devices such as lines and breakers.

The IEEE 141/ANSI C37 method

The short-circuit calculation according to the IEEE 141/ANSI C37 provides some basic and advanced options. The window with basic options is shown in Fig.3.10.

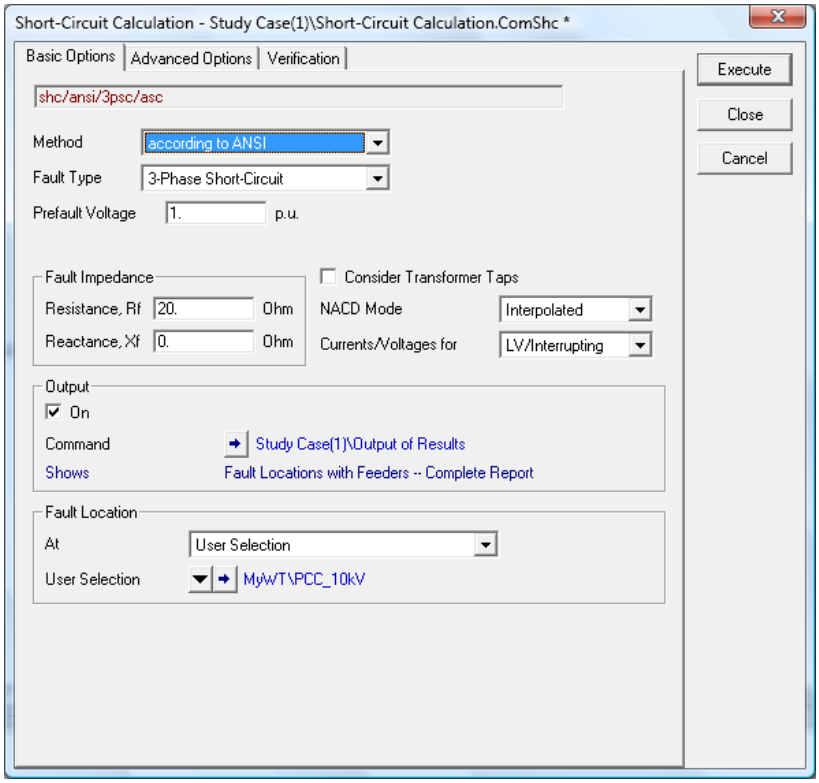

Figure 3.10: *Short-circuit calculation according to IEEE 141/ANSI C37. Basic options.*

The following basic options are available [41]:

- *Fault Type*: the type of short-circuit can be selected.
- *Prefault Voltage*: the value in *p.u.* of the pre-fault voltage can be specified.
- *Fault Impedance*: resistance and reactance of the SC path can be specified.
- *Consider Transformer Taps*: the tap positions of transformers can optionally be considered for the SC calculation.
- *NACD Mode*: four different approximative methods for the determination of the *NACD* factor can be selected; they represent the most common interpretations of the ANSI Standards:
  - *Predominant*: the the *NACD* factor is calculated and if $NACD \geq 0.5$, then only the d.c. decay curve is used, which means that the remote generation is higher than the local generation.
  - *Interpolated*: the *NACD* factor is calculated and the correction factor for the asymmetrical fault current is interpolated between the d.c. decay and a.c./d.c. decay curves with the following equation:

$$MF = a.c./d.c. factor + (d.c. factor - a.c./d.c. factor) * NACD \tag{3.24}$$

If $NACD = 1$, only the d.c. factor is used; if $NACD = 0$, only the a.c./d.c. factor is used.

  - *All remote*: all contributions are set to remote, the *NACD* factor is not calculated but assumed equal to 1 and only the d.c. decay curve is used.
  - *All local*: all contributions are set to local, the *NACD* factor is not calculated but assumed equal to 0 and only the a.c./d.c. decay curve is used.

- *Current/Voltages for*: the calculation mode for the currents and voltages can be set to:
  - *LV/Momentary*: evaluates the subtransient SC currents;
  - *LV/Interrupting*: evaluates the breaking currents;
  - *30 Cycle*: evaluates the 30-cycle (steady-state) current.
- *Output*: if enabled, a report is produced at the end of the SC calculation.
- *Fault location*: the SC can be produced on a used-defined element, at all busbars/junction and internal nodes or at all busbars. If a user-defined element is selected (i.e. busbar, terminal, lines), then the SC current at the faulty elements and the prospective SC currents at all other points are shown as result, otherwise only SC currents at faulty elements are shown.

The window with advanced options is shown in Fig.3.11; the following advanced options are available [41]:

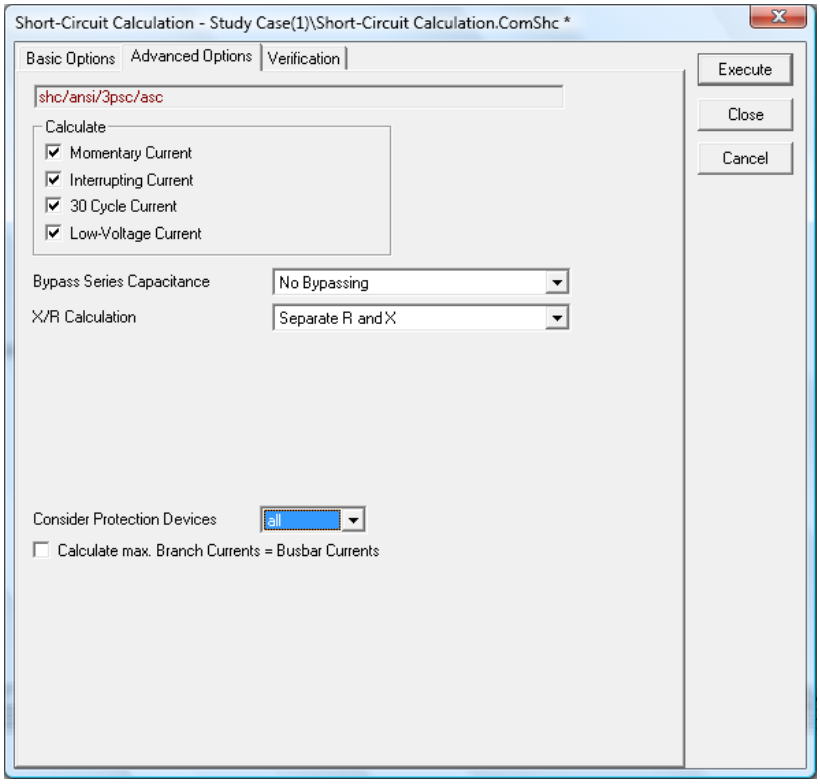

Figure 3.11: *Short-circuit calculation according to IEEE 141/ANSI C37. Advanced options.*

- *Calculate*: it allows the selection of currents of interest to be calculated. Available values are momentary current (first cycle duty), interrupting current (contact-parting duty), 30 cycle current (SC currents for time-delayed relaying devices) and low-voltage current.
- *Bypass Series Capacitance*: series capacitances may not be considered for the ANSI SC calculation. They may be always considered, always bypassed/neglected or this option may be set depending on the type of short-circuit calculated. The available options are:
  - No bypassing;
  - All currents;
  - LV interrupting 30 cycle current;
  - 30 cycle currents;
- *Consider Protection Devices*: it calculates measured currents for all protection devices and evaluates tripping times. This option can be disabled to increase the calculation speed when protection devices do not need to be analyses. The following options are available: none, main, all, backup.
- *Calculate max. Branch Currents = Busbar Currents*: this option is used to check the rating of the circuit breakers against the system breaker currents. Breaker currents are normally calculated as $max[I_{bus} - I_{branch}, I_{branch}]$. If this option is activated, the busbar short-circuit current I_{bus} is used as the breaker current, which is an over-estimation of the SC currents.

The *Verification* option in the third page of ANSI settings will, when enabled, write a loading report to the output window which shows the various maximum and calculated currents for devices such as lines and breakers.

The complete method

The complete method included in DIgSILENT PowerFactory is based on the superposition principle and is therefore identical to the superposition method presented in section 3.4.3. The complete method for SC calculations provides some basic and advanced options. The window with basic options is shown in Fig.3.12; the following basic options are available [41]:

- *Fault Type*: the type of short-circuit can be selected.
- *Multiple faults*: when enabled, it performs multiple faults calculation, such as simultaneous occurrence of more than one fault condition in the network; the complete method must be used in this case.
- *Load-Flow*: as the complete method considers the pre-fault condition in the system, a load flow solution must be specified. The load flow solution is, as default, taken from the currently active study case; to select a different load flow solution, its path must be specified.
- *Fault Impedance*: resistance and reactance of the SC path can be specified.
- *Short-Circuit Duration*: the breaker time is used to calculate the symmetrical SC breaking current I_b of a circuit breaker.
- *Output*: if enabled, a report is produced at the end of the SC calculation.

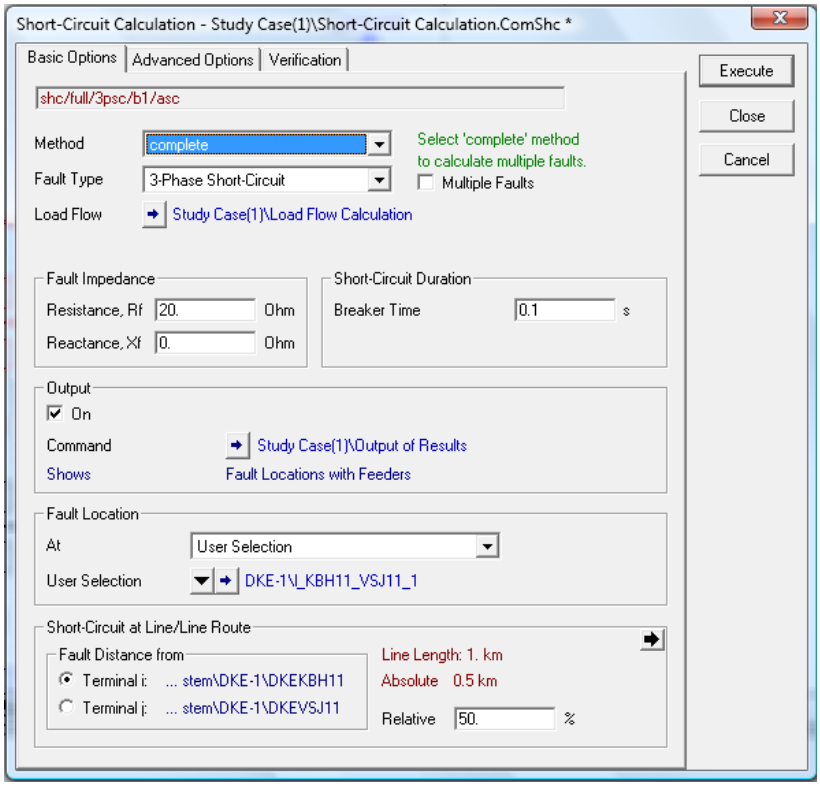

Figure 3.12: *Short-circuit calculation based on the complete method. Basic options.*

- *Fault location*: the SC can be produced on a user-defined element, at all busbars/junction and internal nodes or at all busbars. If a user-defined element is selected (i.e. busbar, terminal, lines), then the SC current at the faulty elements and the prospective SC currents at all other points are shown as result, otherwise only SC currents at faulty elements are shown.

The window with advanced options is shown in Fig.3.13. The advanced short-circuit options are used to tune the short-circuit calculations; they are presented in the following [41]:

- *Decaying Aperiodic Component*: the d.c. component of the SC current at the breaking time T_b is calculated using the R_e/X_e ratio which can be evaluated as follows:
  - method B, corresponding to the method B in IEC 60909/VDC 0102;
  - method C, corresponding to the method C' in IEC 60909/VDC 0102;
  - method C', corresponding to the method C in IEC 60909/VDC 0102.

  Some discrepancy in the notation has been identified between the IEC 60909/VDC 0102 and DIgSILENT PowerFactory (i.e. C and C').
- *Use Generator Impedances*: with this option the time domain for generator impedances can be selected; available options are *subtransient* and *transient*.
- *Calculate* I_k: the symmetrical short-circuit current can be calculated with different ways of considering asynchronous machines; the following options are available:
  - *Without Motors*, which disconnects all asynchronous motors before calculating I_k;

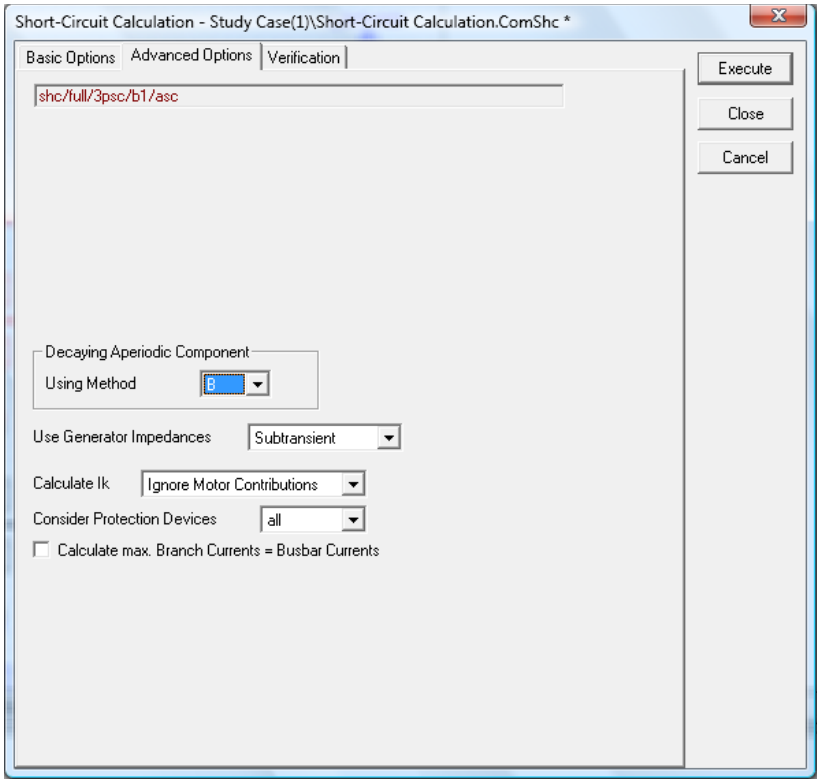

Figure 3.13: *Short-circuit calculation based on the complete method. Advanced options.*

  - *DIgSILENT Method*, which considers all asynchronous motors by their breaker current; the breaker opens after the maximum possible time;
  - *Ignore Motor Contributions*, which considers asynchronous motor impedances during the calculation but it does not consider motor contributions as results.

- *Consider Protection Devices*: it calculates measured currents for all protection devices and evaluates tripping times; if protection devices do not need to be analyses, this option can be disabled to increase the calculation speed.

- *Calculate max. Branch Currents = Busbar Currents*: this option is used to check the rating of the circuit breakers against the system breaker currents. Breaker currents are normally calculated as $max[I_{bus} - I_{branch}, I_{branch}]$. If this option is activated, the busbar short-circuit current I_{bus} is used as the breaker current, which is an over-estimation of the SC currents.

The thermal equivalent short-circuit current I_{th} is only roughly estimated when using the complete method. The thermal current I_{th} is approximated as I_k'', whereas the symmetrical short-circuit breaking current I_b is evaluated according to IEC method. The correct evaluation of I_{th} and I_b is only done when using the IEC calculation method.

The *Verification* option in the third page of settings will, when enabled, write a loading report to the output window which shows the various maximum and calculated currents for devices such as lines and breakers.

The complete method for SC calculation at steady-state conditions is selected for further short-circuit studies in this work. The reasons will be deeply explained in chapter 4 as they are strongly related to the WT model for short-circuit calculations. Such a model is based on the Thevenin

equivalent whose a.c. voltage source can only be taken into consideration for SC calculations only when the complete method is used; in fact, when the IEC or ANSI methods are used, only the pre-fault voltage at the faulty busbar is considered whereas other voltage sources are neglected.

3.7 Summary

This chapter has provided a deep background on the short-circuit current studies normally performed by power system companies as those studies provide the maximum SC current used for the design of electrical components and the minimum SC current for proper relays setting and coordination.

The time behavior of the SC current is analized to identify characteristic values. Depending on the considered standards, different/similar values are used to identify the current. Then, types of short-circuit that can occur in a power system are classified; among them, the balanced three-phase SC is selected for further use in this work as it is often the most severe grid fault.

Methods for SC analysis studies have been introduced and described. It is highlighted how the selection depends on the application (i.e. planning studies or analysis of specific operating conditions) and on the required accuracy.

Standards concerning SC current calculation have been presented. Two main approaches have been identified: the IEC method, according to the IEC 60909/VDE 0102, and the ANSI method, according to the IEEE 141/ANSI C37. Those methods have been deeply described and analyzed in order to identify similarities and differences in the methodologies and approximations. It can be concluded that the IEC method is specificaly designed to lead with sufficient accuracy to results on the safe side; compared with the IEEE 141/ANSI C37, it presents a method that inherently more accurately models the network and therefore it requires significantly more complex modelling of the power system fault contributions than ANSI.

As SC studies will be performed in DIgSILENT PawerFactory to evaluate the current contribution from wind turbines during a grid fault, the implementation of the SC current calculation in the simulation tool is deeply described.

Finally, the complete method for SC calculation at steady-state conditions is selected for further SC studies in this project work. The reasons will be explained in chapter 4 as they are strongly related to the WT model for short-circuit calculations.

Chapter 4

Model of VSC-based wind turbines for short-circuit calculations

Contents

4.1 Introduction

In this chapter an equivalent model of a VSC-based wind turbine for short-circuit studies at steady-state conditions is developed and presented. The wind turbine is assumed to be compliant with the German grid code from E.On regarding fault-ride-through capability and grid voltage support [18]. Although [18] refers to WTs connected to the trasmission level, it is assumed to be the reference grid code for the considered WT which is connected to the distribution level (i.e. $30kV$).

The equivalent model of the WT allows the consideration of the short-circuit current injected into the grid by the WT during a grid fault and therefore the evaluation of the grid support performed by reactive current injection. The model is first described theoretically and then implemented in the commercially available power system simulation tool DigSILENT PowerFactory using DIgSILENT Programming Language (DPL). The model is based on the Thevenin equivalent connected at the LV-side of the WT transformer.

The presented model is suitable for all electrical components connected to the grid by means of a full-rating power converter. The behavior at steady-state condition of any similar component is characterized by the active and reactive current injected into the the connection point (i.e. WT generator terminals for a wind turbine); for wind turbines complying with the German or Spanish grid codes, the reactive current component is specified depending on the voltage at the WT terminal (i.e. LV-side of the WT transformer), whereas the active current component is chosen to avoid excessive overload of the wind turbine and its transformer.

4.2 Model structure

The structure of a suitable model for the wind turbine during the short-circuit is the first issue and strictly connected to the selected simulation tool where the model will be implemented. While performing short-circuit calcualtion in DigSILENT PowerFactory, the current contribution from components connected to the grid by means of power converters is neglected (see section 3.6). This means that alternative components must be used in the model in order to take into consideration the current injection during a grid fault.

In this project the Thevenin equivalen is used to model the wind turbine connected at the LV-side of the WT transformer; this is shown in Fig.4.1.

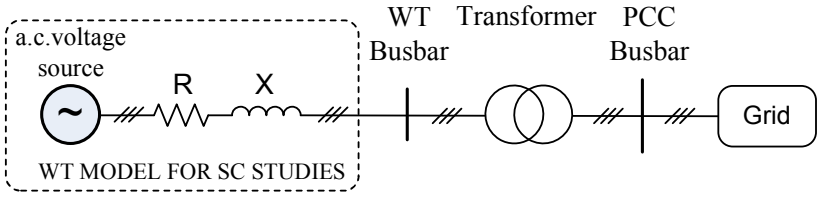

Figure 4.1: *Thevenin equivalent-based model of the WT for short-circuit studies at steady-state conditions.*

It has been noted that:

- the value of the reactance X has a strong effect on the injected reactive current component at steady-state;
- the phase angle of the a.c. voltage source φ and the series resistance R have a strong effect on the injected active current component at steady-state; the voltage magnitude, on the contrary, has a similar effect on both current components and therefore is kept fixed.

Knowing the reference active and reactive current components that the wind turbine shall inject at the WT terminal during a grid fault, the equivalent model can be adjusted by changing X, R and φ to fit with the expected WT behaviour[1].

The grid in Fig.4.1 represents the power system at which the wind turbine is connected; it is characterized by the ratio R_g/X_g and the symmetrical short-circuit power S_k at the PCC, which is a fictitious value determined as the product of the symmetrical SC current, I_k, and the system nominal voltage, U_n, at the short-circuit location [14]:

$$S_k = \sqrt{3} I_k U_n \tag{4.1}$$

In case of bolded short-circuit at the PCC, at steady-state conditions the power grid contribute to the fault with the symmetrical SC current I_k; the higher S_k, the stronger is the grid (i.e. stiff grid).

In the Danish grid code for wind turbines connected to networks with voltages above $100kV$ (see section 2.4.2) the value of the short-circuit power and the ratio R_g/X_g for the simulation test are specified; S_k is assumed to be ten times the wind farm rated power, $S_k = 10PS_{WF,n}$, and the ratio R_g/X_g equal to 0.1, corresponding to a phase angle of 84.3°. No other information for designing the external grid is available in national grid codes. Although the WT in Fig.4.1 is connected to the distribution network, a good estimate for S_k and R_g/X_g are the ones provided by the Danish GC for the trasmission system.

[1]The magnitute of the a.c. voltage source can be arbitrary chosen as, for different values, different solutions for X, R and φ will be obtained to fit the Thevenin equivalent with the expected WT behaviour.

4.3 Algorithm for short-circuit calculations

The basic principle of the algorithm to perfom short-circuit calculations including the current contribution from VSC-based wind turbines is the presented in the following. When a grid fault occurs, it reflects into a voltage dip at the PCC busbar and the WT busbar; knowing the measured WT voltage u_{WT} (i.e. at the LV-side of the WT transformer), the reactive current to be injected by the wind turbine into the WT busbar to support the grid is defined by the the German grid code[2]. Here it is assumed that the wind turbine complies with the German grid code; however the implementation of the the fault-ride-through capability in the control system is beyond the scope of this work.

According to [18], the reactive current injection shall be performed within $20ms$ after a voltage dip on u_{WT} above 10% has occured; it shall act as follows:

- if the voltage drop is $\Delta u_{WT} \leq 0.1pu$, than there are no specifications regarding the reactive current injection; therefore the WT can be operated at unity power factor to maximize the active power injection or at a lower power factor depending on the control strategy chosed by the manufacturer;
- if the voltage drop is $0.1pu < \Delta u_{WT} \leq 0.5pu$, than the reactive current shall be $i_{react} \geq 2\Delta u_{WT}$; in this work $i_{react} = 2\Delta u_{WT}$ is selected;
- if the voltage drop is $\Delta u_{WT} > 0.5pu$, than the reactive current cannot be furhter increased as the rated current has been already achieved; therefore $i_{react} = 1pu$;

The reactive current injection is represented in Fig.4.2. It has to be notice that Fig.4.2 represents

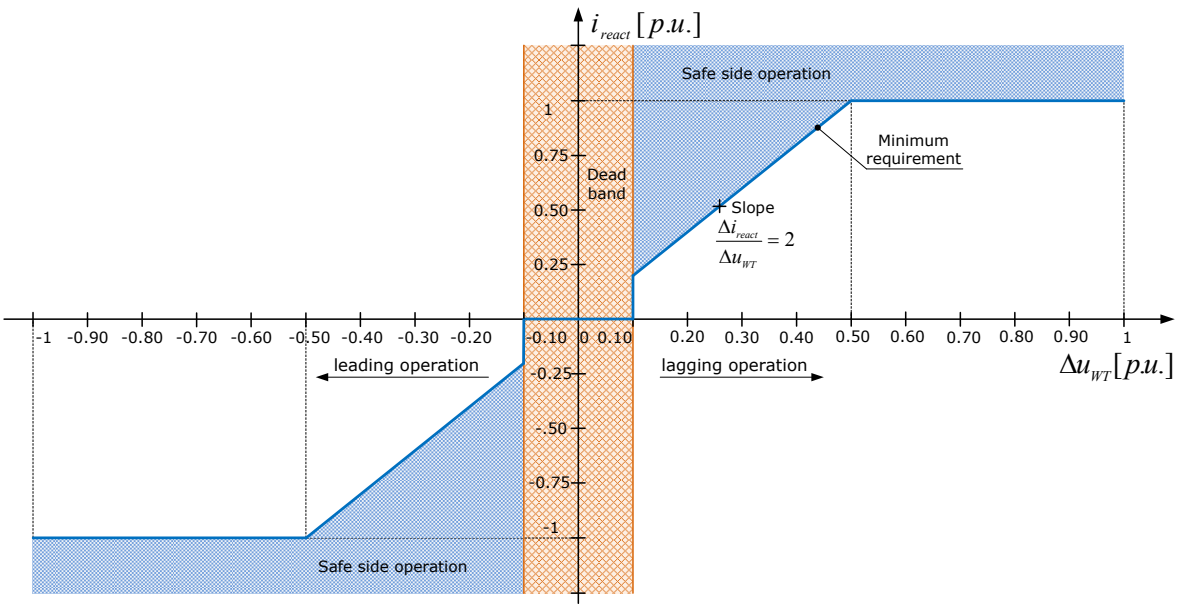

Figure 4.2: *Reactive current injection for grid voltage support according to the German code.*

minimum requirements for FRT capability; however WT manufacturers can decide to support the

[2]In this work specifications regarding the grid support from wind turbines connected to the transmission network are also applied for wind turbines connected at the distribution network as no other similar specifications are available in national grid codes.

grid voltage more than required by injecting more reactive current; moreover, below $\Delta u_{WT} = 0.1pu$, WT manufacturers are free to inject some reactive power depending on the selected control strategy in normal operation. In this work, Fig.4.2 is used to calculate the reference reactive current i^*_{react}. Knowing i^*_{react}, the reference active current component i^*_{act} can be calculated; however it is necessary to use one more constraint: the wind turbine is assumed to work at the rated current, such as at $1pu$. This constraint is resonable as long as the available wind power is higher than the WT output power during the voltage dip[3]. The steady-state reference active current i^*_{act} is calculated as follows:

$$i^*_{act} = \sqrt{1 - {i^*_{react}}^2} \tag{4.2}$$

The wind turbine model shall inject into the WT busbar the reference active and reactive currents at steady-state conditions; to do this, an algorithm has been developed. The algorithm is based on a routine (i.e. an iterative process) that will change the reactance X, the resistance R and the phase angle of the a.c. voltage source, , until $i_{act} = i^*_{act}$ and $i_{react} = i^*_{react}$; in order to limit the number of required iterations, a maximum allowed error is defied; it has been selected $\epsilon_{max} = 0.005pu$. Measured errors are defined as:

$$\epsilon_{act} = i_{act} - i^*_{act} \tag{4.3}$$

$$\epsilon_{react} = i_{react} - i^*_{react} \tag{4.4}$$

The iteration process is stoped when the absolute values $|\epsilon_{act}|$ and $|\epsilon_{react}|$ are both below the maxmum allowed error ϵ_{max}.

At each iteration, depending on the sign and value of ϵ_{react} and ϵ_{act}, X, R and φ will be changed to adjust i_{act} and i_{react}. The injected reactive current i_{react} is adjusted according to the following considerations:

- if $\epsilon_{react} > 0$ (i.e. $i_{react} > i^*_{react}$) and, in the same time $|\epsilon_{react}| > \epsilon_{max}$, in order to reduce the injected reactive current i_{react}, the series reactance X must be increased by multiplying it by $k_{Xi} > 1$ (i.e. $X = k_{Xi} \cdot X$);
- if $\epsilon_{react} < 0$ (i.e. $i_{react} < i^*_{react}$) and, in the same time $|\epsilon_{react}| > \epsilon_{max}$, in order to increase the injected reactive current i_{react}, the series reactance X must be decreased by multiplying it by $k_{Xr} < 1$ (i.e. $X = k_{Xr} \cdot X$).

The injected active current component i_{act} is controlled according to the following considerations:

- if $\epsilon_{act} > 0$ (i.e. $i_{act} > i^*_{act}$) and, in the same time $|\epsilon_{act}| > \epsilon_{max}$, in order to reduce the injected active current i_{act}, the series resistance R can be increased by multiplying it by $k_{Ri} > 1$ and/or the phase angle φ can be decreased by $\Delta\varphi$;
- if $\epsilon_{act} < 0$ (i.e. $i_{act} < i^*_{act}$) and, in the same time $|\epsilon_{act}| > \epsilon_{max}$, in order to increase the injected active current i_{act}, the series resistance R can be reduced by multiplying it by $k_{Rr} < 1$ and/or the phase angle φ can be increased by $\Delta\varphi$.

Regarding the active current control, it has been experienced that:

- at low WT voltages (i.e. $u_{WT} < 0.1pu$), the active current control is better performed by controlling the R instead of φ; in this way the algorithm is more robust but some convergence problems may still be experienced;

[3]It corresponds to the maximum fault current contribution from the wind turbine to the grid and, thus, it is assumed as worst case.

- at WT voltages above $0.1pu$, the active current control is well performed by controlling in the same time φ and R; in this way the algorithm is fast and robust.

The values of k_{Xi}, k_{Xr}, k_{Ri}, k_{Rr} and $\Delta\varphi$ have been carefully chosen as a trade-off between:

- speed of convergence: big variations at each iteration make the eventual convergence faster;
- robustness of the algorithm: big variations at each iteration may lead to non-convergence (e.g. in some conditions $|\epsilon_{react}|$ can not be below ϵ_{max} because possible approximated solutions around the solution X^*, such as $X_1 < X^* < X_2$), both lead to $|\epsilon_{react}| > \epsilon_{max}$).

The above considerations and has led to the following design:

- $k_{Xi} = 1.02$ (i.e small-size perturbation);
- $k_{Xr} = 0.98$ (i.e small-size perturbation);
- $k_{Ri} = 1.02$ for $u_{WT} \geq 0.1pu$ (i.e small-size perturbation);
- $k_{Rr} = 0.98$ for $u_{WT} \geq 0.1pu$ (i.e small-size perturbation);
- $k_{Ri} = 1.10$ for $u_{WT} < 0.1pu$ (i.e big-size perturbation);
- $k_{Rr} = 0.90$ for $u_{WT} < 0.1pu$ (i.e big-size perturbation);
- $\Delta\varphi = \Delta\varphi_{con} + \Delta\varphi_{var} = 0.005^o + 500 \cdot |\epsilon_{act}|$.

Regarding the selection of $\Delta\varphi$, first a constant value $\Delta\varphi = 0.5^o$ was chosen; however a better convergence has been achieved by using a variable step $\Delta\varphi = \Delta\varphi_{con} + \Delta\varphi_{var}$ composed by the following two terms:

- constant term $\Delta\varphi_{con} = 0.005^o$, which is a small-size perturbation especially important when close-to the solution (i.e. small $|\epsilon_{act}|$);
- variable term $\Delta\varphi_{var} = 500 \cdot |\epsilon_{act}|$, which is a variable perturbation especially important when far-from the solution (i.e. big $|\epsilon_{act}|$).

The choice of using a variable term $\Delta\varphi_{var}$ leads to a faster variation towards the solution when far-from it and a robust algorith also when close-to the solution. It is worthy to highlight that the selection of k_{Xi}, k_{Xr}, k_{Ri}, k_{Rr} and $\Delta\varphi$ is based on tests performed in the expected fault conditions; they derive from the analysis of the convergence process. Therefore the selected design cannot necessarily be generalized to other applications or conditions. For the selection, the attention has been paid to balanced three-phase short-circuit fault at the HV-side of the WT transformer with fault reactance X_f and fault resistance $R_f = X_f/5$, as suggested in [20]. Furhermore, power grids with different stiffness have been considered.

The algorithm for the short-circuit calculation including the current contribution from VSC-based wind turbines is graphically represented in Fig.4.3; the flow-chart provides a simple explaination of the code used for the implementation. The following blocks need to be explained:

- *Execute SC*: the short-circuit calculation based on the complete method is launched; it is not possible to use approximated methods, such as the IEC and ANSI methods (see section 3.5), as they do not consider the a.c. voltage source whose phase angle is used to control the active current component (i.e. φ would not have any effect on the WT active power).

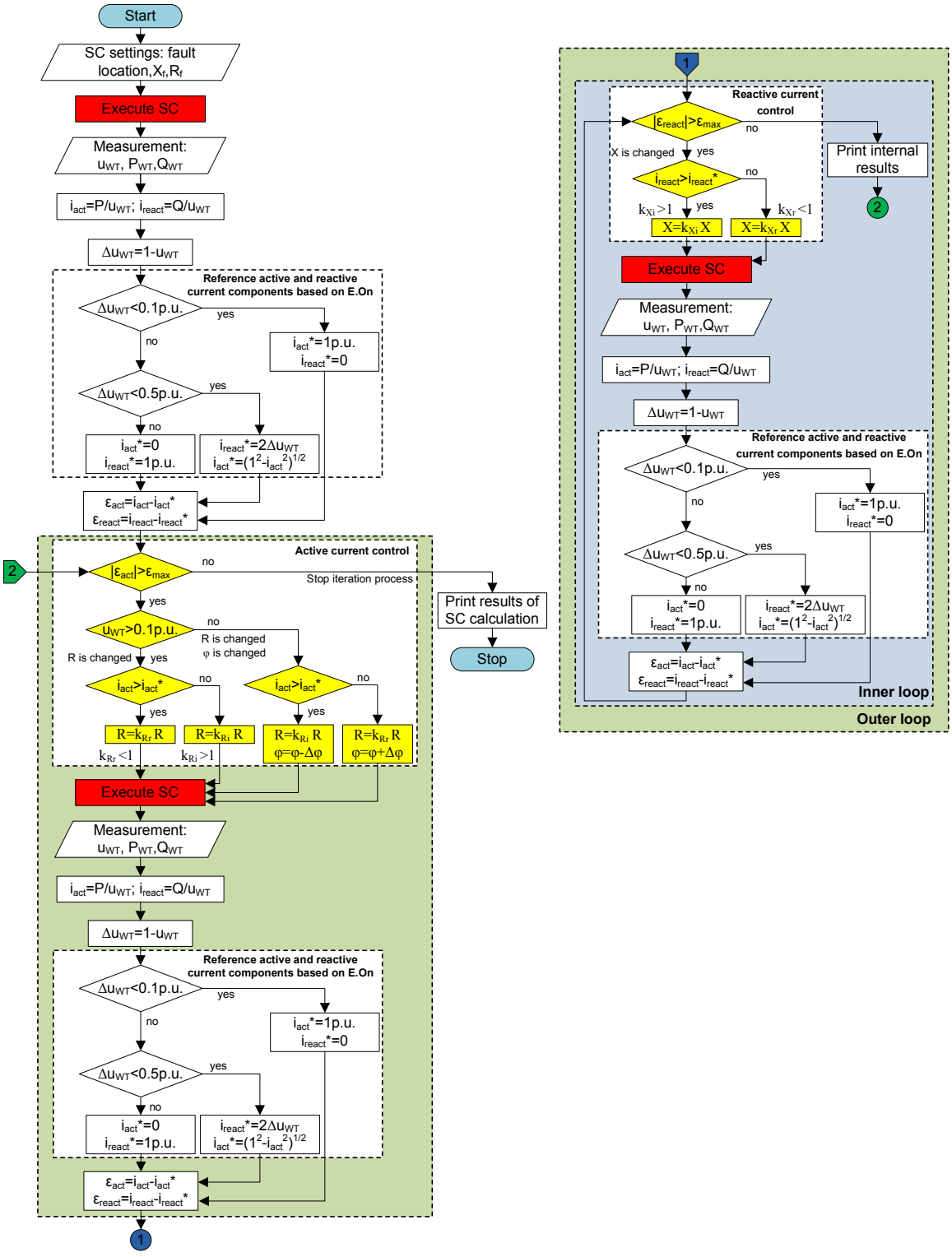

Figure 4.3: *Flow-chart of the algorithm for short-circuit calculation.*

- *Active and reactive current components calculation*: here i_{act} and i_{react} are calculated from the measured values in pu:

$$i_{act} = \frac{P_{WT}}{u_{WT}} \tag{4.5}$$

$$i_{react} = \frac{Q_{WT}}{u_{WT}} \tag{4.6}$$

  where P_{WT} $[pu]$ and Q_{WT} $[pu]$ are measured active and reactive powers and u_{WT} $[pu]$ is the measured voltage at the WT busbar.

- *Reference active and reactive current components based on E.On*: i^*_{react} is calculated according to Fig.4.2 depending on the WT voltage dip; i^*_{act} is then calculated assuming the total current equal to the rated value.

- *Inner loop*: in the inner loop the series reactance X is chanded by an iterative loop until the the reactive current error $|\epsilon_{react}| < \epsilon_{max}$; at the beginning of each iteration, a short-circuit calculation at steady-state condition is performed.

- *Outer loop*: in the outer loop the active current component is adjusted by the series resistance R and phase angle φ for $u_{WT} \geq< 0.1$ or by series resistance R for $u_{WT} < 0.1$; the iteration process is terminated when the active current error $|\epsilon_{act}| < \epsilon_{max}$.

4.4 DIgSILENT Programming Language (DPL) implementation

The algorithm shown in Fig.4.3 has been implemented in DIgSILENT PowerFactory using the DIgSILENT Programming Language DPL. The implementation of an algorithm with a specific programming language requires the adaptation to the specific philosopy. The DPL includes the following sections:

- *Variable definition*: all variables used in the DPL are defined with specified formats (i.e. object, double, integer);

- *Active study case*: the DPL checks if a study case is active; if not, a warning message is printed in the output windows;

- *Short-circuit command*: if a SC command is not included in the active study case, it is created with default settings;

- *Short-circuit calculation method*: the complete method is automatically selected;

- *Fault location*: the fault location is specified; it can the the HV-side of the WT turbine transformer, a generic terminal or line of the power system;

- *Fault impedance*: the fault impedance is specified; as done in [20] the reactance X_f is specified whereas the resistance R_f is calculated as $X_f/5$;

- *Initial conditions*: default initial conditions for the WT model are specified (i.e. series resistance $R = 0.1pu$, series reactance $X = 1pu$ and the phase angle of the a.c. voltage source $\varphi = -30^o$);

- *Execute short-circuit calculation*: the SC calculation is run and the solution is checked; if an error has occured during the calculation, the DPL routine is safely exited;

- *Measurement*: all significant variables in *pu* are taken from the solution of the SC calculation; significant variables are the WT terminal voltage u_{WT} (magnitude u_{WTm}, phase angle $\varphi_{u_{WT}}$, real part u_{WTr} and immaginary part u_{WTi}), the PCC voltage u_{PCC} (magnitude u_{PCCm}, phase angle $\varphi_{u_{PCC}}$, real part u_{PCCr} and immaginary part u_{PCCi}), WT active and reactive powers (P_{WT} and Q_{WT});

- *Print results of the outer loop*: at each execution of the outerloop shown in Fig.4.3, some interesting results are printed in the output windows (i.e. counter, WT voltage u_{WT}, WT active power P_{WT} and reference value P^*_{WT}, WT reactive power Q_{WT} and reference value Q^*_{WT}, active and reactive power errors $\Delta P = P_{WT} - P^*_{WT}$ and $\Delta Q = Q_{WT} - Q^*_{WT}$, active and reactive current errors $\epsilon_{act} = i_{act} - i^*_{act}$ and $\epsilon_{react} = i_{react} - i^*_{react}$.

- *Print results of the SC calculation*: when the iterative process has been terminated, the results of the short-circtuit calculation are shown in the schematic; for every element that connects two busbars, interesting values are SC power S_k, SC current I_k, peak SC power i_p, active power P and reactive power Q, whereas for busbars and terminals interesting values are the busbar voltages. Moreover, depending on the user's need, some results of the WT model may be shown in the output window; significant values could be WT active and reactive power, P_{WT} and Q_{WT}, WT active current i_{act} and the reference value i^*_{act}, WT reactive current i_{react} and the reference value i^*_{react}, final parameters of the WT model, such as X, R and φ.

The fact that, at the end of the DPL execution, $|i_{act} - i^*_{act}| \leq \epsilon_{max}$ and $|i_{react} - i^*_{react}| \leq \epsilon_{max}$ proves that the WT model behaves as expected, which means as required by the reference German grid code [18]. In fact the WT supports the grid during the fault by injecting reactive current according to Fig.4.2.

The developed DPL routine only implements one WT model at a time; however the same algorithm can be adopted to more WT models in a later implementation.

4.5 Summary

An equivalent VSC-based WTs for short-ciruit calculation has been developed and presented. It is based on the Thevenin equivalen where paramenters, such as X, R and φ, are adjusted by a routine in order to force the model to behave as expected. The WT behavior at steady-state condition is characterized by the active and reactive current injected at the WT busbar; as the German grid code has been selected as reference, the reactive current injection during a grid fault is evaluated accordingly as depicted in Fig.4.2. The model has been implemented in DigSILENT PowerFactory using the DPL-Programming Language. At the end of the DPL execution, $|i_{act} - i^*_{act}| \leq \epsilon_{max}$ and $|i_{react} - i^*_{react}| \leq \epsilon_{max}$ proves that there is full control of the injected active and reactive current components. As the grid voltage support is performed according to Fig.4.2, minimum requirements for FRT have been properly implemented in DIgSILENT PowerFactory.

Chapter 5

Model comparison

Contents

5.1 Introduction

This chapter focuses on the evaluation of the wind turbine model for short-circuit calculation presented in chapter 4. Before the developed WT model is extensively used by TSOs for short-circuit investigations, *credibility*, *numerical robustness* and *quality of predicted results* must be verified and be beyond question [53][54]. Therefore the developed DPL-based WT model for SC calculations must be properly evaluated. Therefore the steady-state operating conditions of the developed WT model have been compared with the steady-state results obtained with the dynamic model of the 3.6MW variable-speed wind turbine developed and provided by Siemens Wind Power. The latter model is implemented in DIgSILENT PowerFactory and validated with certified fault-ride-through tests [54]; it complies with the German grid code and therefore is a suitable and accurate reference for the comparison.

The dynamic model provided by Siemens Wind Power is first described. Then some significant study cases for the comparison are defined. Then, some tests are performed to prove that the DPL-based WT model can be successfully used to control the active and reactive current components. Results are finally compared and some conclusions are given.

5.2 Why validation

The model validation is fundamental if the proposed wind turbine model will be used with confidence in short-circuit studies. An uncorrent current contribution from a wind turbine/farm to the grid during a fault may lead to a wrong voltage at the connection point, thus, leading to a different

requirement concerning the reactive current injection [18]. Moreover, a wrong current contribution from a wind farm to the grid may lead to the wrong design and coordination of the protective system of a considerably big portion of the power system.

The validation must ensure that the wind turbine model represents with sufficient accuracy the performance of the real turbine. It involves two distinct processes [53]: *measurement* and *comparison*. *Measurements* shall be perfomed in some significant conditions for which the model is developed; therefore the DPL-based WT model shall require measurements at steady-state conditions in case of persistent SC, without switching of any circuit breaker; however those measurements are impossible to be perfomed experimentally due to the severeness and therefore measurements can be obtained from a validated dynamic model of the WT. The second process involved in the model validation is the *comparison* where measurements in significat conditions are compared with results obtained with the reference model in the same conditons.

In this work, the measurement process is based on simulations performed with the validated dynamic WT model of the 3.6MW variable-speed wind turbine which is briefly introduced in the next section.

It must be noted that the DPL-based WT model is based on a general control routine which does not necessarily represent the exact control applied by Siemens Wind Power. Thus, some discrepancy is expected and cannot be accounted to an uncorrect implementation.

5.3 Wind turbine dynamic model for comparison

Siemens Wind Power (SWP), in cooperation with TNEI Services, has developed a reduced dynamic model representing the SWP 3.6MW variable-speed wind turbine [54]. The model is implemented in the simulation tools DIgSILENT Power Factory and Siemens PTI PSS/E. The reduced model is a r.m.s. positive-sequence model comprising:

- drive-train system;
- the aerodynamic rotor and pitch control;
- advanced fault-ride-through control and grid voltage support;
- relay protection system and other relevant components.

The SWP 3.6MW wind turbine complies with the German grid code which specifies minimum requirements concering FRT and grid support; however higher capability can be expected depending on the real design and behavior of the WT.

Fig.5.1 shows the SWP 3.6MW WT installed onshore. Technical specifications of the SWP 3.6MW WT are presented in Table 5.1.

Rated power	3.6MW	Rotor speed	5-13rpm
Rotor diameter	107m	Generator type	Asyncrhronous
Hub height tower	80m or site specific	Frequency	Variable
Cut-in wind speed	3-5m/s	Synchronous speed	1500rpm
Rated wind speed	12-15/s	Voltage	690V
Cut-out wind speed	25m/s	Power regulation	Pitch and variable-speed

Table 5.1: *Main technical specifications for Siemes Wind Power 3.6MW variable-speed wind turbines.*

Figure 5.1: *Onshore Siemens Wind Power 3.6MW variable-speed wind turbine. Courtesy of Siemens Wind Power.*

Using the SWP dynamic model, a large wind farm can be either represented as single-machine equivalent, a single rescaled wind turbine model representing the whole wind farm or as a detailed multi-component representation comprising all WTs within the wind farm [54].

The SWP dynamic model and the fault ride-through response have been validated by certified tests at the Hovsøre test site in Denmark [54]. The WT has been subjec to a balanced three-phase short-circuit at the PCC (i.e. HV-side of the WT transformer). Measurements required for validation has been obtained with different voltage dips and fault durations. The voltage dip was varied by the fault impedance Z_f.

In [54], the following study cases are presented:

- 0% retain voltage and 250ms fault duration;
- 50% retain voltage and 710ms fault duration.

An example of results of validation tests performed by Siemens Wind Power are shown in the following in case of 0% *retain voltage and* 250ms *fault duration* and kindly given by Siemens Wind Power to this report [54]. Results refer to the SWP WT working at rated conditions when the three-phase SC is initiated. In Fig.s 5.2, 5.3 and 5.4 the following results are shown [54]:

- experimental test resuls (i.e. blue lines);
- simulation results obtained with the SWP dynamic model implemented in Siemens PTI PSS/E (i.e. red lines);
- simulation results obtained with the SWP dynamic model implemented in DIgSILENT PowerFactory (i.e. green lines).

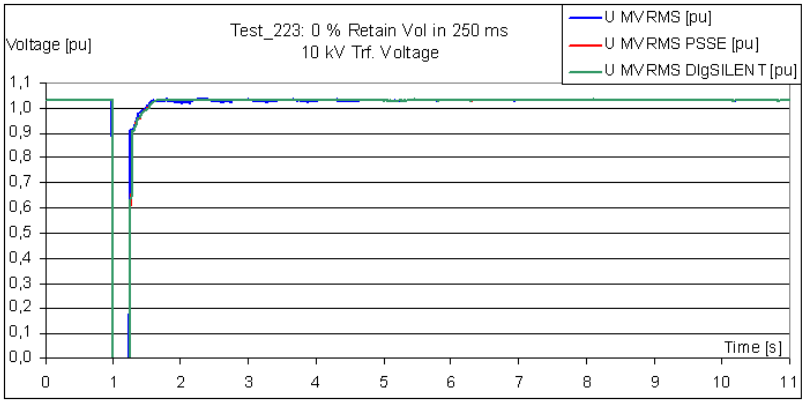

Figure 5.2: *Voltage at the HV-side of the WT transformer (10kV). Courtesy of Siemens Wind Power.*

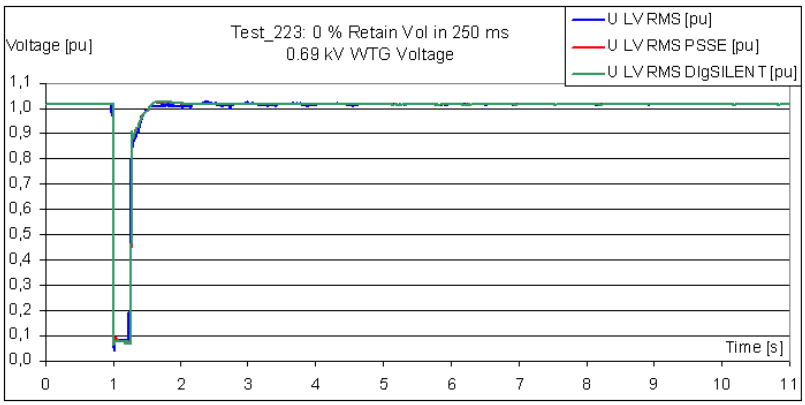

Figure 5.3: *Voltage at the LV-side of the WT transformer (0.69kV). Courtesy of Siemens Wind Power.*

The simulation results obtained with both simulation tools are in good and satisfactory agreement with each other and with the experimental measurements. By performing numerous FRT certified tests, SWP has validated the dynamic model of its SWP 3.6MW variable-speed wind turbine [54]. In Fig.5.2 it can be seen that, in case of bolded SC, the PCC voltage drops to zero. However, the voltage at the LV-side of the WT transformer (see Fig.5.3) does not drop to zero thank to the reactive current injection provided by the WT full-scale power converter. In Fig.5.4 it can be seen that in normal condition the WT injects some reactive for the voltage control; furthermore the reactive current support to the grid during the voltage dip exceeds $1pu$. (the operation during the grid fault is on the safe side of the German grid code).

The validated WT dynamic model represents the accurate implementation of the FRT capability of the 3.6MW wind turbine. This means that results obtained with such a model can be further used for comparison with the developed model of VSC-based wind turbines for short-circuit calculations based on the DPL routine described in chapter 4. As the real wind turbine works on the safe side of the German grid code during the grid fault and the developed WT model implements minimum requirements, some discrepances are expected in the comparison.

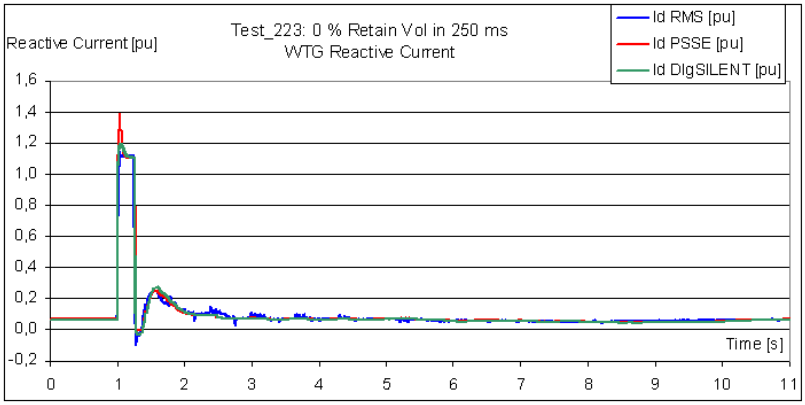

Figure 5.4: *Wind turbine reactive current. Courtesy of Siemens Wind Power.*

5.4 Study cases

By common agreement, short-circuit studies are carried out for balanced three-phase short-circuit faults because they usually result in the largest SC currents and voltage dips; therefore they are considered the worst case situation for the grid voltage recovery [55]. Tests has been executed with different voltage dips, and thus different fault impedances Z_f, and different short-circuit power S_k of for the grid. The desired voltage dip is achieved by varing the fault reactance X_f with fixed ratio $R_f/X_f = 0.2$ as in [20]. Depending on the SC power of the grid, the same fault impedance will lead to different voltage dips; therefore Z_f has to be changed to achieve the desired voltage dip with a different grid.

The fault current contribution from a 3.6MW wind turbine is analyzed[1]. The following three study cases are considered:

- *study case 1 - weak grid*: power grid with $S_k = 10MVA$ and ratio $R_g/X_g = 0.1$;
- *study case 2 - normal grid*: power grid with $S_k = 10P_n = 36MVA$ and ratio $R_g/X_g = 0.1$, as specified by the Danish grid code [35];
- *study case 3 - stiff grid*: power grid with $S_k = 100MVA$ and ratio $R_g/X_g = 0.1$.

Since the DPL does not converge to a steady-state solution for $u_{WT} < 0.07pu$, $u_{WTC} = 0.1pu$ is considered as the lowest WT voltage.

The comparison between steady-state measurements obtained with both models is based on the following results:

- voltage at point of common coupling, u_{PCC} $[pu]$;
- injected reactive current for grid voltage support, i_{react} $[pu]$;
- WT reactive power, Q_{WT} $[pu]$.

For confidentiality reasons, some results obtained with the SWP dynamic model (e.g. the steady-state active current i_{act} injected by the WT into the grid during a grid fault) are not provided by Siemens Wind Power.

[1]The fault current contribution from a wind farm to the grid will be considered in chapter 6

5.5 Test results with the DPL-based WT model

In this section important test results are shown. However, numeric results are presented in Appendix A.

5.5.1 Test scenario

The scenario is shown in Fig.5.5 as a single-line schematic.

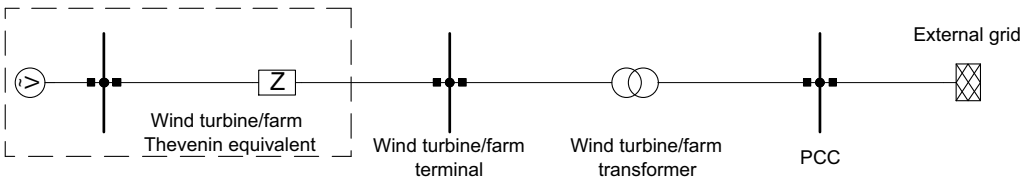

Figure 5.5: *WT model for SC calculation connected to an external grid by means of a transformer.*

The considered wind turbine has a rated power $S_{WT,n} = 3.6MW$. The schematic includes:

- the WT Thevenin equivalent that implements the WT fault current contribution (i.e. fault ride-through capability and grid voltage support according to the German code); the series impedance has rated power $S_{imp,n} = S_{WT,n} = 3.6MVA$;
- the three-phase WT transformer with the following data:
  - rated power $S_{Tn} = 3.6MVA$;
  - nominal frequency $f_n = 50Hz$;
  - rated voltages $V_{LV} = 0.69kV$ and $V_{HV} = 30kV$;
  - short-circuit voltage $u_{k\%} = 6\%$;
- external grid with symmetrical SC power S_k and ratio $R_g/X_g = 0.1$.

Since only balanced faults are considered in this project, the vector group of the transformer is not relevant.

5.5.2 Test example

An example of short-circuit calculation in case of weak grid is shown in the following where a three-phase short-circuit fault with fault reactance $X_f = 50\Omega$ and resistance $R_f = X_f/5 = 10\Omega$ is considered at the PCC. Results of the short-circuit calculation performed using the developed DPL routine are shown in Fig.5.6 on the single-line schematic.

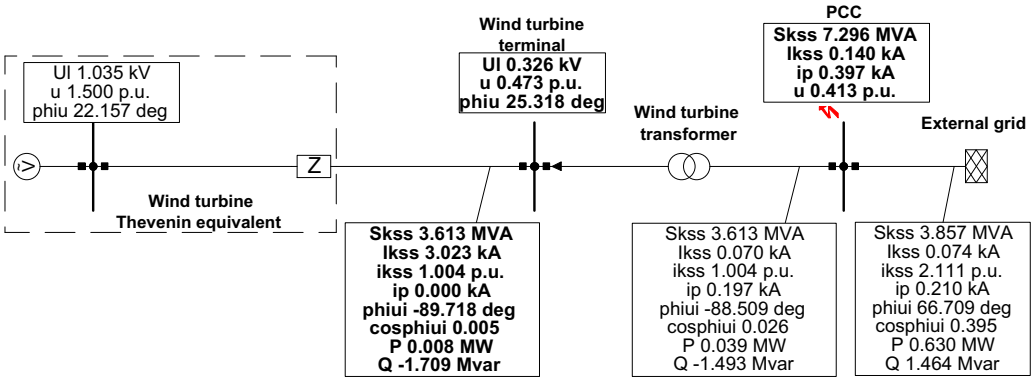

Figure 5.6: *Example of short-circuit calculation. DigSILENT schematic.*

Table 5.2 presents significant results from the schematic in Fig.5.6.

WT terminal voltage u_{WT}	[pu]	0.473
PCC voltage u_{PCC}	[pu]	0.413
WT symmetrical SC power S_k	[MVA]	3.613
WT symmetrical SC current I_k	[kA]	3.023
WT symmetrical SC current i_k	[pu]	1.004

Table 5.2: *Example of short-circuit calculation. Results from the DigSILENT schematic.*

Detailed results regarding the wind turbine model are given in the DIgSILENT output window and reshown in Table 5.3.

Reference active current $i_{act,ref}$	[pu]	0.0000
Active current i_{act}	[pu]	-0.0049
Reference reactive current $i_{react,ref}$	[pu]	1.0000
Reactive current i_{react}	[pu]	1.0037
WT active power P_{WT}	[MW]	-0.0084
WT reactive power Q_{WT}	[MVAr]	1.7087
WT model - reactance X	[Ω]	1.0214
WT model - resistance R	[Ω]	0.0774
WT model - phase angle a.c. voltage source φ	[^{o}]	-7.8429

Table 5.3: *Detailed results from the DIgSILENT output window.*

As shown in Table 5.3, the wind turbine injects 100% reactive current (i.e. $i_{react} = 1.0037pu$) in order to support the grid voltage as required by the German grid code.

5.5.3 Results

Numeric results are presented in Appendix A; for a simpler understanding, some results for each study case are plotted as a function of the WT voltage u_{WT}.

Study case 1 - weak grid

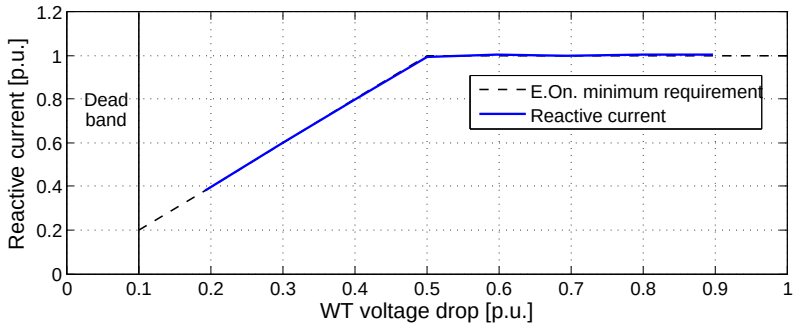

Figure 5.7: *Wind turbine reactive current i_{react} and minimum requirement of the German grid code. Weak grid.*

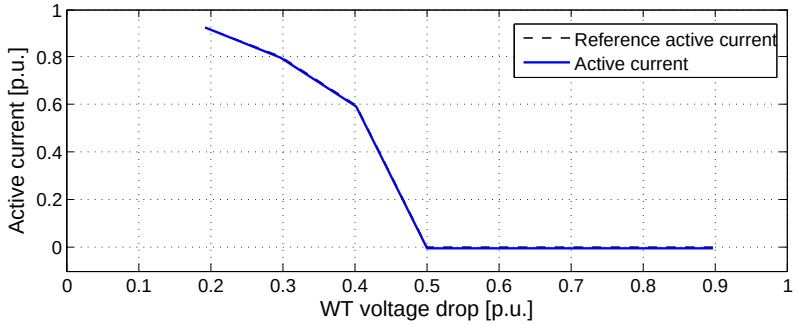

Figure 5.8: *Wind turbine active current i_{act} and reference i^*_{act}. Weak grid.*

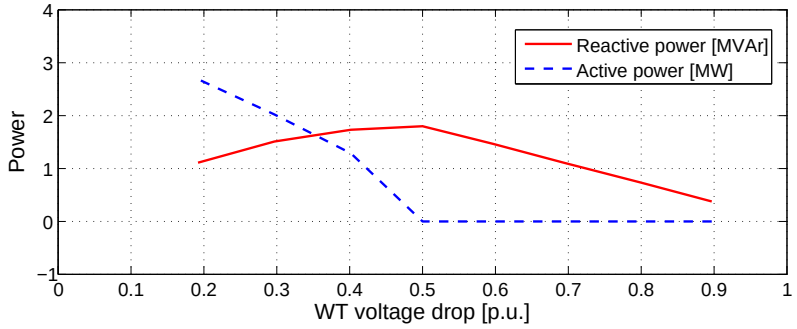

Figure 5.9: *Wind turbine active and reactive powers. Weak grid.*

Study case 2 - normal grid

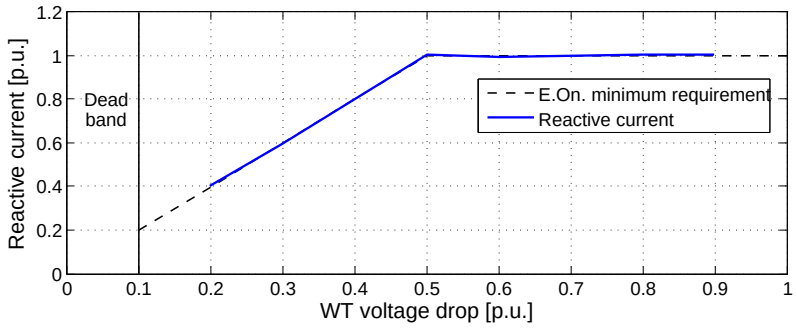

Figure 5.10: *Wind turbine reactive current i_{react} and minimum requirement of the German grid code. Normal grid.*

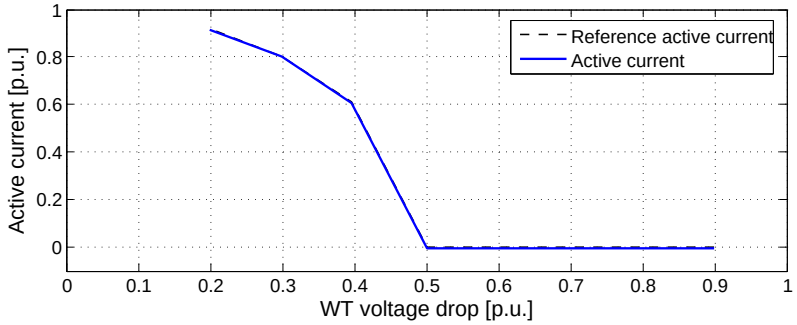

Figure 5.11: *Wind turbine active current i_{act} and reference i^*_{act}. Normal grid.*

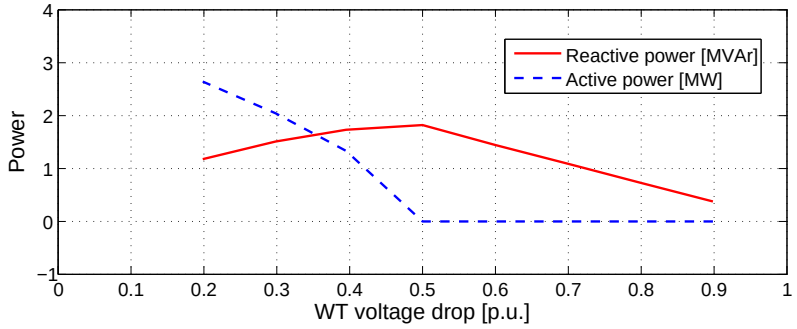

Figure 5.12: *Wind turbine active and reactive powers. Normal grid.*

Study case 3 - stiff grid

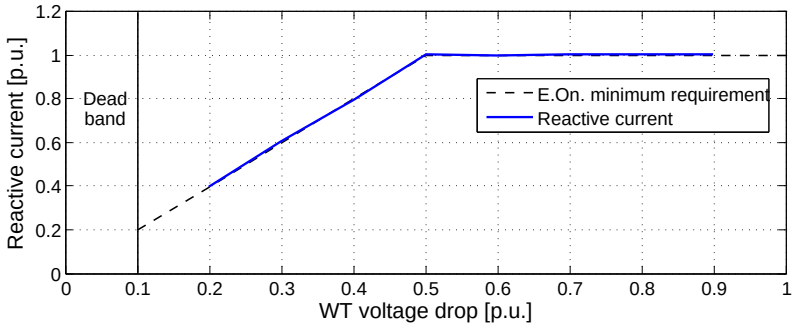

Figure 5.13: *Wind turbine reactive current i_{react} and minimum requirement of the German grid code. Stiff grid.*

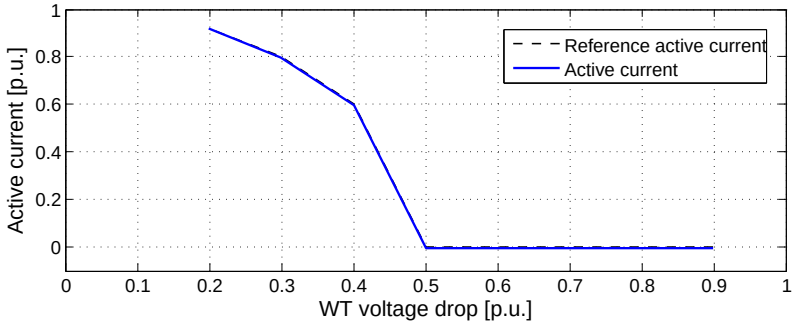

Figure 5.14: *Wind turbine active current i_{act} and reference i^*_{act}. Stiff grid.*

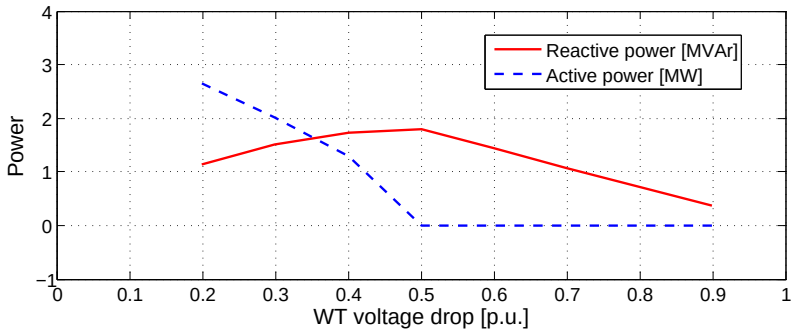

Figure 5.15: *Wind turbine active and reactive powers. Stiff grid.*

5.5.4 Conclusions

Analysing the results presented in this section and in Appendix A, the following considerations can be given:

- the DPL routine has always converged for WT voltages between 0.1 and 0.8pu;
- the convergence time is always below 10s; in most cases it is below 5s;

- the grid voltage support implemented in the DPL reflects exactly minimum requirements of the German grid code and provides a general algorithm without specific details of the SWP control; this is proven in Fig.s 5.7, 5.10 and 5.13.

- the DPL routine has been successfully used to control active and reactive current injected by the wind turbine at the LV-side of the WT transformer; this is shown in Fig.s 5.16 and 5.17, where the reactive and active current errors, ϵ_{react} and ϵ_{act}, are plotted.

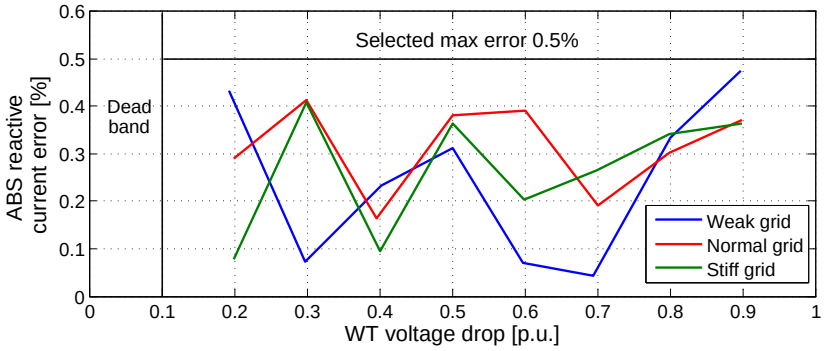

Figure 5.16: *Reactive current error* $|\epsilon_{react}| = |i^*_{react} - i_{react}|$ *in %.*

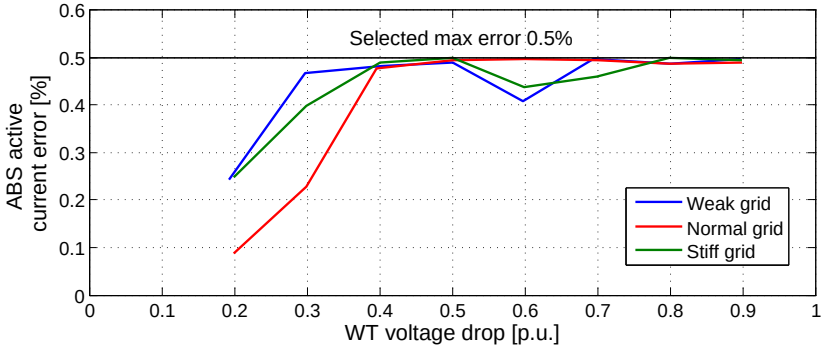

Figure 5.17: *Active current error* $|\epsilon_{act}| = |i^*_{act} - i_{act}|$ *in %.*

It can be seen that they are always below 0.5% as fixed in section 4.3;

- as shown in Fig.5.16 and 5.17, $|\epsilon_{act}|$ is bigger then $|\epsilon_{react}|$; in fact, it has been experienced that the reactive current i_{react} converges fast to the reference $i_{react,ref}$ and then the routine is stopped as soon as $|\epsilon_{act}|$ is below the selected accuracy (i.e. there are no further iterations to reduce $|\epsilon_{act}|$);

- for WT voltages above $0.80pu$, some non-systematic convergence problems have been experienced (i.e. the outer loop of Fig.4.3 does not converge as the active current error $|\epsilon_{act}| > \epsilon_{max} = 0.005$); the convergence problem can, for example, be solved by increasing the maximium error ϵ_{max} or by acting on the active current control;

- the selected accuracy $\epsilon_{max} = 0.005pu$, which means $\epsilon_{max\%} = 0.5\%$, leads to an acceptable speed of execution. In case of higher accuracy, such as $\epsilon_{max\%} = 0.25\%$, the convergence requires in most cases more that $15s$ which is considered unacceptable;

- the short-circuit current contribution to the grid from the wind turbine is only slightly affected by the voltage at the WT terminal voltage; in fact, in all considered cases, S_k and I_k are always within some narrow intervals around the rating values (i.e. S_k and I_k are both around $1pu$);

- the wind turbine current contribution during the grid fault is never above the rating, meaning that r.m.s. current is always below the rated value. However the reactive current injection according to the German grid code strongly affects the voltage level at the connection point; in fact, while in normal operation the rated current is injected with high power factor (i.e. within $0.9 - 1.0$ inductive), during the grid fault the rated current is injected with low power factor (i.e. even 0 in case of WT voltage dip above $0.5pu$).

5.6 Comparison: DPL vs SWP dynamic model

In this section, the steady-state results obtained with the developed DPL-based wind turbine model for short-circuit calculations are compared with the results provided by Siemens Wind Power and obtained with the SWP 3.6MW WT dynamic model; the latter results are shown in Appendix B. Since both sets of results refer to different fault conditions (i.e. different WT voltages), the comparison in not performed analitically according to the available mearements but graphically. The graphical interpolation between available points allows the comparison within the entire WT voltage range. The comparison is based on the above described study cases.

5.6.1 Study case 1 - weak grid

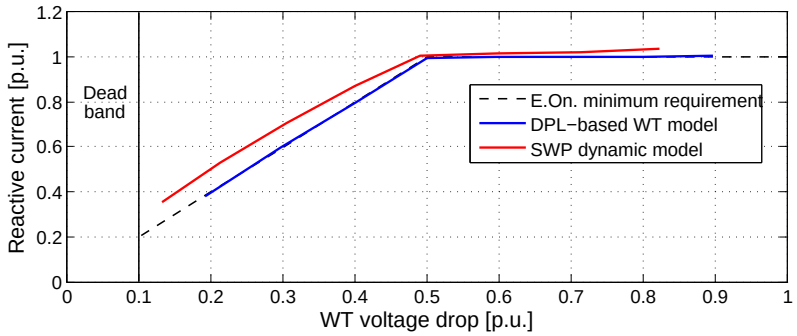

Figure 5.18: *WT reactive current. Comparison between the DPL-based WT model and the SWP dynamic model. Weak grid.*

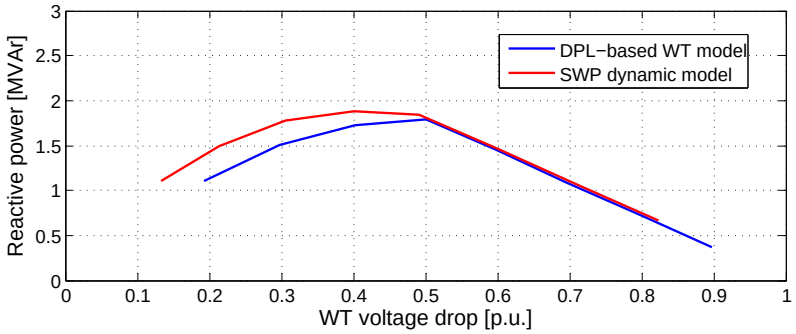

Figure 5.19: *WT reactive power. Comparison between the DPL-based WT model and the SWP dynamic model. Weak grid.*

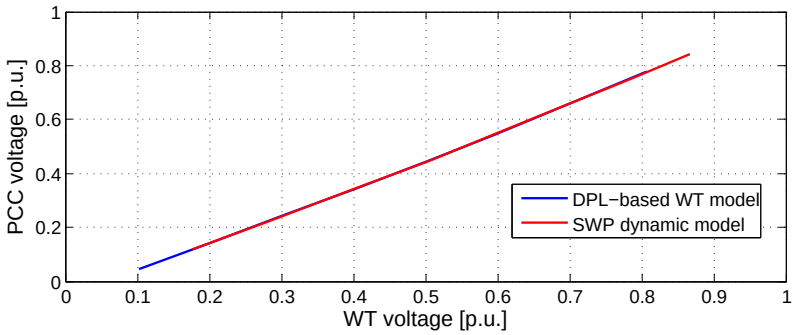

Figure 5.20: *PCC voltage. Comparison between the DPL-based WT model and the SWP dynamic model. Weak grid.*

5.6.2 Study case 2 - normal grid

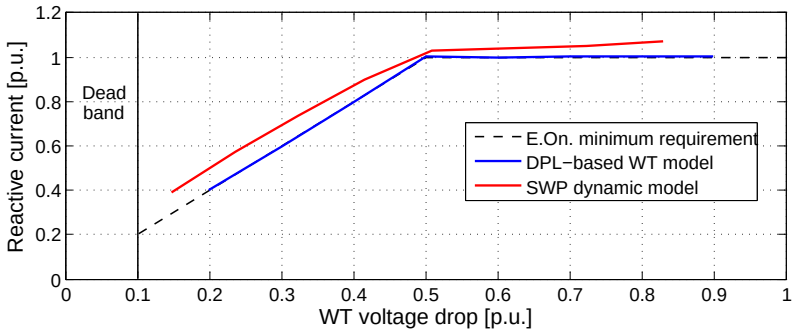

Figure 5.21: *WT reactive current. Comparison between the DPL-based WT model and the SWP dynamic model. Normal grid.*

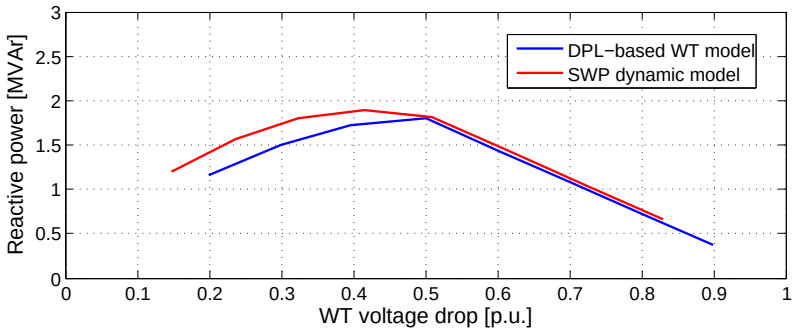

Figure 5.22: *WT reactive power. Comparison between the DPL-based WT model and the SWP dynamic model. Normal grid.*

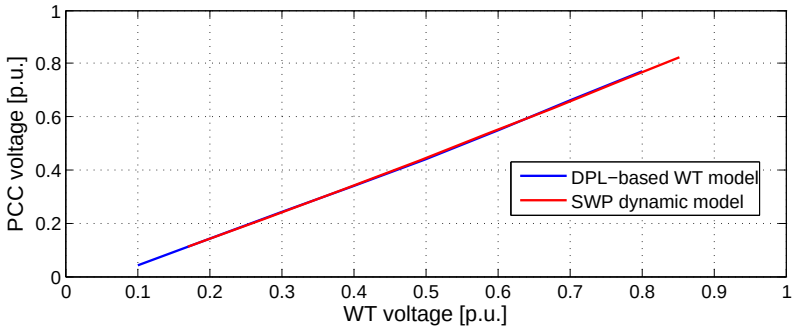

Figure 5.23: *PCC voltage. Comparison between the DPL-based WT model and the SWP dynamic model. Normal grid.*

5.6.3 Study case 3 - stiff grid

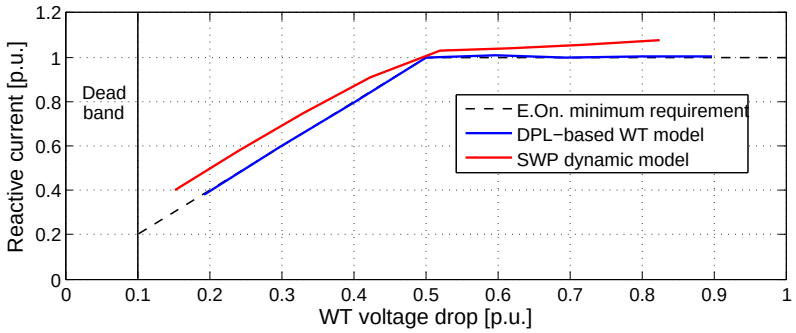

Figure 5.24: *WT reactive current. Comparison between the DPL-based WT model and the SWP dynamic model. Stiff grid.*

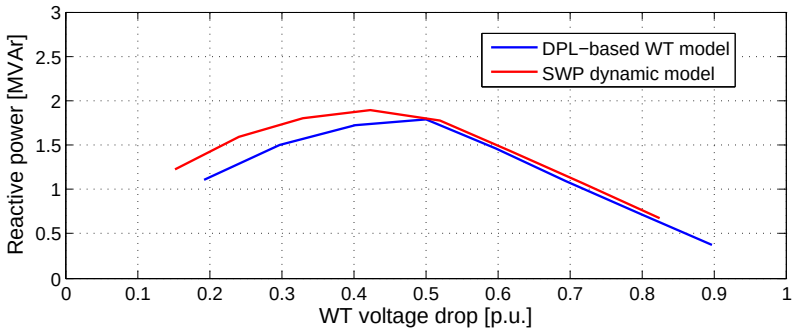

Figure 5.25: *WT reactive power. Comparison between the DPL-based WT model and the SWP dynamic model. Stiff grid.*

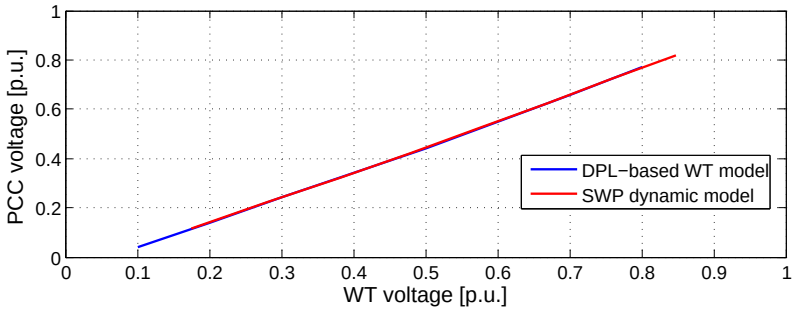

Figure 5.26: *PCC voltage. Comparison between the DPL-based WT model and the SWP dynamic model. Stiff grid.*

5.6.4 Conclusions

Analysing results of the comparison between the the developed DPL-based WT model and the SWP dynamic model, the following condiderations can be given:

- the comparison can only be performed graphically and, thus, the error can not be analytically evaluated; this is due to the fact that available measures obtained with the DPL-based WT model and the SWP dynamic model do not refer to the same WT voltages;
- discrepances on the reactive current i_{react} and power Q_{WT} are justified by the different implementation of fault ride-through cabability; in fact, while the developed WT model implements minimum requirements of the German grid code concerning the grid voltage support (see Fig.4.2), the SWP 3.6MW WT operates on the safe side during the voltage support by injecting more reactive current/power than required;
- even injecting sligthly different reactive current due to the different implementation of the faul ride-through capability, the PCC voltage is not strongly affected and therefore the error between the two models is very small;
- as it can be seen in Fig.s 5.20, 5.23 and 5.26, the voltage drop on the WT turbine transformer, $\Delta_T = u_{WT} - u_{PCC}$, is the same in all study cases and for both models; since the same transformer model has been used, this means that the rms currents on LV and HV-sides are always the same and, thus, the fault current contribution is always close to $1pu$;

Some discrepancy has been obtained when comparing the results of the DPL-based general model and the manufacturer specific model provided by Siemens Wind Power. The discrepancy is present because the DPL-based general model is built up on a general algorithm regarding the grid-compliance rules of the German TSO E.On Netz and does not necessarily includes specific control details used by Siemens Wind Power. The DPL-based model is developed as a general model to represent expected behaviour of wind turbines with full-rating power converters without direct relation to a specific manufacturer.

The results and discrepancy have been discussed with Siemens Wind Power which agreed that the DPL-based general model is implemented in a correct and sufficiently accurate way, but not necessarily represents the specific control of Siemens Wind Power wind turbines. Indeed, the discrepancy might be expected since a general algorithm has been compared to the manufacturer specific control algorithm. It is also agreed that the applied algorithm is general and can be applied for evaluation of SC contribution from the wind turbines with full-scale power converters in a general and common way, i.e. independent from specific design of manufacturers, regarding the present grid-compliance rules.

5.7 Summary

In this chapter the developed DPL-based wind turbine model for short-circuit calculations has been compared with the valiadated dynamic model of the SWP 3.6WM variable-speed WT provided by Siemens Wind Power. Since the SWP 3.6MW wind turbines are with ful-rating power converters, the comparison seems reasonable. The comparison in some significant cases with a good dynamic model is required to assess the credibility, numerical robustness and quality of predicted results of the new model.

The comparison is first based on short-circuit studies with different types of external networks (i.e. weak, normal and stiff grids); the fault impedance is used to obtain the desired voltage at the WT terminal. This first comparison proves that the DPL routine accurately implements the injection of the desired active and reactive current components. Therefore, having a reference reactive current to be injected to support the grid according to the German grid code, the WT model is adjusted so that the steady-state reactive current error is within the chosen accuracy; also the steady-state active current is accurately controlled to be equal to the reference upon which there are no general specifications.

Some discrepancy between the general DPL-based model and the dynamic model of SWP has been obtained. The discrepancy is caused by the diffenence between the applied general approach and the exact control algorithm of Siemens Wind Power. The discrepancy could be reduced if the exact control system is implemented in the DPL-based model; however this work is beyond the target of this project.

Siemens Wind Power agreed that the implemented DPL-based model represents an accurate and satisfatory behavior of a generic algorithm which can be applied for WTs with full-rating converters for FRT.

Chapter 6

Application in the Danish Power System Model

Contents

6.1 Introduction

In this chapter the developed VSC-based wind turbine model for short-circuit calculations at steady-state conditions is used with different scenarios. The goal is to demonstrate how it can be used to perform short-circuit investigations in power systems including large wind farms.

The Danish transmission system is considered and the fault current contribution from a large offshore wind farm to the grid is included in the investigation. First, the DPL-based WT model is rescaled to the rated power of the large offshore wind farm; the obtained DPL-based wind farm model is then used to perform short-circuit calculations in a realistic scenario including the Danish transmission system model. Several study cases are considered including balanced three-phase faults at some significant fault locations.

6.2 Fault current contribution from the Nysted/Rødsand offshore wind farm to the grid

The largest wind farm in Denmark is Nysted offshore wind farm at Rødsand built in 2003. The wind farm is located approximately $10km$ south of the town of Nysted on Lolland in the south of Denmark and consists of 8 rows with 9 turbines each, yielding 72 wind turbines and a the total installed capacity of $165.6MW$ [60]. Fig.6.1 shows the offshore Nysted wind farm and its location.

Figure 6.1: *The Nysted offshore wind farm is located 10km south of Lolland on Rødsand Bank. Courtesy of Siemens Wind Power.*

The annual electricity production of the wind farm is $600GWh$, enough to supply 145000 (Danish) households (e.g. the entire ciiy of Odense). The wind turbine towers are $69m$ tall and the rotor blades $41m$ long [61]. They were delivered by the Danish wind turbine manufacturer BONUS Energy A/S, which was acquired by Siemens Wind Power A/S in December 2004. The wind farm is owned by a joint venture, in which DONG Energy owns 80% and E.ON Sweden 20% [61].

The Nysted offshore wind farm is equipped with $2.3MW$ fixed-speed active-stall controlled wind turbines. This means that the actual wind farm configuration does not include VSC-based wind turbines. Furthermore, since the wind farm is installed in Denmark, it complies with the Danish grid code which does not require the grid voltage support in case of grid fault. It yields that it is not appropiate to represent the real Nysted offshore wind farm using the DPL-based wind farm model that implements the German grid code.

In the following, it is considered that a large offshore wind farm replaces the Nysted wind farm; it is assumed that:

- it has the same installed capacity of the Nysted wind farm (i.e. $165.6MW$);
- it is connected at the same busbars;
- it comprises wind turbines with full-rating power converters;
- it complies with the German grid code with respect to the grid voltage support in case of grid fault.

Since they have the same total installed capacity, the large offshore wind farm can be identified as Nysted-size offshore wind farm. The Nysted-size offshore wind farm can be included in the short-circuit investigation; it is therefore represented by the Thevenin equivalent-based model introduced in section 4.2, which is connected at the LV-side of the WF transformer (see Fig.6.2). The short-circuit calculation can be performed by using the the developed DPL routine where the following external objects have been defined:

- a.c. voltage source of the Thevenin equivalent and its terminal;

- impedance of the Thevenin equivalent, whose rated power is equal the wind farm rating, such as $165.6MW$;
- wind farm terminal;
- HV-voltage side terminal of the WF transformer;
- fault location.

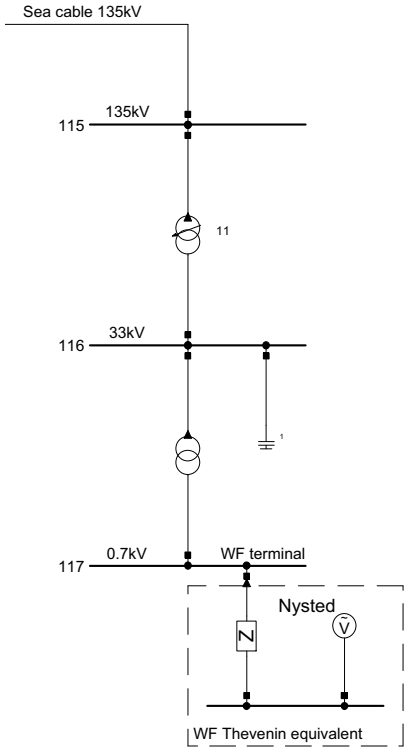

Figure 6.2: *Nysted-size offshore wind farm with full-rating converters-based wind turbines. Thevenin equivalent connected at the LV-side of the wind farm transformer.*

The fault location can be any terminal, busbar or line in the entire power system, meaning that also remote fault can be analyzed.

Example of short-circuit calculation including the fault current contribution from the Nysted-size offshore wind farm

In this section the developed DPL-based WT model is rescaled to obtain an aggregated model of the Nysted-size offshore wind farm suitable for short-circuit studies; the model is obtained by rescaling, to the wind farm rating, the rated power of both the series impedance and the WF transformer.

The single-line schematic is represented in Fig.6.3.

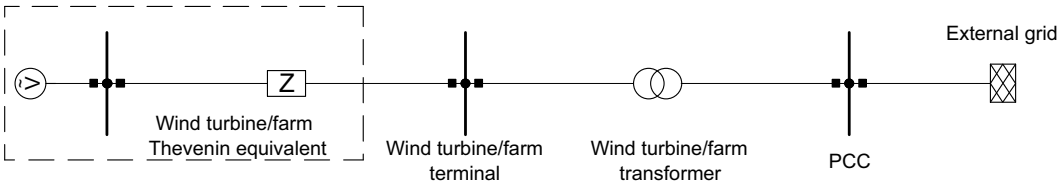

Figure 6.3: *Wind farm model for short-circuit calculations connected to an external grid.*

It includes:

- the Thevenin equivalent of the wind farm with adjustable series resistance, reactance and a.c. voltage source phase angle; the series impedance has rated power $S_{imp,n} = S_{WF,n} = 165.6MVA$, where $S_{WF,n}$ is the wind farm rated power;
- an equivalent three-phase transformer with the following data:
  - rated power $S_n = S_{WF,n} = 165.5MVA$;
  - nominal frequency $f_n = 50Hz$;
  - rated voltages $V_{LV} = 0.69kV$ and $V_{HV} = 30kV$;
  - short-circuit voltage $u_{k\%} = 6\%$;
- external grid with symmetrical short-circuit power $S_k = 10S_{WF,n} = 1656MVA$ and ratio $R_g/X_g = 0.1$, as specified by the Danish grid code regarding the simulation test model for wind farms connected at the transmission level [35].

In the following, an example of short-circuit calculation is shown. A three-phase short-circuit is considered at the PCC; the fault impedance Z_f is chosed such that the retain WT voltage is $u_{WT} = 0.25pu$, with $R_f = X_f/5$. Results of the short-circuit calculation performed using the developed DPL routine are shown in Fig.6.4 on the single-line schematic.

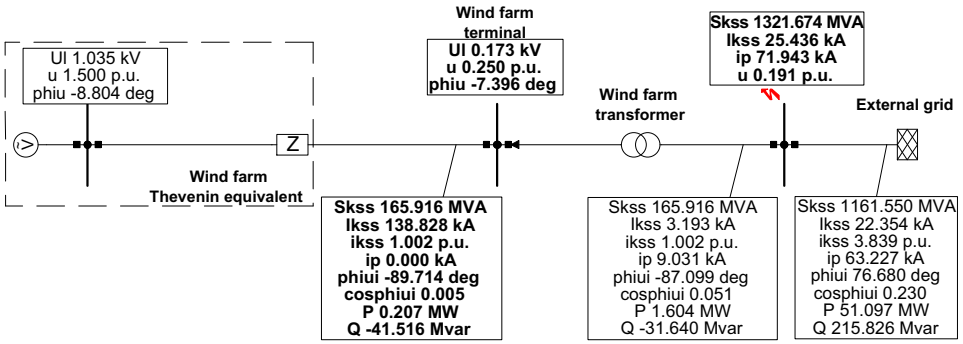

Figure 6.4: *Results of the short-circuit calculation.*

Table 6.1 presents significant results from the schematic in Fig.6.4.

WF terminal voltage u_{WF}	[pu]	0.2503
PCC voltage u_{PCC}	[pu]	0.1911
WF symmetrical SC power S_k	[MVA]	165.92
WF symmetrical SC current I_k	[kA]	138.83
WF symmetrical SC current i_k	[pu]	1.0022

Table 6.1: *Short-circuit calculation results from the DigSILENT schematic.*

Detailed results regarding the wind farm model are given in the DIgSILENT output window and reshown in table 6.2.

Reference active current i^*_{act}	[pu]	0.0000
Active current i_{act}	[pu]	-0.0050
Reference reactive current i^*_{react}	[pu]	1.0019
Reactive current i_{react}	[pu]	1.0019
WF active power P_{WF}	[MW]	-0.2072
WF reactive power Q_{WF}	[MVAr]	41.516
WF model - reactance X	[Ω]	1.2471
WF model - resistance R	[Ω]	0.0306
WF model - phase angle a.c. voltage source φ	[^{o}]	-8.8040

Table 6.2: *Detailed results from the DIgSILENT output window.*

As shown in table 6.2, the wind farm injects 100% reactive current (i.e. $i_{react} = 1.0019pu$) in order to support the grid voltage as required by the German grid code.

When using the DPL-based WF model, the DPL routine has the same performance and, thus, no significant differences can be identified for the convergence.

6.3 Small test model of the Danish transmission system

A realistic model of the power system is useful to evaluate the fault ride-through capability of wind turbines and their control strategies. However those models are normally developed and maintained by power grid companies and TSOs; therefore they are usually too detailed and not available for confidentiality reasons. In [60], a small test model of the Eastern Danish transmission system is presented; it has been developed by the Danish TSO Energinet.dk and submitted to the Centre of Energy Technology (CET) of the Danish Technical University (DTU), other universities and companies for education and research projects on wind power integration. As the transmission system is represented on a generic level, the model is available to all interested parties, such as power companies, wind turbine manufactures, universities and research centers. The model is implemented in the power system simulation tool DIgSILENT PowerFactory and shown in Fig.6.5. The small test model contains 17 buses with voltages from $0.7kV$ to $400kV$, four central power plants and their control, a static VAR Compensator (SVC), several consumption centers, a lumped equivalent local onshore wind farm and an equivalent of a large offshore wind farm. The central power plants are given by the synchronous generator G1 to G4 and the models of their control systems. The local onshore wind farm includeds fixed-speed wind turbines equipped with conventional asynchronous generators; it is considered operating at 60% of the rated power [60]. The buses from 115 to 117 are located offshore. The large offshore wind farm is connected to the bus 117, has the rating of $165MW$ and is close to the rated operating point. It comprises fixed-speed active-stall controlled wind

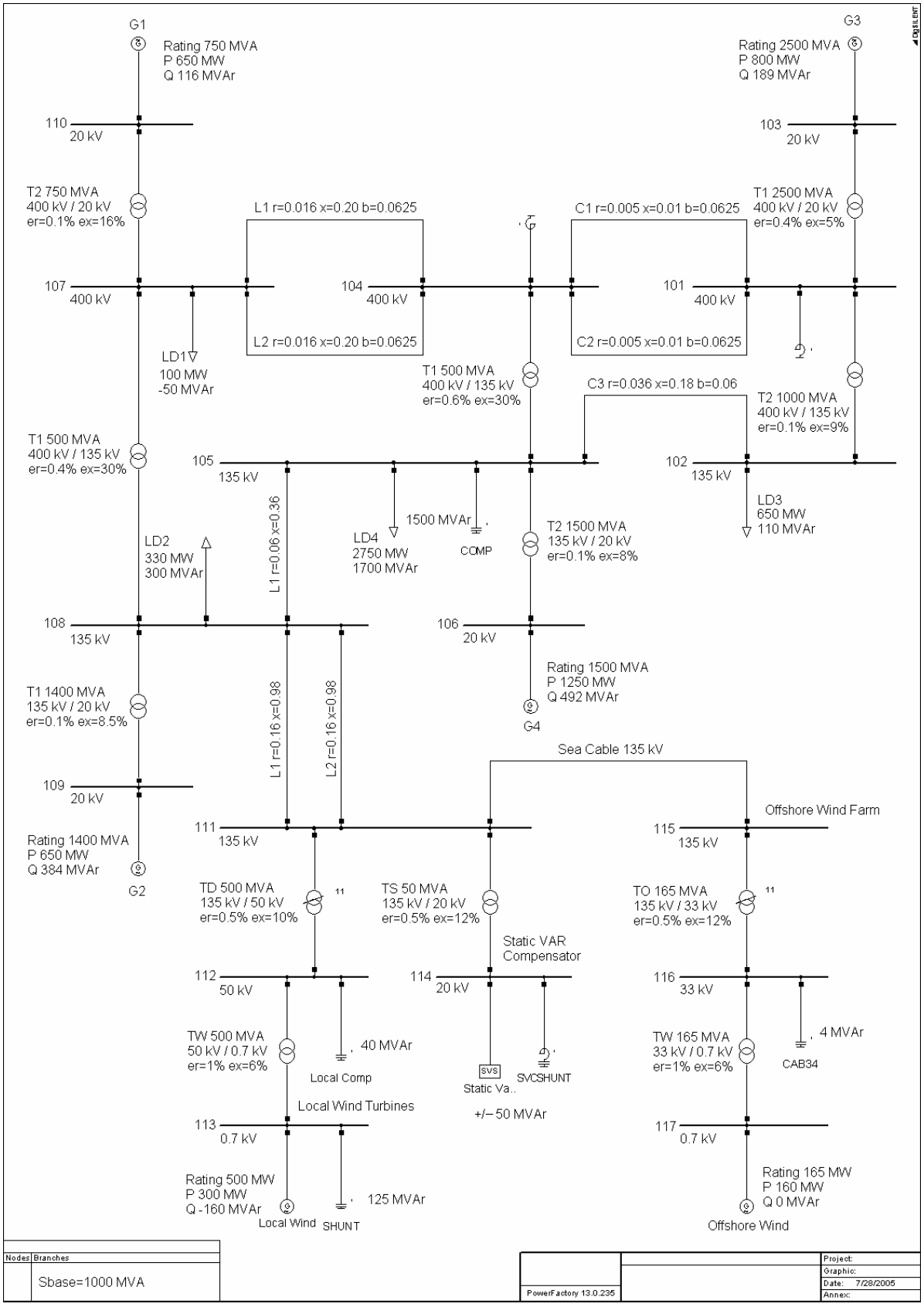

Figure 6.5: *DigSILENT generic model of the Danish transmission system [60].*

turbines and generically represents the Danish offshore wind farm commissioned at Nysted/Rødsand in the year 2003 [60]. The dynamic model of the large offshore wind farm is based on the single-machine approach, which considers a rescaled model representation of the asynchronous generator with the rating of 165 MW [62]. The generator is modelled by the standardized asynchronous generator model included in DIgSILENT Powerfactory. The shaft system, the active-stall control, the FRT and the protective system of the wind farm are modelled by user-written models [60].

The small test model of the Eastern Danish transmission system can be used to compute the dynamic response of the central power plants, the local wind turbines, the large offshore wind farm and the dynamic reactive compensation unit to grid disturbances [60].

In the following, the dynamic model of the large offhore wind farm (i.e. Nysted/Rødsand) will be substituted by the DPL-based wind farm model for short-circuit calculations presented in section 6.2; this will allow performing short-circuit investigations with the fault current controbution from such a wind farm. On the contrary, the model of the onshore wind farm will not be changed because this would require a DPL routine for SC calculations with the inclusion of several wind farms; however, due to time constraints, in this work only the fault current contribution from one wind farm is implemented in the DPL routine.

6.4 Study cases

The developed DPL routine for short-circuit calculations can only be used for balanced grid faults which mostly occur in substations. For this reason, although the single-phase fault on overhead lines has the highest probability in Denmark (see [24]), three-phase short-ciruits in substations are mainly considered in the following.

The above considerations lead to the selection of the following study cases:

- study case 1 - three-phase short-circuit fault at the $33kV$ busbar 116;
- study case 2 - three-phase short-circuit fault at the $135kV$ busbar 115 (i.e. offshore connection point of the Nysted/Rødsand wind farm);
- study case 3 - three-phase short-circuit fault at the $135kV$ busbar 111 (i.e. onshore connection point of the Nysted/Rødsand wind farm);
- study case 4 - three-phase short-circuit fault at the $135kV$ busbar 105;
- study case 5 - three-phase short-circuit fault at the $400kV$ busbar 104;
- study case 6 - three-phase short-circuit fault at 50% of the line $L1$ between busbars 108 and 111.

Since short-circuit calculations are often extreme-case studies, the fault impendance is normally assumed to be zero; however, in some of the considered study cases, convergence problems have been experienced and, thus, a small fault impedance is used when needed. This limitation shall be improved as future work.

6.5 Results of short-circuit calculations with the DPL-based wind farm model

In this section results of the short-circuit calculations are presented. At the end, general conlusions are given.

6.5.1 Case 1. Three-phase short-circuit at the $33kV$ busbar 116

A balanced three-phase short-circuit fault is considered at the $33kV$ busbar 116. The fault impedance Z_f is such that the retain WF voltage is $u_{WF} = 0.1pu$[1]. The DPL routine for the SC calculation converges within $10s$ to the solution shown in Fig.6.6, where significant result boxes are bolded. Table 6.3 presents significant results from the schematic in Fig.6.6 (see result box $B1 - B4$).

WF terminal voltage u_{WF}	[pu]	0.1000
PCC voltage u_{PCC}	[pu]	0.0470
WF symmetrical SC power S_k	[MVA]	166.37
WF symmetrical SC current I_k	[kA]	139.21
WF symmetrical SC current i_k	[pu]	0.9040

Table 6.3: *Short-circuit calculation results from the DigSILENT schematic. Case 1.*

Detailed results regarding the wind farm model are given in the DIgSILENT output window and reshown in table 6.4.

Reference active current i^*_{act}	[pu]	0.0000
Active current i_{act}	[pu]	-0.0049
Reference reactive current i^*_{react}	[pu]	1.0000
Reactive current i_{react}	[pu]	1.0046
WF active power P_{WF}	[MW]	-0.0818
WF reactive power Q_{WF}	[MVAr]	16.638
WF model - reactance X	[Ω]	1.3935
WF model - resistance R	[Ω]	0.0011
WF model - phase angle a.c. voltage source φ	[^{o}]	-10.348

Table 6.4: *Detailed results from the DIgSILENT output window. Case 1.*

As shown in table 6.4, the wind farm injects 100% reactive current (i.e. $i_{react} = 1.0046pu$) in order to support the grid voltage as required by the German grid code. In Fig.6.6, it can be seen that the short-circuit strongly affects the busbar voltages at both the offshore and onshore connection points of the Nysted wind farm, such as busbars 115 and 111; in fact voltages are $u_{115} = 0.555pu$ and $u_{111} = 0.761pu$. However, moving closer to central power plants (see result boxes $B7 - B11$), voltages are above $0.959pu$, meaning that the fault does not affect them strongly.

The wind farm reactive current operating point is represented in Fig.6.7, where it can be seen that it corresponds to the minimum requirement of the E.On. grid code regarding the grid voltage support by means of reactive current injection.

[1]In case of bolded short-circuit at the $33kV$ busbar 116, the WF terminal voltage is equal to the transformer short-circuit voltage, such as $0.06pu$; in this case convergence problems are experienced and therefore the fault impedance is fixed to $Z_f = 0.07pu$, with $R_f = X_f/5$.

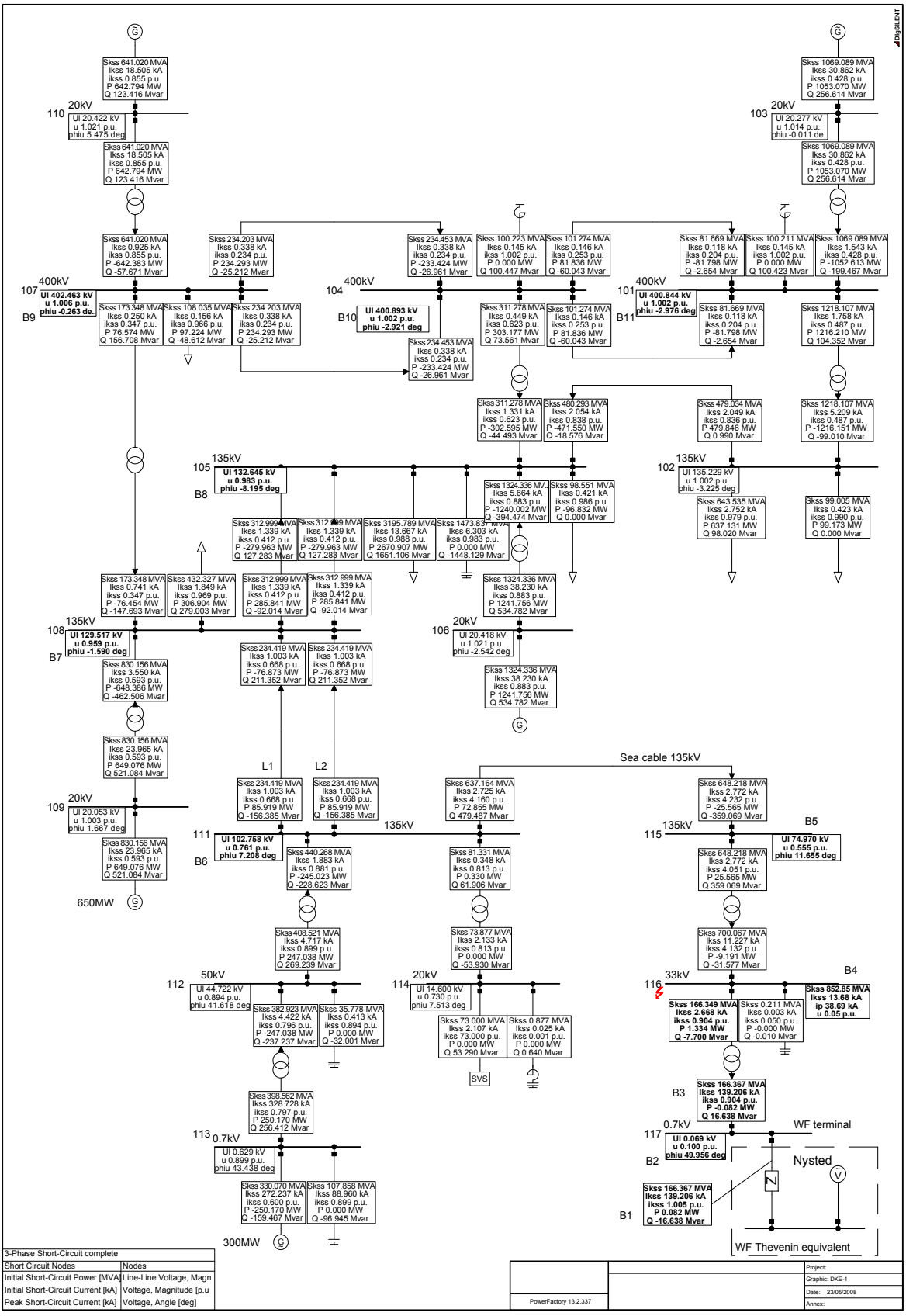

Figure 6.6: *Three-phase short-circuit fault at the 33kV busbar 116. Case 1.*

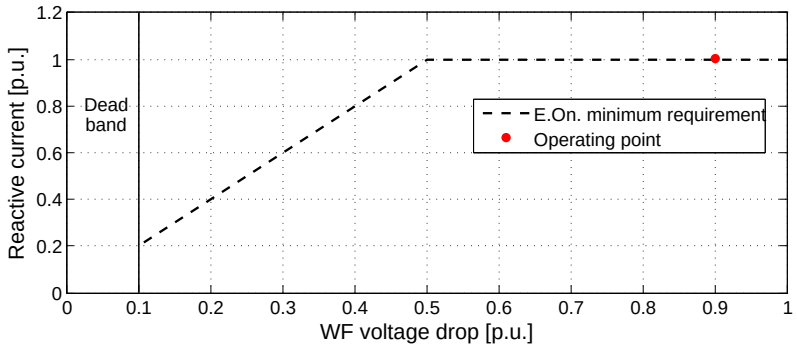

Figure 6.7: *Reactive current operating point. Comparison with minimum requirement of the German grid code. Case 1.*

Fig.6.7 proves that the grid voltage support has been succesfully implemented in the Nysted-size offshore wind farm model for SC calculations and, thus, also its fault current contribution.

6.5.2 Case 2. Three-phase short-circuit at the $135kV$ busbar 115

A balanced three-phase short-circuit fault is considered at the $33kV$ busbar 115. The fault impedance is $Z_f = 0.5\Omega$, with $R_f = X_f/5$. The DPL routine for the SC calculation converges within $10s$ to the solution shown in Fig.6.8, where significant result boxes are bolded. Table 6.5 presents significant results from the schematic in Fig.6.8 (see result box $B1 - B4$).

WF terminal voltage u_{WF}	[pu]	0.2032
PCC voltage u_{PCC}	[pu]	0.1498
WF symmetrical SC power S_k	[MVA]	166.01
WF symmetrical SC current I_k	[kA]	138.91
WF symmetrical SC current i_k	[pu]	0.9022

Table 6.5: *Short-circuit calculation results from the DigSILENT schematic. Case 2.*

Detailed results regarding the wind farm model are given in the DIgSILENT output window and reshown in table 6.6.

Reference active current i^*_{act}	[pu]	0.0000
Active current i_{act}	[pu]	-0.0049
Reference reactive current i^*_{react}	[pu]	1.0000
Reactive current i_{react}	[pu]	1.0024
WF active power P_{WF}	[MW]	-0.1115
WF reactive power Q_{WF}	[MVAr]	33.730
WF model - reactance X	[Ω]	1.2936
WF model - resistance R	[Ω]	0.0025
WF model - phase angle a.c. voltage source φ	[^{o}]	-13.462

Table 6.6: *Detailed results from the DIgSILENT output window. Case 2.*

Also in this case, as the WF voltage is reduced down to $u_{WF} = 0.2032pu < 0.5pu$, according to the German grid code the wind farm injects 100% reactive current (i.e. $i_{react} = 1.0024pu$) in order to support the grid voltage.

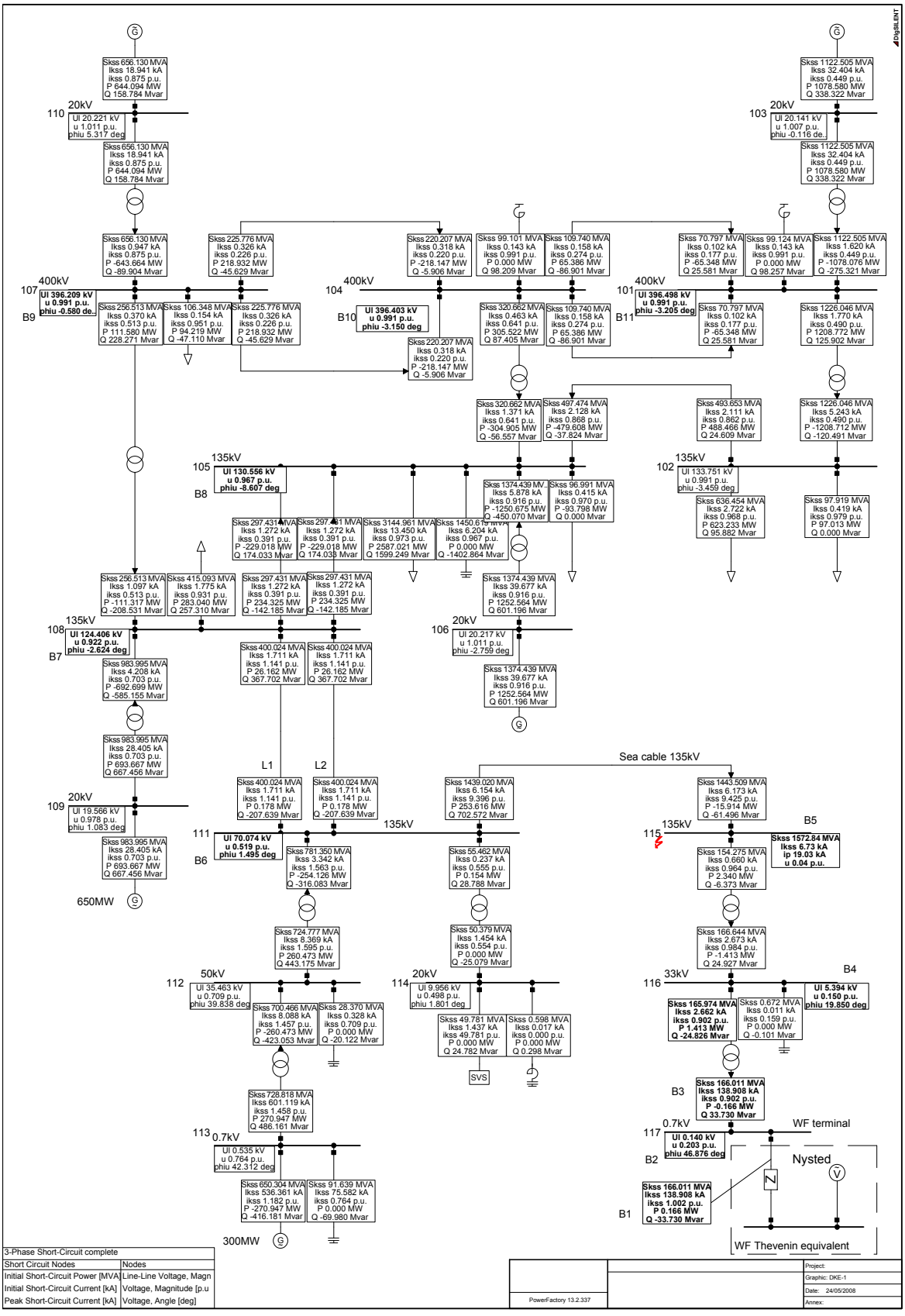

Figure 6.8: *Three-phase short-circuit fault at the* 135kV *busbar 115. Case 2.*

In Fig.6.8, it can be seen that the short-circuit strongly affects the busbar voltage at the onshore connection point of the Nysted wind farm, such as busbar 111; in fact voltages are $u_{111} = 0.519pu$ (see result box $B6$). Voltages at $135kV$ busbars 105 and 108 are affected but they are still above $0.922pu$. Moving closer to central power plants, such as to $400kV$ busbars (see result boxes $B9 - B11$), voltages are above $0.990pu$, meaning that the fault does not affect them strongely.

The wind farm reactive current operating point is represented in Fig.6.9, where it can be seen that it corresponds to the minimum requirement of the E.On. grid code regarding the grid voltage support.

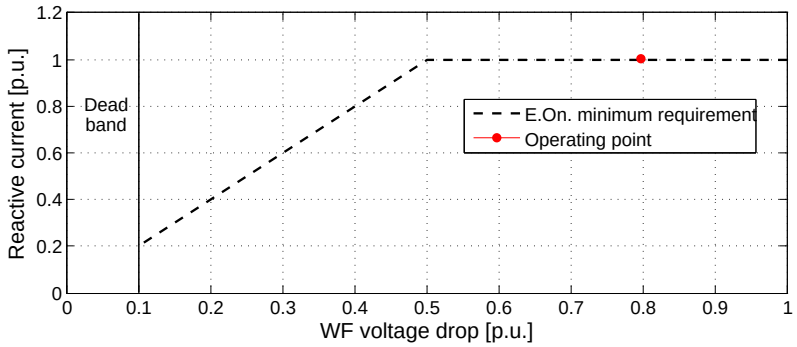

Figure 6.9: *Reactive current operating point. Comparison with minimum requirements of the German grid code. Case 2.*

6.5.3 Case 3. Three-phase short-circuit at the $135kV$ busbar 111

A balanced three-phase short-circuit fault is considered at the $135kV$ busbar 111, which is the onshore conncetion point of the Nysted offshore wind farm. The fault impedance is $Z_f = 0.5\Omega$, with $R_f = X_f/5$. The DPL routine for the SC calculation converges within $10s$ to the solution shown in Fig.6.10, where significative result boxes are bolded. Table 6.7 presents significant results from the schematic in Fig.6.10 (see result box $B1 - B4$).

WF terminal voltage u_{WF}	[pu]	0.2802
PCC voltage u_{PCC}	[pu]	0.2266
WF symmetrical SC power S_k	[MVA]	166.37
WF symmetrical SC current I_k	[kA]	139.21
WF symmetrical SC current i_k	[pu]	0.9042

Table 6.7: *Short-circuit calculation results from the DigSILENT schematic. Case 3.*

Detailed results regarding the wind farm model are given in the DIgSILENT output window and reshown in Table 6.8.

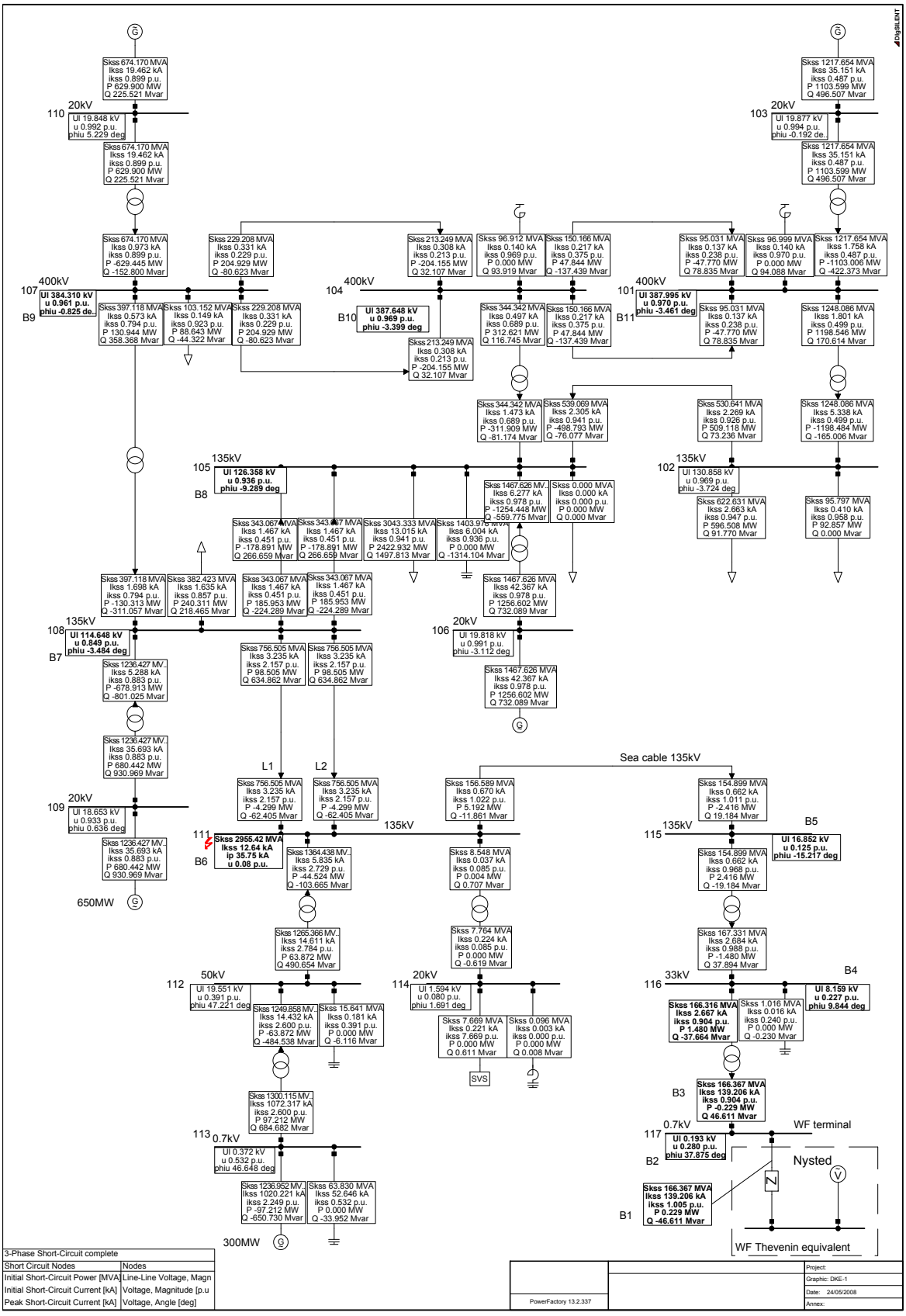

Figure 6.10: *Three-phase short-circuit fault at the* 135*kV busbar 111. Case 3.*

Reference active current i^*_{act}	[pu]	0.0000
Active current i_{act}	[pu]	-0.0049
Reference reactive current i^*_{react}	[pu]	1.0000
Reactive current i_{react}	[pu]	1.0046
WF active power P_{WF}	[MW]	-0.2290
WF reactive power Q_{WF}	[MVAr]	46.611
WF model - reactance X	[Ω]	1.2141
WF model - resistance R	[Ω]	0.0163
WF model - phase angle a.c. voltage source φ	[^{o}]	-22.981

Table 6.8: *Detailed results from the DIgSILENT output window. Case 3.*

Also in this case the wind farm provides full reactive current injection (i.e. $i_{react} = 1.0046pu$) in order to support the grid voltage as required by the German grid code for $u_{WF} < 0.5pu$.

In Fig.6.10, it can be seen that the short-circuit strongly affects voltages at every busbar in the power system. In fact, the voltage at the offshore connection point of the Nysted wind farm is $u_{115} = 0.125pu$; the voltages at the $135kV$ busbars are $u_{108} = 0.849pu$ and $u_{105} = 0.936pu$. Also voltages at the $400kV$ busbars are affected, being below $0.970pu$ (see result box $B9 - B11$).

The wind farm reactive current operating point is represented in Fig.6.11, where it can be seen that it corresponds to the minimum requirement of the E.On. grid code regarding the grid voltage support by means of reactive current injection.

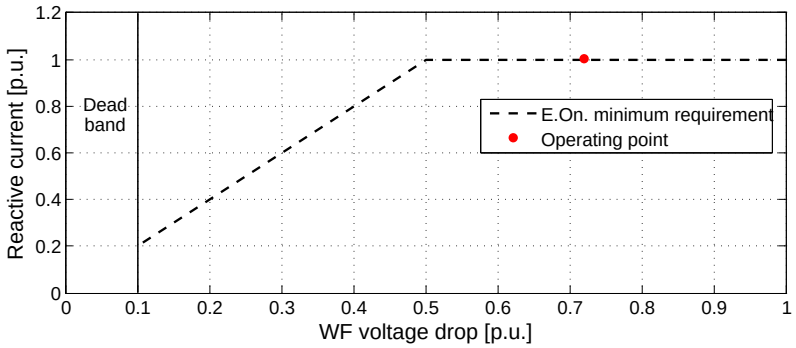

Figure 6.11: *Reactive current operating point. Comparison with minimum requirement of the German grid code. Case 3.*

6.5.4 Case 4. Three-phase short-circuit at the $135kV$ busbar 105

A balanced three-phase short-circuit fault is considered at the $135kV$ busbar 105. The fault impedance is $Z_f = 0$. The DPL routine for the SC calculation converges within $7s$ to the solution shown in Fig.6.12, where significant result boxes are bolded. Table 6.9 presents significant results from the schematic in Fig.6.12 (see result box $B1 - B4$).

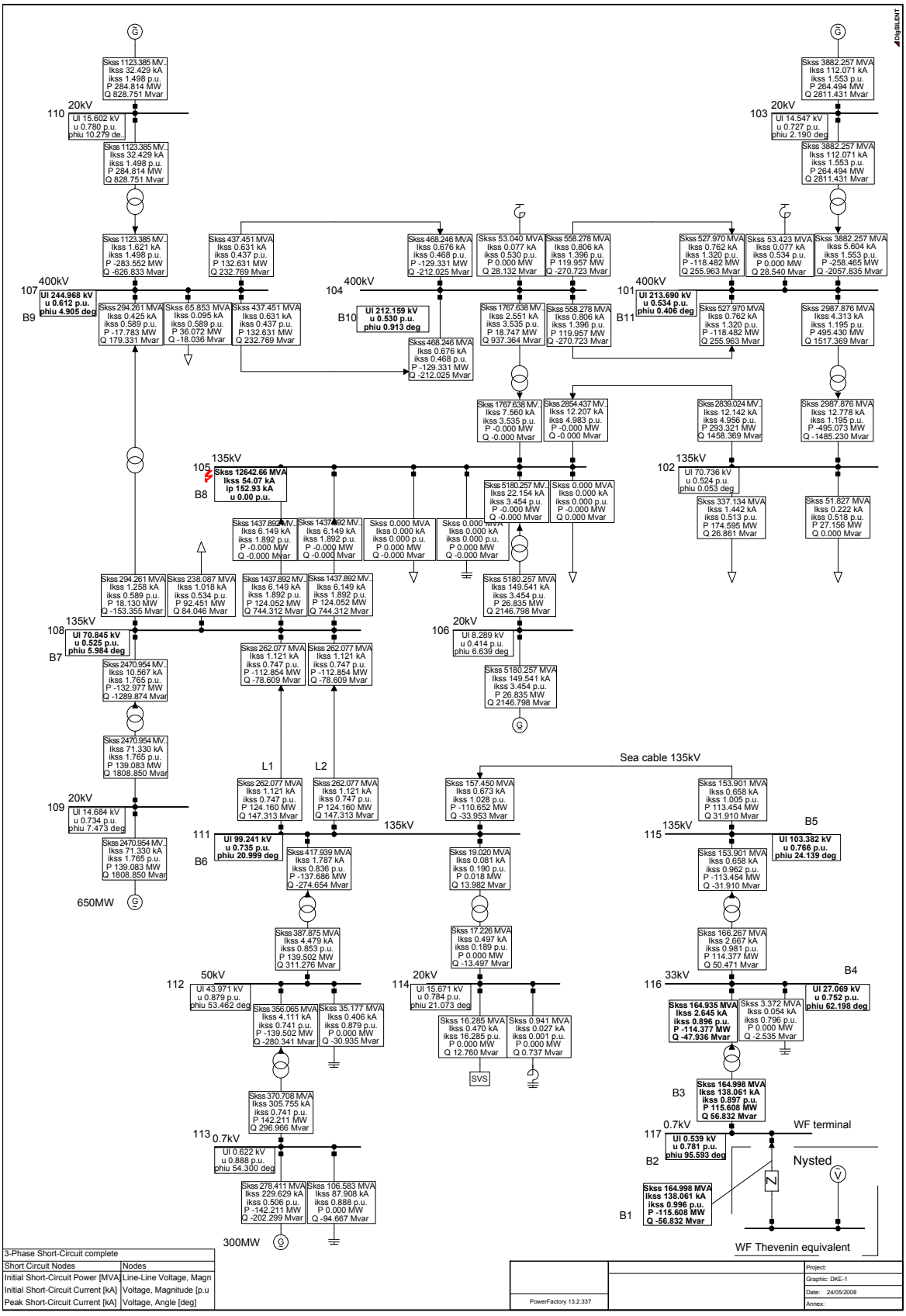

Figure 6.12: *Three-phase short-circuit fault at the* $135kV$ *busbar 105. Case 4.*

WF terminal voltage u_{WF}	[pu]	0.7807
PCC voltage u_{PCC}	[pu]	0.7519
Symmetrical SC power S_k	[MVA]	154.00
Symmetrical SC current I_k	[kA]	138.06
Symmetrical SC current i_k	[pu]	0.8967

Table 6.9: *Short-circuit calculation results from the DigSILENT schematic. Case 4.*

Detailed results regarding the wind farm model are given in the DIgSILENT output window and reshown in Table 6.10.

Reference active current i^*_{act}	[pu]	0.8987
Active current i_{act}	[pu]	0.8942
Reference reactive current i^*_{react}	[pu]	0.4385
Reactive current i_{react}	[pu]	0.4396
WF active power P_{WF}	[MW]	115.61
WF reactive power Q_{WF}	[MVAr]	56.832
WF model - reactance X	[Ω]	0.9218
WF model - resistance R	[Ω]	0.10920
WF model - phase angle a.c. voltage source φ	[^{o}]	66.760

Table 6.10: *Detailed results from the DIgSILENT output window. Case 4.*

As shown in table 6.9, the WF voltage has dropped to $u_{WF} = 0.7807pu > 0.5pu$; therefore, according to the German grid code, the wind farm in not required to inject 100% reactive current in order to support the grid voltage but it must inject at least $i_{react} = 2\Delta u_{WF} = 0.4385pu$.

In Fig.6.12, it can be seen that the short-circuit affects strongly voltages at every busbar in the power system. In fact, the voltage at the offshore connection point of the Nysted-size wind farm is $u_{115} = 0.766pu$; the voltages at the $135kV$ busbars are $u_{111} = 0.735pu$ and $u_{108} = 0.525pu$. Also voltages at the $400kV$ busbars are strongly affected; in fact $u_{101} = 0.534pu$, $u_{104} = 0.530pu$ and $u_{107} = 0.612pu$ (see result box $B9 - B11$).

The wind farm reactive current operating point is represented in Fig.6.13, where it can be seen the it corresponds to the minimum requirements of the E.On. grid code regarding the grid voltage support by means of reactive current injection.

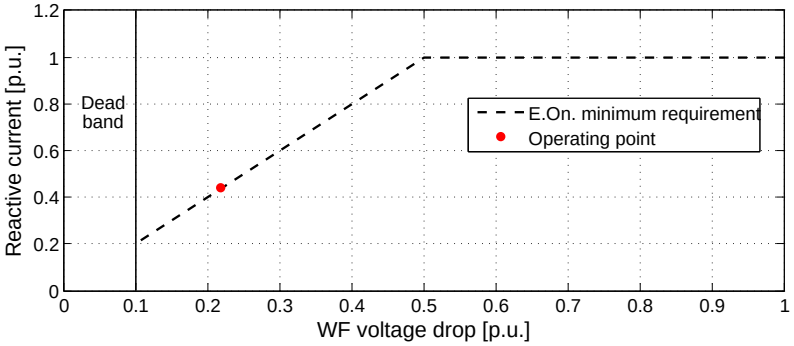

Figure 6.13: *Reactive current operating point. Comparison with minimum requirement of the German grid code. Case 4.*

6.5.5 Case 5. Three-phase short-circuit at the $400kV$ busbar 104

A balanced three-phase short-circuit fault is considered at the $135kV$ busbar 105. The fault impedance is $Z_f = 0$. The DPL routine for the SC calculation converges within $7s$ to the solution shown in Fig.6.14, where significant result boxes are bolded. Table 6.11 presents significant results from the schematic in Fig.6.14 (see result box $B1 - B4$).

WF terminal voltage u_{WF}	[pu]	0.8153
PCC voltage u_{PCC}	[pu]	0.7900
WF symmetrical SC power S_k	[MVA]	164.99
WF symmetrical SC current I_k	[kA]	138.05
WF symmetrical SC current i_k	[pu]	0.8967

Table 6.11: *Short-circuit calculation results from the DigSILENT schematic. Case 5.*

Detailed results regarding the wind farm model are given in the DIgSILENT output window and reshown in table 6.12. As in the previous case, the wind farm is not required to inject 100%

Reference active current i^*_{act}	[pu]	0.9293
Active current i_{act}	[pu]	0.9245
Reference reactive current i^*_{react}	[pu]	0.3693
Reactive current i_{react}	[pu]	0.3713
WF active power P_{WF}	[MW]	124.83
WF reactive power Q_{WF}	[MVAr]	50.128
WF model - reactance X	[Ω]	0.9092
WF model - resistance R	[Ω]	0.1309
WF model - phase angle a.c. voltage source φ	[°]	65.855

Table 6.12: *Detailed results from the DIgSILENT output window. Case 5.*

reactive current in order to support the grid voltage as the WF voltage has dropped to $u_{WF} = 0.8153pu > 0.5pu$.

In Fig.6.14, it can be seen that the short-circuit strongly affects voltages at voltages at the $400kV$ busbars; in fact $u_{101} = 0.054pu$ and $u_{107} = 0.294pu$ (see result box $B11$ and $B9$).

The wind farm reactive current operating point is represented in Fig.6.15, where it can be seen that it corresponds to the minimum requirements of the E.On. grid code regarding the grid voltage support by means of reactive current injection.

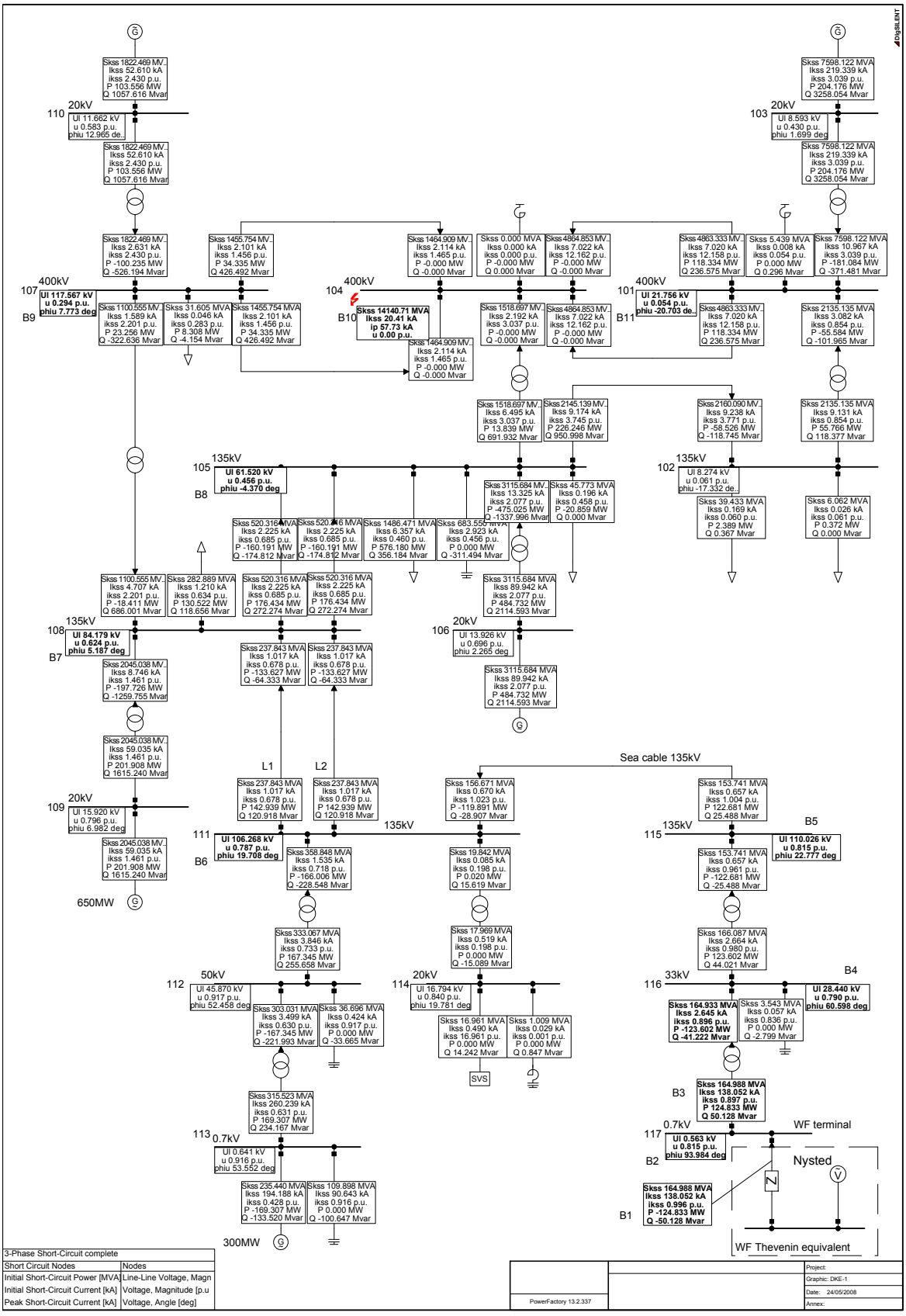

Figure 6.14: *Three-phase short-circuit fault at the 400kV busbar 104. Case 5.*

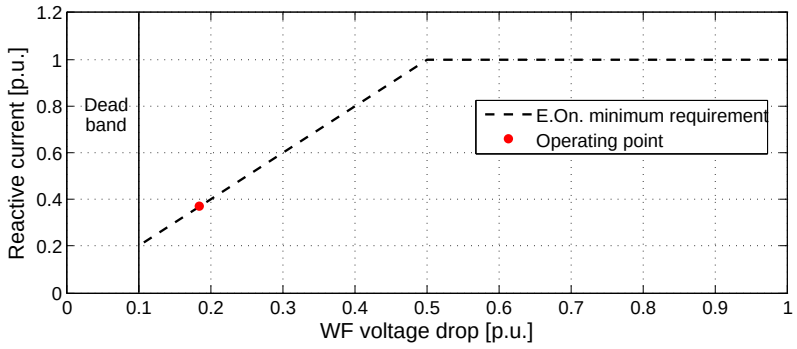

Figure 6.15: *Reactive current operating point. Comparison with minimum requirement of the German grid code. Case 5.*

6.5.6 Case 6. Three-phase short-circuit at 50% of the line $L1$ between busbars 108 and 111

A balanced three-phase short-circuit fault is considered at 50% of length on the line 1 between busbars 108 and 111. This study case proves that, when using the DPL-based routine for SC calculations, the fault location can also be a line. The fault impedance is $Z_f = 0$. The DPL routine for the SC calculation converges within $10s$ to the solution shown in Fig.6.16, where significant result boxes are bolded. Table 6.13 presents significant results from the schematic in Fig.6.16 (see result box $B1 - B4$).

WF terminal voltage u_{WF}	[pu]	0.6409
PCC voltage u_{PCC}	[pu]	0.5982
WF symmetrical SC power S_k	[MVA]	165.14
WF symmetrical SC current I_k	[kA]	138.18
WF symmetrical SC current i_k	[pu]	0.8975

Table 6.13: *Short-circuit calculation results from the DigSILENT schematic. Case 6.*

Detailed results regarding the WF model are given in the DIgSILENT output window and reshown in table 6.14.

Reference active current i^*_{act}	[pu]	0.6959
Active current i_{act}	[pu]	0.6910
Reference reactive current i^*_{react}	[pu]	0.7118
Reactive current i_{react}	[pu]	0.7189
WF active power P_{WF}	[MW]	73.348
WF reactive power Q_{WF}	[MVAr]	76.311
WF model - reactance X	[Ω]	0.9476
WF model - resistance R	[Ω]	0.0758
WF model - phase angle a.c. voltage source φ	[^{o}]	56.619

Table 6.14: *Detailed results from the DIgSILENT output window. Case 6.*

Also in this case the wind farm is not required to inject 100% reactive current in order to support the grid voltage as the WF voltage has dropped to $u_{WF} = 0.6463pu > 0.5pu$.

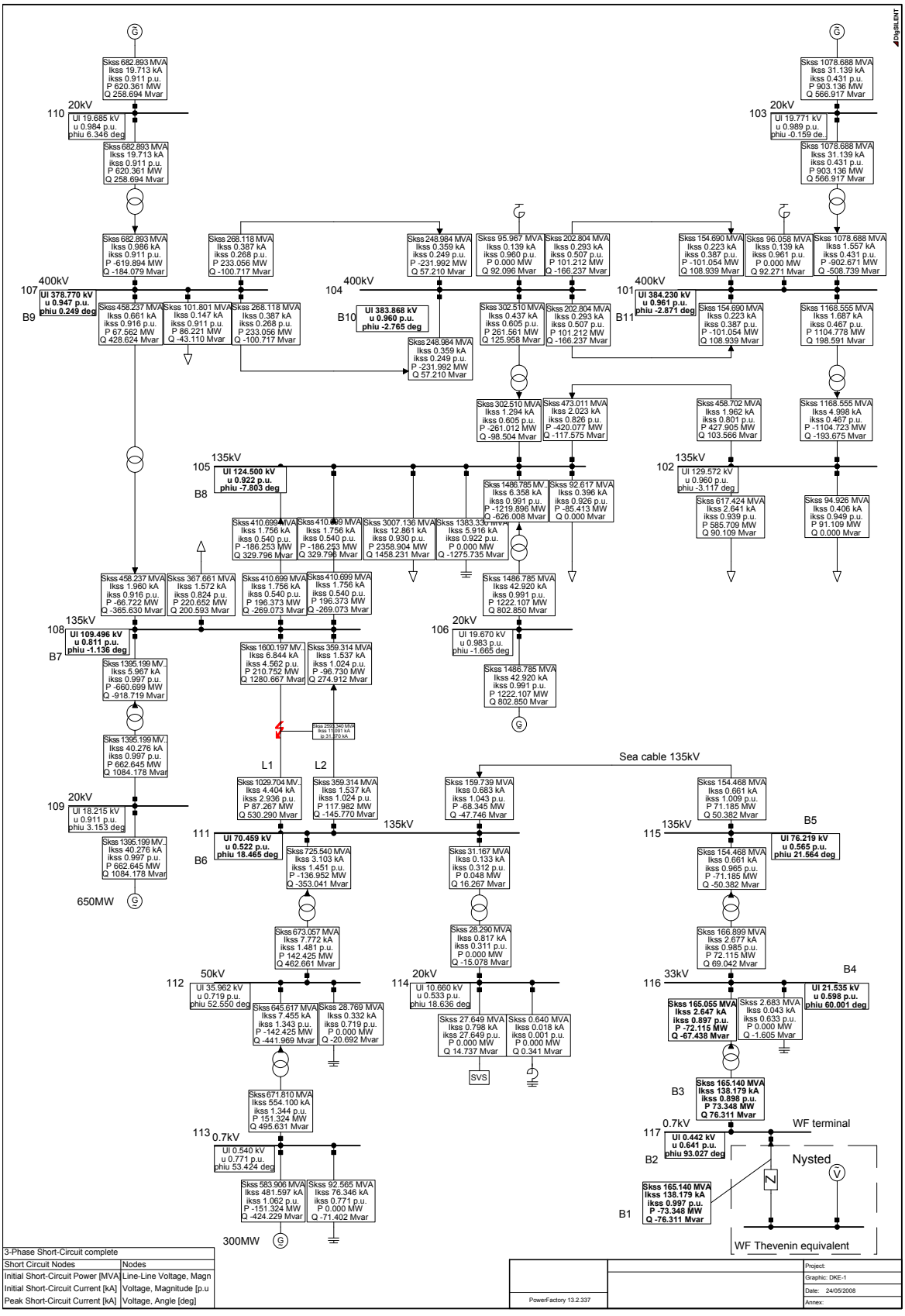

Figure 6.16: *Three-phase short-circuit fault at* 50% *of the line 1 between busbars* 108 *and* 111. *Case 6.*

The wind farm reactive current operating point is represented in Fig.6.17, where it can be seen that it corresponds to the minimum requirements of the E.On. grid code regarding the grid voltage support.

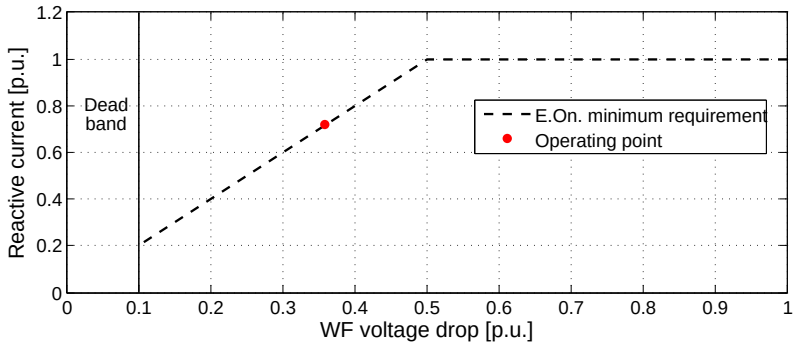

Figure 6.17: *Reactive current operating point. Comparison with minimum requirement of the German grid code. Case 6.*

6.5.7 Conclusions

The fault current contribution from a large scale wind farm to the grid have been successfully implemented in DIgSILENT PowerFactory; the fault contribution is based on the injection of specified active and reactive currents complying with the German grid code.

The DPL routine for short-circuit calculation has been successfully used for investigations in a real scenario including the Danish transmisson system. The analysis have been performed for different fault locations, such as significant terminals and lines; this has proven that also remote faults can be analysed.

Some convergence issues have been experience in sections 6.5.3, 6.5.3 and 6.5.2; in those cases, a short-circuit with zero fault impedance yields a WF voltage too low to be able to control the injected active current according to the reference value; on the contrary, the reactive current is properly controlled even at low WF voltage. In those case, since i_{act} does not converge the the reference i^*_{act}, the DPL routine is safely stopped. This has to be further improved as future work.

As expected, the convergence is slower when considering an entire transmission system instead of an external power grid as in section chapter 6.2, which is also to be improved as future work; however a computational time below $10s$ is considered acceptable.

6.6 Summary

In this chapter an aggregate DPL-based wind farm model for short-circuit calculations at steady-state conditions is developed by rescaling the wind turbine model presented in chapter 4. The Nysted-size offshore wind farm is modelled as equipped with full-rating converters-based WTs and the Danish transmission system is considered for the analysis. Since the real Nysted wind farm does not include VSC-based wind turbines and complies with the Danish grid code, it is not appropiate to represent it using the DPL-based wind farm model. For this reasons it is assumed that it complies with the German grid code with respect to the grid voltage support and comprises wind turbines with full-scale power converter; with those assumptions the Nysted wind farm has been modelled by means of the DPL-based WF model and included in short-circuit studies.

Several study cases have been considered at some significant fault locations, such as some busbars and a line; it has been proven that also remote three-phase short-circuit faults can be analysed. Test results prove that the grid voltage support has been successfully implemented in the Nysted-size wind farm model for SC calculations. In fact, in each case, the DPL-based wind farm model injects into the grid at least the minimum reactive current required by the German grid code; also the active current is fully controlled being equal to its reference within the chosen accuracy. This means that the wind farm fault current contribution has been successfully implemented.

Conclusions

When performing short-circuit investigations in power systems including wind power, valuable and accurate results can only be obtained by considering the real behaviour of wind turbines which is specified in national grid codes. This requires the consideration of the exact active and reactive current injections. Requirements for fault ride-through capability and grid voltage support are fundamental in this work as the study of the short-circuit current contributions from wind turbines to the grid makes sense only if WTs are required to remain connected and support the grid in case of grid fault in order to ensure the stability of the power system.

At the beginning of this work, it was not possible to perform short-circuit studies at steady-state conditions that include the fault current contribution from VSC-based grid wind turbines; it could only be evaluated by performing full dynamic simulations based on a detailed dynamic network model. However, since this approach is time consuming and requires detailed models, power system companies normally prefer to refer to international standards that provide sufficiently accurate methods for short-circuit calculations at steady-state.

The most important goals of this work are *(i)* the development of an equivalent model of VSC-based wind turbines for short-circuit calculations at steady-state conditions, *(ii)* the development of a general routine for short-circuit calculations including the fault current contribution from VSC-based WTs to the grid and *(iii)* evaluation of the developed WT model by comparison with the validated WT dynamic model provided by Siemens Wind Power.

In chapter 1, entitled **Project definition**, a background on the wind energy technology is provided where several WT concepts are presented; then, the problem of the fault current contribution from wind turbines to the grid is defined. Project limitations are given regarding the considered WT concept, such as VSC-based wind turbine, the considered grid fault, such as balanced three-phase fault, and the power system simulation tool used to carry out the short-circuit investigations. Finally, project goals are summarized in a compact way and an outline of the report is provided.

In chapter 2, entitled **Requirements for fault ride-through capability for wind turbines**, general technical requirements for wind turbines from national grid codes are briefly presented.Then, the attention is paid on the most relevant grid codes for the project; the Danish, the German and the Spanish grid codes are deeply analyzed concerning the fault ride-through and grid voltage support specifications. The Danish grid code is important because it provides a detailed description of the simulation model, including the power grid model, to verify basic stability properties of WTs. The German and Spanish grid codes are important because they are the only ones requiring the grid voltage support during a grid fault.The German grid code is assumed as reference with respect to grid voltage support specifications.

In chapter 3, entitled **Short-circuit calculation**, short-circuit calculations at steady state conditions are introduced. Short-circuit studies are frequently performed by power system companies such that the power systems can be correctly dimensioned and protected, allowing safe and economic operation. The time behaviour of the SC current is analized to identify characteristic values and types of short-circuit that can occur in a power system are classified. Then, four methods for SC

calcuations are presented; they are *nodal method*, *symmetrical component method*, *superposition method* and *dynamic time-based simulations*; it is highlighted how the selected method depends on the application (i.e. planning studies or analysis of specific operating conditions) and on the required accuracy. Power system companies normally perform those investigations at steady-state conditions and using approximations provied by international standars; therefore standards regarding SC calculations are analysed in order to identify differences and similarities about requirements, approximations and methodologies. Two main approaches have been identified: the IEC method, according to the IEC 60909/VDE 0102, and the ANSI method, according to the IEEE 141/ANSI C37. Finally, the implementation of short-circuit methods in DIgSILENT PowerFactory is deeply described.

In chapter 4, entitled **Model of VSC-based wind turbines for short-circuit calculations**, an equivalent VSC-based wind turbine model for short-ciruit calculations has been developed and presented. It is based on the Thevenin equivalent where paramenters are adjusted by a general routine in order to force the model to behave as required by the German grid code; in fact the reference reactive current i^*_{react} is calculated according to the minimum requirement of the German grid code whereas the reference active current i^*_{act} is calculated to avoid overloading of the full-scale frequency converter. The desired active and reactive currents are achieved by adjusting paramenters of the Thevenin equivalent-based WT model. The routine, including the adjustable WT model, has been implemented in DigSILENT PowerFactory using the DPL-Programming Language.

In chapter 5, entitled **Model validation**, the developed DPL-based wind turbine model for short-circuit calculations has been compared with the validated dynamic model of the SWP 3.6MW variable-speed WT provided by Siemens Wind Power. The comparison in some significant cases proves that the DPL routine accurately implements the injection of the desired WT active and reactive current components. The general DPL routine, based on the general implementation of the German grid code, has given good and satisfactory results; it has always converged within $10s$ for WT voltages between 0.1 and $0.8pu$. Some discrepancy is obtained when comparing the generic DPL routine with the dynamic model provided by Siemens Wind Power; this is justified as the DPL routine does not necessarily includes specific control details but, on the contrary, it is based on a general algorithm. The manufacturer Siemens Wind Power, which has supported this work, agreed that the implemented algorithm represent a general behavior of full-rating converters-based WTs in a suitable way, although SWP does not necessarily applies the same control. The discrepancy is explained by the use of a general algorithm that represents the expected behaviour of wind turbines with full-rating power converters without direct relation to a specific manufacturer.

In chapter 6, entitled **Application in the Danish Power System**, the developed DPL-based wind turbine model is rescaled to obtain an aggregate DPL-based wind farm model. This model is then used to perform short-circuit investigations in a real power system including wind power. The Nysted/Rødsand offshore wind farm is modelled as equipped with full-rating converters-based WTs and the Danish transmission system is considered for the analysis. Several study cases have been considered at some significant fault locations, such as some busbars and a line. Test results prove that the current contribution from the Nysted-size offshore wind farm has been successfully implemented.

It can be concluded that project goals presented in section 1.6 have been completely achieved.

Future work

The future work of the project includes:

- *improvement of the convergence of the DPL routine*: the speed and stability of the DPL routine convergence can be improved, presumably, using a better convergence criterion which considers the derivative of the active and reactive current variations at each iteration. The *Secant method* is a possible method; at each iteration, it would evaluate the new solutions for X, R and φ respectively from two previous solutions; however, as a disadvantage, this method would require two initial guesses to start the iterative process [63]).

- *development of a DPL routine addressed to a specific control designed of a wind turbine*: this is possible only if the manufacturer-used control strategy in fault conditions is applied and therefore it is addressed to manufacturers producing full-rating converters-based wind turbines.

- *implementation of the fault current contribution from several wind farms included in the power system*: in case of high wind power penetration, the results accuracy of short-circuit studies can be improved by including the fault current contribution from all wind farms included in the power system. This can be done by developing a main DPL routine including several DPL subroutines (i.e. a DPL subroutine for each wind farm); at each iteration the main routine could run all subroutines, which are copies of the developed DPL routine, and stop the process when all fault current contributions have been successfully considered.

- *analysis of the Danish power system in* 2025 *when additional* $3000MW$ *of wind power will be installed*: among the scheduled $3000MW$ that will be installed in Denmark until 2025, it can be reasonably assumed that $1000MW$ will be installed on the East coast and connected at the Eastern power system. It is therefore interesting to investigate how the new installed wind power will support the grid assuming that, until 2025, the grid voltage support will be also included in the Danish grid code. It is expected that useless results will be obtained if the fault current contribution from the wind generation is not considered in short-circuit studies at steady-state conditions.

- *implementation of user-defined reactive current profile for the grid voltage support*: requirements for the reactive current injection could be specified by the user independently on requirements of national grid codes. The user-defined profile could be as shown in Fig.6.18 and characterized by the following values:

  - dead band DB in $[pu]$;
  - reactive current i^0_{react} within the dead band;
  - slope S;

– maximum reactive current support i_{react}^{max}.

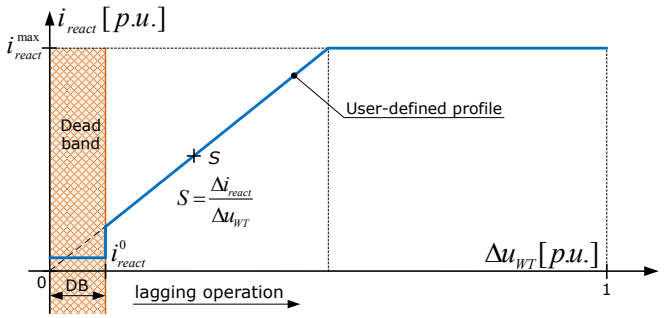

Figure 6.18: *Example of user-defined reactive current profile for the grid voltage support.*

- *implementation of the fault current contribution from VSC-based wind turbines to the grid in other simulation tools*: the implementation in a different tool may require a different approach.

Bibliography

[1] "Worldwide wind energy capacity at 47616MW-8321MW added in 2004," World Wind Energy Association, Press Release March 2005.

[2] V. Akhmatov, *Analysis of Dynamic Behaviour of Electric Power Systems with Large Amount of Wind Power*. PhD thesis, Technical University of Denmark, April 2003. ISBN Softbound 87-91184-18-5; ISBN CD ROM 87-91184-19-3. Available on line: http://www.elektro.dtu.dk/upload/institutter/_oersted/eltek/research/00-05/05-va-thesis.pdf.

[3] C. Eping, J. Stenzel, M. Poller, and H. Muller, "Impact of large scale wind power on power system stability," DIgSILENT publication available on line: http://www.digsilent.de/Consulting/Publications/PaperGlasgow_DIgSILENT.pdf.

[4] S. M. Bolik, *Modelling and Analysis of variable speed Wind Turbines with Induction Generator during grid fault*. PhD thesis, Aalborg University, October, 2004.

[5] J. G. Slootweg, *Wind Power: Modelling and Impact on Power System Dynamics*. PhD thesis, University of Delft, October 2003. ISBN 90-9017239-4.

[6] F. D. Bianchi, H. D. Battista, and R. J. Mantz, *Wind Turbine Control System*. Springer, 2007. ISBN 1-8462-8492-9.

[7] F. Blaabjerg and F. Iov, "Wind power - a power source now enabled by power electronics," 30 September - 4 October 2007. Keynote paper in Proc of 9th Brazilian Power Electronics Conference COBEP 07, Blumenau Santa Catarina, Brazil, ISBN 978-85-99195-02-4.

[8] M. Valentini, T. Ofeigsson, and A. Raducu, "Control of a variable speed variable pitch wind turbine with full power converter." Unpublished project at the Institute of Energy Technology, Aalborg University, Denmark, 17 December 2007.

[9] F. Blaabjerg, F. Iov, Z. Chen, and R. Teodorescu, "Power electronics in renewable energy systems," Keynote paper at EPE-PEMC 2006 Conference, August 30 - September 1 2006, Portoroz , Slovenia, p.17, IEEE Catalog Number: 06EX1405C, ISBN 1-4244-0449-5.

[10] F. Blaabjerg, R. Teodorescu, M. Liserre, and A. Timbus, "Overview of control and grid synchronization for distributed power generation systems," *IEEE Transactions on Industrial Electronics*, vol. 53, issue 5, pp. 1398-409, Oct. 2006. Digital Object Identifier 10.1109/TIE.2006.881997.

[11] F. Hansen, L. Helle, F. Blaabjerg, E. Ritche, S. Munk-Nielsen, H. Bindner, P. Sørensen, and B. Bak-Jensen, "Conceptual survey of generators and power electronics for wind turbines," RISØ National laboratory, December 2001. Available on line: http://www.risoe.dk/rispubl/VEA/veapdf/ris-r-1205.pdf.

[12] H. Saadat, *Power System Analysis*. McGraw-Hill, 1999. ISBN 0-07-561634-3.

[13] "VDE 0102:2002-07: Short-circuit currents in three-phase a.c. systems - part 0: Calculation of currents (IEC 60909-0:2001)," VDE - Verband Deutscher - Electrotechniker, July 2007. German version EN 60909-0:2001.

[14] "European standard EN 60909. short-circuit currents in three-phase a.c. systems. part 0: Calculation of currents (IEC 60909-0:2001)," CENELEC (European Committee for Electrotechnical Standardzation), August 2001.

[15] P. Kundur, *Power System Stability and Control*. McGraw-Hill, Inc, 1994. ISBN 0-07-035958-X.

[16] *DIgSILENT Technical Documentation: PWM Converter*, 30.03.2007. TechRef ElmVsc V1.

[17] T. Boutsika, S. Papathanassiou, and N. Drossos, "Calculation of the fault level contribution of distributed generation according to IEC standard 60909," Available on line: http://users.ntua.gr/stpapath/Paper_2.52.pdf.

[18] "Grid code. high and extra high voltage," E.ON Netz BmbH, Bayreuth, 1 August 2006.

[19] F. Iov, R. Teodorescu, F. Blaabjerg, B. Andersen, J. Birk, and J. Miranda, "Grid code compliance of grid-side converter in wind turbine systems," *Power Electronics Specialists Conference, 2006. PESC '06. 37th IEEE*, pp. 1 – 7, 18-22 June 2006. ISSN: 0275-9306, ISBN: 0-7803-9716-9.

[20] F. Iov, A. D. Hansen, P. Sørensen, and N. A. Cutululis, "Mapping of grid faults and grid codes," Risø National Laboratory and Technical University of Denmark, Roskilde, Denmark, July 2007. Risø-R-1617(EN), ISSN 0106-2840, ISBN 978-87-550-3622-2. Available on line: http://www.risoe.dk/rispubl/reports/ris-r-1617.pdf.

[21] A. Mullane, G. Lightbody, and R. Yacamini, "Wind-turbine fault ride-through enhancement," *Power Systems, IEEE Transactions on*, vol. 20, issue 4, pp. 1929-1937, Nov. 2005. ISSN: 0885-8950.

[22] C. Abbey and G. Joos., "Effect of low voltage ride through (LVRT) characteristic on voltage stability," in *Power Engineering Society General Meeting, 2005. IEEE*, vol. 2, pp. 1901-1907, 12-16 June 2005. ISBN: 0-7803-9157-8, Digital Object Identifier: 10.1109/PES.2005.1489659.

[23] M. Molinas, J. A. Suul, and T. Undeland, "A simple method for analytical evaluation of LVRT in wind energy for induction generators with STATCOM or SVC," *Power Electronics and Applications, 2007 European Conference on*, pp. 1-10, 2-5 Sept. 2007. ISBN: 978-92-75815-10-8, Digital Object Identifier: 10.1109/EPE.2007.4417780.

[24] "Grid disturbance and fault statistics," Nordel, 2006. Available on line: http://195.18.187.215/Common/GetFile.asp?PortalSource=1907&DocID=5338&mfd=off&pdoc=1.

[25] P. M. Anderson, *Analysis of faulted power systems*. IEEE Press Power Systems Engineering Series, 1995. ISBN: 0-7803-1145-0.

[26] "DIgSILENT powerfactory software: DIgSILENT programming language (DPL)," 7-8 February 2008. Industrial and PhD course of 1.5ECTS, Institute of Energy Technology IET, Aalborg University (DENMARK).

[27] DIgSILENT GmbH, Heinrich-Hertz-Strasse 9, D-72810 Gomaringen, *Chapter 29: The DIgSILENT Programming Language - DPL*. DIgSILENT 13.23337, User manual.

[28] I. Erlich and U. Bachmann, "Grid code requirements concerning connection and operation of wind turbines in Germany," pp. 2230-2234, June 12-16, 2005.

[29] "Large scale integration of wind energy in the european power syupply: analysis, issues and recommendations," EWEA - European Wind Energy Association, December 2005. Available on line: http://www.ewea.org/fileadmin/ewea_documents/documents/publications/grid/051215_Grid_report.pdf.

[30] T. Ackermann, *Wind Power in Power Systems*. John Wiley & Sons, Ltd, 2005. Royal Institute of Technology, Stockolm (Sweden), ISBN 10: 0-470-85508-8.

[31] F. Iov and F. Blaabjerg, "Advanced power converters for universal and flexible power management in future electricity network," UNIFLEX-PM, 20 February 2007. Project Number: 019794 (SES6).

[32] V. Cataliotti, *Impianti Elettrici. Sistemi elettrici di potenza: analisi - gestione- tecniche realizzative*, vol. II. Flaccovio Editore, 1998. ISBN: 8878041602.

[33] S. M. Bolik, "Grid requirements challenges for wind turbines," *Fourth International Workshop on Large Scale Integration of Wind Power and Transmission Networks for Offshore Wind Farms*, October 2003.

[34] Energinet.dk, "Grid connection of wind turbines to networks with voltages below 100 kV," in *Technical Regulations TF 3.2.6*, Energinet.dk, May 2004.

[35] Energinet.dk, "Grid connection of wind turbines to networks with voltages above 100 kV," in *Technical Regulations TF 3.2.5*, Energinet.dk, December 2004.

[36] "Generation in the medium voltage network-guidelines for the connection and operation of generation units in the medium voltage network," VDE - Verband Deutscher - Electrotechniker, 1998.

[37] "Requisitos de respuesta frente a huecos de tension de las instalaciones de produccion de regimen especial," REE, November 2005. PO 12.3.

[38] "Going mainstream at the grid face. Examining grid codes for wind," in *Windpower Monthly*, September 2005.

[39] A. Berizzi, A. Silvestri, D. Zaninelli, and S. Massucco, "Short-circuit current calculation: a comparison between methods of IEC and ANSI standards using dynamic simulation as reference," vol. 2, pp. 1420-1427, 2-8 Oct. 1993. ISBN: 0-7803-1462-X.

[40] I. Kasikci, *Short Circuits in Power Systems: A Practical Guide to IEC 60909*. WILEY-VCH, 2002. ISBN 3-527-30482-7.

[41] DIgSILENT GmbH, Heinrich-Hertz-Strasse 9, D-72810 Gomaringen, *Chapter 14: Short-Circuit Calculations*. DIgSILENT 13.23337, User manual.

[42] "IEEE recommended practice for electric power distribution for industrial plants (ieee red book)," IEEE-Institute of Electrical and Electronics Engineers, 1994. E-ISBN: 0-7381-1142-2, ISBN: 1559373334. Sponsored by: IEEE Industry Applications Society.

[43] J. Das, *Power System Analysis: Short-Circuit Load Flow and Harmonics*. CRC - 2002-04-17, 2002. ISBN-10: 0824707370, ISBN-13: 9780824707378.

[44] DIgSILENT GmbH, Heinrich-Hertz-Strasse 9, D-72810 Gomaringen, *Chapter 22: Time-domain Simulations*. DIgSILENT 13.23337, User manual.

[45] A. Tleis, "Experience in transmission systems," *Fault Level Assessment - Guessing with Greater Precision?, IEE Colloquium on*, vol. 5, pp. 1-3, 30 Jan 1996. INSPEC Accession Number: 5237850.

[46] "IEEE Std C37.010-1999 (R2005). application guide for ac high-voltage circuit breakers rated on a symmetrical current basis," Reaffirmed 20 March 2005, Approved 16 September 1999. ISBN Print: 0-7381-1837-3 SH94796, ISBN PDF: 0-7381-1828-1 SS94796, 1999 (R2005). Revision of IEEE Std C37.010-1979.

[47] "ANSI C37.5 methods for determining the rms value of a sinusoidal current wave and normal-frequency recovery voltage, and for simplified calculation of fault currents," ANSI-American National Standards Institute.

[48] G. Knight and H. Sieling, "Comparison of ANSI and IEC 909 short-circuit current calculation procedures," in *Petroleum and Chemical Industry Conference*, pp. 229-235, 9-11 Sep 1991. Record of Conference Papers., Industry Applications Society 38th Annual, Toronto, Ont., Canada. ISBN: 0-7803-0193-5.

[49] "IEEE Std C37.013a-2007 - IEEE standard for ac high voltage generator circuit breakers rated on a symmetrical current basis-Amendment 1: Supplement for use with generators rated 10-100 MVA," IEEE-Institute of Electrical and Electronics Engineers, 18 Oct 2007.

[50] V. Cataliotti, *Implianti Elettrici. Generalitá - Componenti*, vol. I. Flaccovio Editore, 2005. ISBN: 8878042706.

[51] "Short-circuit currents in three-phase a.c. systems. part 1: Factors for the calculation of short-circuit currents in three-phase a.c. systems according to IEC 60909-0," IEC-International Electrotechnical Commission, August 2001.

[52] C. Hartman, "Understanding asymmetry," *IEEE Transaction on Industry Applications*, vol. IA-2 1, n.A4, pp. 842-848, July/August 1985.

[53] Y. Coughlan, P. Smith, A. Mullane, and M. O'Malley, "Wind turbine modelling for power system stability analysis-a system operator perspective," *Power Systems, IEEE Transactions on*, vol. 22, issue 3, pp. 929-936, Aug. 2007.

[54] J. N. Nielsen, V. Akhmatov, J. Thisted, E. Grondahl, P. Egedal, M. N. Frydensbierg, and K. H. Jensen, "Modelling and fault-ride-through tests of Siemens Wind Power 3.6MW variable-speed wind turbine," *Wind Engineering*, vol. 31, No. 6, 2007.

[55] V. Akhmatov and P. Eriksen, "A large wind power system in almost island operation-a Danish case study," *Power Systems, IEEE Transactions on*, vol. 22, issue 3, pp. 937-943, Aug. 2007. Digital Object Identifier 10.1109/TPWRS.2007.901283.

[56] R. Teodorescu, F. Iov, and F. Blaabjerg, "Modelling and control of grid converter. Phase 1a: Basic grid inverter control," Gamesa Wind Engineering, Enertron, Aalborg University, February 2006.

[57] M. L. Remus Teodorescu and P. Rodriguez, "Power electronics for renewable energy systems-in theory and practice," 13-15 May 2008. Industrial/PhD course, Aalborg University.

[58] F. Kazmierkowski, R. Krishnan, and F. Blaabjerg, *Control in Power Electronics*. Academic Press, 2002. ISBN-0124027725.

[59] Bimal K. Bose, "An adaptive hysteresis-band current control technique of a voltage-fed PWM inverter for machine drive system," vol. 37, issue 5, pp. 402-408, Oct. 1990.

[60] V. Akhmatov and A. Nielsen, "A small test model of the transmission grid with a large offshore wind farm for education and research at Technical University of Denmark," in *Power Systems Conference and Exposition, 2006. PSCE '06. 2006 IEEE PES*, Oct. 29 2006-Nov. 1 2006. Pag.650-654, ISBN: 1-4244-0177-1. Digital Object Identifier 10.1109/PSCE.2006.296395.

[61] "Nysted offshore wind farm," 29 April 2008. http://www.nystedwindfarm.com.

[62] V. Akhmatov and H. Knudsen, "An aggregate model of grid-connected, large-scale, offshore wind farm for power stability investigations - importance of windmill mechanical system," *Int. Journal of Electrical Power and Energy Systems*, vol. 24, pp. 709-717, 2002.

[63] Erwin Kreyszig, *Advanced Engineering Mathematics*. 9^{th} edition, John Wiley Sons, New York, 2006. ISBN-978-0-471-72897-9.

Acronyms

Acronym	Description
WT	Wind turbine
WF	Wind farm
WECS	Wind Energy Conversion System
VSC	Voltage Source Converter
CSC	Current Source Converter
FSWT	Fixed Speed Wind Turbine
PVSWT	Partial Variable Speed Wind Turbine
DFIGWT	Doubly-Fed Induction Generator-based Wind Turbine
SCIG	Squirrel Cage Induction Generator
WRIG	Wound Rotor Induction Generator
SC	Short-circuit
IEC	International Electrotechnical Commission
VDE	Verband Deutscher - Electrotechniker (German Association for Electrical, Electronic and Information Technologies)
ANSI	American National Standards Institute
IEEE	Institute of Electrical and Electronics Engineers
FRT	Fault Ride-Through
PM	Permanent Magnet
DG	Distributed Generation
DIgSILENT	DIgital SImuLator for Electrical NeTwork
GFA	General Fault Analysis
DPL	DIgSILENT Programming Language
GC	Grid Code
PCC	Point of Common Coupling
TSO	Transmission System Operator
HVL	High Voltage Limit

Continued on next page

Acronyms - continued

LVL	Low Voltage Limit
pu	Per unit
a.c.	Alternating Current
d.c.	Direct Current
SCTM	Symmetrical Component Tranformation Matrix
HV	High Voltage
LV	Low Voltage
SWP	Siemens Wind Power
SVC	Static VAR Compensator
CET	Centre of Energy Technology
DTU	Danish Technical University
VOC	Synchronous Voltage Oriented Control
PLL	Phase Locked Loop
PI	Poportional-integral controller
ABH	Adaptive band hysteresis

Nomenclature

Parameter	Description
Z_f	Fault impedance [Ω]
X_f	Fault reactance [Ω]
R_f	Fault resistance [Ω]
S_k	Symmetrical short-circuit power [MVA]
P_{actual}	Wind farm active power during the simulated fault [MW]
V_{actual}	PCC voltage during the simulated fault [V]
$P_{t=0}$	Pre-fault power [MW]
$V_{t=0}$	Pre-fault voltage [V]
I_k''	Initial symmetrical short-circuit current [A]
I_k	Symmetrical short-circuit current [A]
i_p	Peak short-circuit current [A]
i_{dc}	Decaying dc aperiodic component of the SC current [A]
A	Initial value of the dc aperiodic component [A]
I_1	Positive-sequence current [A]
I_2	Negative-sequence current [A]
I_0	Zero-sequence current [A]
$\mathbf{I}_{abc}$	Phase currents vector [A]
Z_{k1}	Positive-sequence impedance at the fault location [Ω]
Z_{k2}	Negative-sequence impedance at the fault location [Ω]
Z_{k0}	Zero-sequence impedance at the fault location [Ω]
I_{op}	Load current [A]
U_i	Voltage at bus i [V]
$U_{n,i}$	Rated voltage at bus i [V]
U_{bF}	Pre-fault voltage at the faulty bus [V]
c	Correction factor [pu]
c_{max}	Maximum correction factor [pu]
	Continued on next page

Nomenclature - continued

c_{min}	Minimum correction factor [pu]
I_b	Symmetrical short-circuit breaking current [A]
I_{th}	Thermal equivalent short-circuit current [A]
I''_{kM}	Initial symmetrical short-circuit current calculated without motors [A]
Z_k	Magnitude of the equivalent impedance at the short-circuit location [Ω]
K_G	Correction factorfor the correct calculation of the generator impedance [pu]
Z_Q	Impedance of the network feeder (upstream grid) [Ω]
Z_T	Impedance of the transformer [Ω]
I_{rG}	Generator rated current [Ω]
Δt	Maximum duration of the fault contribution [s]
Z_M	Impedance of the induction generator [Ω]
U_{rG}	Generator rated voltage [V]
S_{rG}	Generator rated power [W]
I_{LR}/I_{rG}	Ratio of the locked-rotor current to the rated current [pu]
R_G	Generator resistance [Ω]
X_G	Generator reactance [Ω]
i_{pi}	Peak short-circuit current of the network branch i [A]
f_c	Equivalent frequency [Hz]
X_{ci}	Positive-sequence reactance for network branch i [Ω]
t_m	Instant of contact separation of the first pole of the switching device [s]
I_{ri}	Rated current of the machine in the i-th branch [A]
p	Number of pole pairs [pu]
P_{rG}	Generator rated active power [W]
$NACD$	Ratio of remote current contribution and the total fault current [pu]
Z_{fc}	Impedance of the first-cycle network at the fault location [Ω]
X_{fc}	Reactance of the first-cycle network at the fault location [Ω]
E	Ideal voltage source [V]
I_{Ad}	Asymmetrical duty [A]
I_{Pd}	Peak value of the first-cycle SC current [A]
Z_{int}	Equivalent impedance of the interrupting network [Ω]
X_{int}	Equivalent reactance of the interrupting network [Ω]
X_{del}	Reactance of the network comprising only generators and passive elements [Ω]
I_{bus}	Busbar short-circuit current [A]
X	Reactance of the Thevenin equivalent-based WT model for short-circuit studies [Ω]

Continued on next page

Nomenclature - continued

R	Resistance of the Thevenin equivalent-based WT model [Ω]
φ	Phase angle of the a.c. voltage source of the Thevenin equivalent-based WT model [^{o}]
X_g	Grid reactance [Ω]
R_g	Grid resistance [Ω]
$S_{WF,n}$	Wind farm rated apparent power [MVA]
u_{WT}	Wind turbine terminal voltage [pu]
u_{WF}	Wind farm terminal voltage [pu]
Δu_{WT}	Wind turbine voltage dip due to a grid fault [pu]
i_{react}	Wind turbine reactive current [pu]
i_{act}	Wind turbine active current [pu]
i^*_{react}	Reference wind turbine reactive current [pu]
i^*_{act}	Reference wind turbine active current [pu]
ϵ_{max}	Maximum current error [pu]
ϵ_{act}	Active current error [pu]
ϵ_{react}	Reactive current error [pu]
R_1	Small-size variation of the series resistance of the Thevenin equivalent-based WT model [Ω]
R_2	Big-size variation of the series resistance of the Thevenin equivalent-based WT model [Ω]
X	Variation of the series reactance of the Thevenin equivalent-based WT model [Ω]
φ	Variation of the phase angle of the a.c. voltage source of the Thevenin equivalent-based WT model [^{o}]
φ_{con}	Constant component of the variation of the phase angle of the a.c. voltage source [^{o}]
φ_{var}	Variable component of the variation of the phase angle of the a.c. voltage source [^{o}]
R^*	Final value of the series resistance [Ω]
X^*	Final value of the series reactance [Ω]
φ^*	Final value of the phase angle of the a.c. voltage source [^{o}]
S_{Tn}	WT transformer rated apparent power [MVA]
$u_{k\%}$	Transformer short-circuit voltage [%]
u_{111}	Voltage at busbar 111 [pu]

Base values

In the project, the Siemens Wind Power 3.6MW variable speed wind turbine is considered as reference. Therefore, the DPL-based wind turbine model is developed to have the same rating of the reference WT. This has made the comparison possible. Throughout the work *pu* values have been used. It is therefore required to define base values so that absolute values can be calculated. When considering the Nysted wind farm, new base values are defined by taking into consideration the number of SWP 3.6MW wind turbines included in the wind farm (i.e. $n = 46$). Base values are listed in the following tables, respectively referring to the wind turbine and the wind farm.

Base value - Wind turbine	**Description**
Base WT active power P_b	$3.6MW$
Base WT base apparent power S_b	$3.6MVA$
Base WT terminal voltage U_{WTb}	$690V$
Base WT current I_{WTb}	$3.012kA$
Base PCC voltage U_{PCCb}	$10kV$

Table 6.15: *Base values when considering the wind turbine.*

Base value - Wind farm	**Description**
Base WF active power P_b	$165.6MW$
Base WF base apparent power S_b	$165.6MVA$
Base WF terminal voltage U_{WFb}	$690V$
Base WT current I_{WTb}	$216.864kA$
Base voltage U_{PCCb} of the Nysted WF	$33kV$

Table 6.16: *Base values when considering the wind farm.*

Appendices

Appendix A

Test results with the DPL-based WT model

In this appendix, results of short-circuit calculations performed with the developed WT model implemented in DIgSILENT PowerFactory by means of a DPL are shown. As described in section 5.4, the following study cases are analyzed:

- *study case 1 - weak grid*: power grid with $S_k = 10MVA$ and ratio $R_g/X_g = 0.1$;
- *study case 2 - normal grid*: power grid with $S_k = 10P_n = 36MVA$ and ratio $R_g/X_g = 0.1$, as specified by the Danish grid code [35];
- *study case 3 - stiff grid*: power grid with $S_k = 100MVA$ and ratio $R_g/X_g = 0.1$;

In each study cases 8 measures are performed with the following voltage levels at the WT: $0.10 - 0.20 - 0.30 - 0.40 - 0.50 - 0.60 - 0.70 - 0.80$ $[pu]$. The desired voltage dip is achieved by varing the fault reactance X_f with fixed ratio $R_f/X_f = 0.2$ as in [20].

At each measure, the following steady-state values have been considered:

- PCC voltage u_{PCC} (i.e. voltage at the HV-side of the WT transformer);
- WT voltage u_{WT} (i.e. voltage at the LV-side of the WT transformer);
- WT active and reactive power, P_{WT} and Q_{WT};
- fault reactance X_f and resistance $R_f = X_f/5$;
- reference active and reactive currents, i^*_{act} and i^*_{react};
- active and reactive currents, i_{act} and i_{react};
- WT symmetrical short-circuit power S_k and current I_k.

Study case 1 - weak grid

Results regarding the study case 1 are presented in Tables A.1 and A.2.

No.	u_{WT} [pu]	u_{PCC} [pu]	P_{WT} [MW]	Q_{WT} [MVAr]	Z_f [Ohm]
1	0.1026	0.0439	-0.0018	0.3713	3.569
2	0.1990	0.1397	-0.0035	0.7189	12.44
3	0.3049	0.2457	-0.0055	1.0981	24.48
4	0.4019	0.3422	-0.0059	1.4568	38.24
5	0.4992	0.4401	-0.0088	1.7915	56.60
6	0.5983	0.5465	1.2729	1.7254	85.66
7	0.7026	0.6619	2.0213	1.5063	137.7
8	0.8067	0.7779	2.6852	1.1103	255.0

Table A.1: *Test results: power grid with $S_k = 10MVA$ and ratio $R_g/X_g = 0.1$ (i.e. weak grid). Part 1.*

No.	i^*_{react} [pu]	i_{react} [pu]	i^*_{act} [pu]	i_{act} [pu]	WT S_k [MVA]	WT I_k [kA]
1	1.0000	1.0047	0.0000	-0.0050	3.617	3.027
2	1.0000	1.0033	0.0000	-0.0049	3.612	3.022
3	1.0000	1.0004	0.0000	-0.0050	3.602	3.014
4	1.0000	1.0070	0.0000	-0.0041	3.625	3.033
5	1.0000	0.9969	0.0000	-0.0049	3.589	3.003
6	0.8035	0.8011	0.5954	0.5905	3.583	2.998
7	0.5948	0.5956	0.8038	0.7992	3.588	3.002
8	0.3867	0.3823	0.9222	0.9246	3.602	3.014

Table A.2: *Test results: power grid with $S_k = 10MVA$ and ratio $R_g/X_g = 0.1$ (i.e. weak grid). Part 2.*

Study case 2 - normal grid

Results regarding the study case 2 are presented in Tables A.3 and A.4.

No.	u_{WT} [pu]	u_{PCC} [pu]	P_{WT} [MW]	Q_{WT} [MVAr]	Z_f [Ohm]
1	0.1007	0.0420	-0.0018	0.3694	1.122
2	0.2005	0.1413	-0.0035	0.7241	4.181
3	0.3000	0.2407	-0.0054	1.0820	8.005
4	0.3995	0.3405	-0.0071	1.4327	12.95
5	0.4989	0.4394	-0.0089	1.8027	19.48
6	0.6043	0.5531	1.3193	1.7181	30.59
7	0.7009	0.6603	2.0279	1.4989	47.93
8	0.8005	0.7706	2.6400	1.1581	82.60

Table A.3: *Test results: power grid with $S_k = 36MVA$ and ratio $R_g/X_g = 0.1$ (i.e. normal grid). Part 1.*

No.	i^*_{react} [pu]	i_{react} [pu]	i^*_{act} [pu]	i_{act} [pu]	WT S_k [MVA]	WT I_k [kA]
1	1.0000	1.0037	0.0000	-0.0049	3.613	3.023
2	1.0000	1.0030	0.0000	-0.0049	3.611	2.021
3	1.0000	1.0019	0.0000	-0.0050	3.607	3.018
4	1.0000	0.9961	0.0000	-0.0050	3.586	3.000
5	1.0000	1.0038	0.0000	-0.0050	3.614	3.014
6	0.7914	0.7898	0.6113	0.6065	3.585	3.000
7	0.5982	0.5940	0.8014	0.8037	3.598	3.010
8	0.3990	0.4019	0.9170	0.9161	3.601	3.013

Table A.4: *Test results: power grid with $S_k = 36MVA$ and ratio $R_g/X_g = 0.1$ (i.e. normal grid). Part 2.*

Study case 3 - stiff grid

Results regarding the study case 3 are presented in Tables

No.	u_{WT} [pu]	u_{PCC} [pu]	P_{WT} [MW]	Q_{WT} [MVAr]	Z_f [Ohm]
1	0.1003	0.0420	-0.0018	0.3622	0.418
2	0.2005	0.1412	-0.0036	0.7244	1.581
3	0.3001	0.2407	-0.0050	1.0832	3.039
4	0.4002	0.3410	-0.0063	1.4376	4.946
5	0.5000	0.4405	-0.0090	1.8064	7.496
6	0.6000	0.5483	1.2853	1.7260	11.52
7	0.7005	0.6593	2.0093	1.5208	18.36
8	0.8008	0.7711	2.6512	1.1464	31.92

Table A.5: *Test results: power grid with $S_k = 100MVA$ and ratio $R_g/X_g = 0.1$ (i.e. stiff grid). Part 1.*

No.	i^*_{react} [pu]	i_{react} [pu]	i^*_{act} [pu]	i_{act} [pu]	WT S_k [MVA]	WT I_k [kA]
1	1.0000	1.0036	0.0000	-0.0050	3.613	3.023
2	1.0000	1.0034	0.0000	-0.0050	3.612	3.023
3	1.0000	1.0027	0.0000	-0.0046	3.610	3.020
4	1.0000	0.9980	0.0000	-0.0044	3.593	3.006
5	1.0000	1.0036	0.0000	-0.0050	3.613	3.023
6	0.8000	0.7991	0.6000	0.5951	3.587	3.001
7	0.5990	0.6031	0.8008	0.7968	3.597	3.010
8	0.3985	0.3977	0.9172	0.9197	3.607	3.018

Table A.6: *Test results: power grid with $S_k = 100MVA$ and ratio $R_g/X_g = 0.1$ (i.e. stiff grid). Part 2.*

Appendix B

Test results provided by Siemens Wind Power

In this appendix, the results of short-circuit calculations performed with the SWP dynamic model of the 3.6MW variable speed WT are presented; they have been provided by Siemens Wind Power. For confidentiality reasons, some results obtained with the SWP dynamic model (i.e the steadystate active current iact injected by the WT into the grid during a grid fault) are not provided by Siemens Wind Power as they reflects the implemented control strategy during voltage dips.

As for the DPL-based WT model, the following study cases are analyzed:

- *study case 1 - weak grid*: power grid with $S_k = 10MVA$ and ratio $R_g/X_g = 0.1$;
- *study case 2 - normal grid*: power grid with $S_k = 10P_n = 36MVA$ and ratio $R_g/X_g = 0.1$, as specified by the Danish grid code [35];
- *study case 3 - stiff grid*: power grid with $S_k = 100MVA$ and ratio $R_g/X_g = 0.1$;

In each study cases 8 measures are performed with the following voltage levels at the WT: $0.10 - 0.20 - 0.30 - 0.40 - 0.50 - 0.60 - 0.70 - 0.80$ $[pu]$. The desired voltage dip is achieved by varing the fault reactance X_f with fixed ratio $R_f/X_f = 0.2$ as in [20].

Study case 1 - weak grid

Results regarding the study case 1 are presented in table B.1.

No.	u_{WT} [pu]	u_{PCC} [pu]	Q_{WT} [MW]	i_{react} [MVAr]	Z_f [Ohm]
1	0.1767	0.1190	0.6600	1.0375	7.954
2	0.2857	0.2283	1.0524	1.0232	16.62
3	0.4002	0.3429	1.4671	1.0183	27.53
4	0.5081	0.4512	1.8404	1.0061	40.28
5	0.5997	0.5487	1.8863	0.8737	57.82
6	0.6947	0.6517	1.7719	0.7085	86.68
7	0.7866	0.7526	1.4989	0.5293	136.7
8	0.8672	0.8423	1.1028	0.3532	226.4

Table B.1: *Test results: power grid with $S_k = 10MVA$ and ratio $R_g/X_g = 0.1$ (i.e. weak grid).*

Study case 2 - normal grid

Results regarding the study case 2 are presented in table B.2.

No.	u_{WT} [pu]	u_{PCC} [pu]	Q_{WT} [MW]	i_{react} [MVAr]	Z_f [Ohm]
1	0.1701	0.1110	0.6556	1.0706	2.753
2	0.2760	0.2175	1.0438	1.0505	6.017
3	0.3847	0.3266	1.4372	1.0377	10.30
4	0.4912	0.4334	1.8175	1.0278	15.81
5	0.5853	0.5332	1.8928	0.8983	23.25
6	0.6773	0.6329	1.7986	0.7377	34.67
7	0.7642	0.7280	1.5720	0.5714	53.03
8	0.8517	0.8247	1.1994	0.3912	90.76

Table B.2: *Test results: power grid with $S_k = 36MVA$ and ratio $R_g/X_g = 0.1$ (i.e. normal grid).*

Study case 3 - stiff grid

Results regarding the study case 3 are presented in table B.3.

No.	u_{WT} [pu]	u_{PCC} [pu]	Q_{WT} [MW]	i_{react} [MVAr]	Z_f [Ohm]
1	0.1747	0.1152	0.6772	1.0768	1.122
2	0.2820	0.2233	1.0715	1.0555	2.448
3	0.3834	0.3251	1.4371	1.0412	4.079
4	0.4797	0.4218	1.7792	1.0303	6.119
5	0.5770	0.5242	1.8931	0.9114	9.178
6	0.6709	0.6260	1.8077	0.7485	13.87
7	0.7591	0.7224	1.5873	0.5808	21.42
8	0.8474	0.8199	1.2252	0.4016	37.02

Table B.3: *Test results: power grid with $S_k = 100MVA$ and ratio $R_g/X_g = 0.1$ (i.e. stiff grid).*

Appendix C

Algorithm-based discrepancy of the DPL-based wind turbine model

In this appendix numeric results of the tests performed to highlight the weakness of the DPL-based wind turbine model are presented. They are shown and compared in tables C.1 and C.2.

No.	Z_f [Ω]	u_{PCC} [pu] SWP	u_{PCC} [pu] DPL	$\epsilon_{u_{PCC}}$ [%]	u_{WT} [pu] SWP	u_{WT} [pu] DPL	$\epsilon_{u_{WT}}$ [%]
1	1.122	0.1152	0.1044	-9.36	0.1747	0.1635	-6.38
2	2.448	0.2233	0.2032	-9.00	0.2820	0.2623	-6.99
3	4.079	0.3251	0.2988	-8.08	0.3834	0.3580	-6.64
4	6.119	0.4218	0.3907	-7.37	0.4797	0.4498	-6.24
5	9.178	0.5242	0.4911	-6.32	0.5770	0.5478	-5.05
6	13.87	0.6260	0.5936	-5.18	0.6709	0.6411	-4.44
7	21.42	0.7224	0.6931	-4.05	0.7591	0.7309	-3.71
8	37.02	0.8199	0.7962	-2.89	0.8474	0.8232	-2.86

Table C.1: *Comparison: power grid with $S_k = 100MVA$ and ratio $R_g/X_g = 0.1$ (i.e. stiff grid). Part 1.*

No.	Z_f [Ω]	Q_{WT} [MVAr] SWP	Q_{WT} [MVAr] DPL	$\epsilon_{Q_{WT}}$ [%]	i_{react} [pu] SWP	i_{react} [pu] DPL	$\epsilon_{i_{reac}}$ [%]
1	1.122	0.6772	0.5900	-12.9	1.0768	1.0021	-6.93
2	2.448	1.0715	0.9429	-12.0	1.0555	0.9986	-5.39
3	4.079	1.4371	1.2858	-10.53	1.0412	0.9978	-4.17
4	6.119	1.7792	1.6133	-9.33	1.0303	0.9964	-3.29
5	9.178	1.8931	1.7776	-6.10	0.9114	0.9013	-1.10
6	13.87	1.8077	1.6607	-8.13	0.7485	0.7196	-3.86
7	21.42	1.5873	1.4264	-10.1	0.5808	0.5421	-6.67
8	37.02	1.2252	1.0388	-15.2	0.4016	0.3505	-12.7

Table C.2: *Comparison: power grid with $S_k = 100MVA$ and ratio $R_g/X_g = 0.1$ (i.e. stiff grid). Part 2.*

Appendix D

Enclosed CD-ROM

The enclosed CD-ROM contains the project report in Latex and Adobe PDF formats, documentations used throughout the report. If questions arise regarding the CD-ROM and something seems to be missing, please contact the author at the following email: masvalentini@gmail.com.

The content of the CD-ROM is summarized in the following.

- *References*: this folder contains all public references used throughout the report and listed in the bibliography.
- *DIgSILENT PowerFactory project*: this folder contains all DIgSILENT projects uses;
- *Latex project*: this folder contains the Latex project for further use;
- *Report in PDF format.*